IN VIVO FUNCTIONS OF MYELOID CELL TRAF3

By

ALMIN IQBALALI LALANI

A dissertation submitted to the

Graduate School-New Brunswick

And

The Graduate School of Biomedical Sciences

Rutgers, The State University of New Jersey

In partial fulfillment of the requirements

For the degree of

Doctor of Philosophy

Graduate Program in Cellular and Molecular Pharmacology

Written under the direction of

Dr. Ping Xie

And approved by

_____

_____

_____

_____

New Brunswick, New Jersey

January, 2017

ABSTRACT OF THE DISSERTATION

In Vivo Functions of Myeloid Cell TRAF3

by ALMIN IQBALALI LALANI

Dissertation Director:

Dr. Ping Xie

Tumor necrosis factor receptor-associated factor 3 (TRAF3) is a member of the TRAF family of cytoplasmic adaptor proteins that is ubiquitously expressed in various cell types of the immune system. It is shared for signaling by a variety of adaptive and innate immune receptors as well as cytokine receptors. Previous studies examining conditional TRAF3-deficient mouse models that have the *traf3* gene specifically deleted in B lymphocytes or T lymphocytes have revealed the diverse and critical *in vivo* functions of TRAF3 in adaptive immunity. Although *in vitro* evidence points to a pivotal and indispensable role for TRAF3 in type I interferon production induced by pattern recognition receptors in macrophages and dendritic cells, the *in vivo* functions of TRAF3 in myeloid cells had long remained unclear. My dissertation research has addressed this gap in knowledge by generating and characterizing myeloid cell-specific TRAF3-deficient (M-TRAF3$^{-/-}$) mouse model, which allowed us to gain insights into the *in vivo* functions of TRAF3 in myeloid cells. We found that TRAF3 ablation did not affect the maturation or homeostasis of myeloid cells in young adult mice, even though TRAF3-deficient macrophages and neutrophils exhibited constitutive NF-κB2 activation. However, in response to injections with LPS (a bacterial mimic) or polyI:C (a viral mimic), M-TRAF3$^{-/-}$ mice exhibited an altered profile of cytokine production. M-TRAF3$^{-/-}$ mice immunized with T cell-

independent (TI) and -dependent (TD) antigens displayed elevated TI IgG3 as well as TD IgG2b responses. Interestingly, 15-22 months old M-TRAF3$^{-/-}$ mice spontaneously developed chronic inflammation and tumors including TRAF3-sufficient B lymphoma and hepatocellular adenoma and TRAF3-deficient histiocytic sarcoma. Moreover, diseased M-TRAF3$^{-/-}$ mice displayed expanded population of myeloid derived suppressor cells that were highly immunosuppressive and blocked the proliferation of CD8 T cells *in vitro*. To further investigate the role of TRAF3 in MDSC physiology, we developed a new chronic inflammatory model in young adult M-TRAF3$^{-/-}$ mice using repeated injections of heat-killed BCG. Our results obtained from this model established TRAF3 as a suppressor of MDSC expansion and showed that chronic inflammation led to greater *de novo* synthesis of MDSC in the spleen of M-TRAF3$^{-/-}$ mice as compared to littermate control mice. In addition, characterization of B lymphomas spontaneously developed in aging M-TRAF3-/- mice confirmed their germinal center or post-germinal center origin as they displayed somatic hypermutations and had undergone Ig isotype switching. Interestingly, we discovered reactivation of endogenous retroviruses in these B lymphomas. Furthermore, we found that antibiotic treatment of mice prevents chronic inflammation and B lymphoma development in aging M-TRAF3-/- mice, indicating the requirement of commensal bacteria for the development of chronic inflammation and B lymphomas in these mice. Importantly however, antibiotic treatment did not affect the development of histiocytic sarcomas in aging M-TRAF3-/- mice, demonstrating a cell intrinsic role of TRAF3 in suppressing the oncogenesis of this tumor type. Taken together, the results from my dissertation research has established myeloid cell TRAF3 as a critical regulator of innate immune responses and a potent inhibitor of chronic inflammation, MDSC expansion and

tumor development. Our findings suggest that restoration of TRAF3 signaling pathways in myeloid cells could be a potential therapeutic strategy for the treatment of a variety of human diseases, including chronic inflammatory diseases, chronic infectious diseases and cancers.

DEDICATION AND ACKNOWLEDGEMENTS

DEDICATION

Shukran Allah, Alhumdulillah

To my family, especially my parents for investing in my higher education early on even in financially difficult times and believing in me and supporting me throughout this journey. This is the best gift any parents can give and I am very grateful for that. To my younger siblings, Reshma and Altaf for supporting me and taking more and more responsibilities so that I would have an easier time getting through this. I am also grateful to my entire family for making a sincere attempt to understand what I really do, because, trust me, sometimes even I don't get it ☺!

To my life partner and best friend Nabila for taking the biggest gamble of her life and falling in love with me and agreeing to marry me. Thank you for your patience and belief in me and for being the source of my inspiration, support and love. I promise your gamble will pay off big.

To my friends, for being there for me when I needed them. Thank you to all of you! Especially, Noorali, for your support, encouragement and interesting conversations. Rahim, for good times and your silly jokes – they are refreshing at times. Swapnil, Namit, Megha, Abdul, Saurabh, Anand and Shafiq for adventures, parties and good times.

ACKNOWLEDGEMENTS

MY ADVISOR AND COMMITTEE MEMBERS

Thank you very much to my advisor, Dr. Ping Xie, for this opportunity, your mentorship, guidance, support and for setting high expectations from me – it helped to bring the best out of me. Dr. Lori Covey, thank you for your help, guidance, advice and humor. Drs. Bertino and Zhou, thank you for critically evaluating my work and keeping me on track.

XIE LAB

Thank you to all members of Xie lab for helping me get through the past five years. Especially, Chang, Patty, Vishnu, Vidish, Arushi, Debanjan and Sining for your help with experiments – it meant a lot specially on long days. Carissa, for starting a great project and Ying Ying, for your overall support. Shanique, thank you for being the first PhD student to graduate – made things a lot easier for me ☺. On a serious note, thank you for being a great lab mate.

TABLE OF CONTENTS

LIST OF FIGURES

LIST OF TABLES

INTRODUCTION

IMMUNE RESPONSE AND MYELOID CELLS

Mammals have evolved an elaborate and complex immune response over time, which can be divided into two different types that are intricately interconnected: innate and acquired immune response[1]. Innate immune response is the foremost and non-specific defense mechanism launched by the mammalian host against pathogens, which, if needed, is followed by a highly specific acquired immune response that culminates in immunological memory[1,2]. The innate immune response is orchestrated by phagocytes which include macrophages, granulocytes and dendritic cells (DCs)[1,2]. Macrophages and granulocytes arise from the myeloid progenitor cells in the bone marrow (BM), whereas DCs arise from both myeloid and lymphoid progenitors in the BM[2,3]. Tissue resident macrophages are the first phagocytes to encounter most pathogens at the site of infection and they are very quickly reinforced by the recruitment of neutrophils. Although, these innate immune cells do not have the specificity of adaptive immune cells like B and T lymphocytes, they are able to differentiate between self and non-self. This is made possible by the presence of several cell-surface and cytoplasmic receptors that are collectively known as pattern recognition receptors (PRRs)[1,4]. PRRs are germline encoded receptors that recognize microbial components known as pathogen associated molecular patterns (PAMPs)[1]. Different types of PAMPs can lead to activation of distinct PRRs, which will eventually lead to a pathogen specific response via activation of a particular signaling pathway.

Tumor necrosis factor receptor (TNF-R) associated factor (TRAF) family of intracellular proteins play a significant role in signaling via various receptors including PRRs [4-6]. TRAF adaptor proteins were initially identified as signal transducers of TNF-R superfamily [4,7-9]. However, it is now widely accepted that TRAFs also play an indispensible role in signaling by various PRRs including Toll-like receptors (TLRs), RIG-I like receptors (RLRs) and NOD-like receptors (NLR). The structure of TRAF3 and an overview of its role in signaling by these PRRs are discussed below.

STRUCTURE OF TRAF3 AND OTHER TRAF FAMILY MEMBERS

TRAF family consists of seven members (TRAF1-7), however TRAF7 is controversial because it does not contain the TRAF homology domain which is a signature of this family [4]. TRAFs have a modular structure which consists of several functional domains [5] (Figure i). TRAF is one of the domains which is located at the C-terminus. It can be sub-divided into amino-terminal region (TRAF-N) which promotes TRAF homotrimerization and C-terminal β-sandwich (TRAF-C) region which mediates TRAF oligomerization and also promotes interactions with upstream regulators and downstream effectors [4,5].

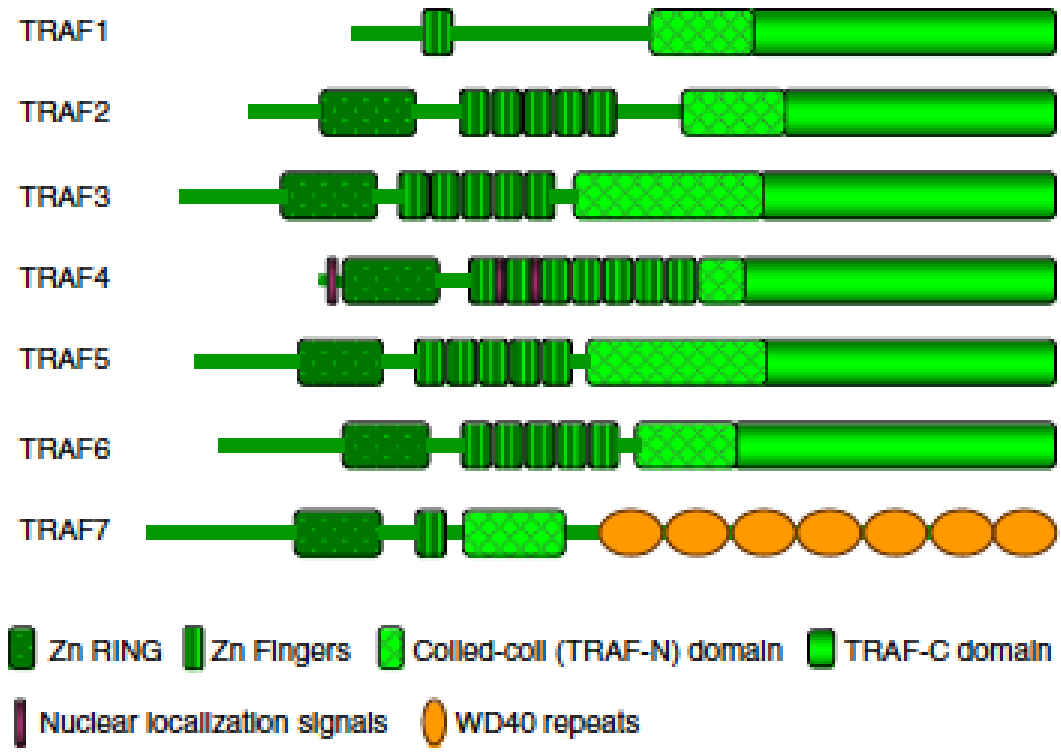

Figure i: Domain structure of the seven TRAF proteins. Symbols for different domains are shown, including zinc RING (Zn RING), zinc fingers (Zn Fingers), coiled-coil (TRAF-N) domain, TRAF-C domain, nuclear localization signals, and WD40 repeats. Adapted from Xie, Ping. TRAF molecules in cell signaling and in human disease[10].

Apart from their function as adaptor proteins, some TRAFs are also known to act as E3 ubiquitin ligases, including TRAF3 [4,11].This function is mediated by the N-terminal really interesting new gene (RING) finger motif, which is absent only in TRAF1. The RING finger motif is followed by variable number of zing fingers in different TRAFs (Figure i). RING finger motif is found in many E3 ubiquitin ligases and signal transduction via protein ubiquitination is an important mechanism used by TRAFs [5]. Moreover, auto-ubiquitinated TRAFs serve as docking sites for adaptors and kinases with ubiquitin-binding motifs, which lead to activation of downstream signaling events. In fact, differential

ubiquitation of TRAF3 is an important mechanism by which TRAF3 is used by cells to carry out opposing functions, as described in later section.

TRAF3 IN IMMUNE CELL HOMEOSTASIS AND DEVELOPMENT

We and Gardam et al. previously reported that B cell-specific TRAF3-deficient (B-TRAF3$^{-/-}$; TRAF3$^{flox/flox}$CD19$^{+/Cre}$) mice exhibit severe peripheral B cell hyperplasia and autoimmunity, due to vastly prolonged B cell survival and constitutive activation of the NIK-NF-κB2 pathway [12,13]. These mice eventually develop splenic marginal zone lymphomas (MZL) or B1 lymphomas by 18 months of age [14]. We also found that TRAF3$^{-/-}$ B cells display enhanced production of cytokines and type I interferons (IFN) as well as elevated Ig isotype switching in response to signaling by TLR3, 4, 7/8, and 9 [15]. These observations indicate that TRAF3 is a critical regulator of peripheral B cell homeostasis and autoimmunity, and serves as an important tumor suppressor in B lymphocytes.

In contrast, T cell-specific TRAF3-deficient (T-TRAF3$^{-/-}$; TRAF3$^{flox/flox}$CD4-Cre) mice exhibit normal homeostasis of CD4 and CD8 T cells, but are defective in T cell-dependent IgG1 responses and in T cell-mediated immunity to infection with *Listeria monocytogenes* [16]. The defects in T cell-mediated immune responses are caused by compromised T cell receptor (TCR)/CD28 signaling in both TRAF3$^{-/-}$ CD4 and CD8 T cells [16]. Interestingly, T-TRAF3$^{-/-}$ mice contain markedly increased frequency and numbers of regulatory T cells (Treg) cells [16], but decreased numbers of CD8 central memory T (Tcm) cells [17] and invariant natural killer T (iNKT) cells [18]. It was revealed that TRAF3 inhibits IL-2 signaling by facilitating the recruitment of the tyrosine phosphatase TCPTP to the IL-2 receptor complex to dephosphorylate Jak1, Jak3 and STAT5, thereby restraining thymic Treg development [19]. On the other hand, TRAF3 is required for TCR-

induced expression of T-bet and CD122, two molecules required for IL-15 signaling, and as a consequence, IL-15-mediated homeostasis of CD8 Tcm cells and development of iNKT cells are impaired in T-TRAF3$^{-/-}$ mice [17,18]. Furthermore, Treg cell-specific TRAF3-deficient (Treg-TRAF3$^{-/-}$; TRAF3$^{flox/flox}$Foxp3-Cre) mice exhibit heightened formation of germinal centers (GCs) and increased production of high-affinity IgG antibodies, resulting from decreased numbers of follicular Treg cells (T_{FR} cells) and increased numbers of follicular T helper cells (T_{FH} cells) [20]. It is found that TRAF3 signaling in Treg cells is required to maintain high level expression of the inducible co-stimulator (ICOS), which in turn is essential for T_{FR} cell generation in GCs and inhibition of antibody responses [20]. Both T-TRAF3$^{-/-}$ and Treg-TRAF3$^{-/-}$ mice have increased numbers of CD4 effector/memory T cells, suggesting that TRAF3$^{-/-}$ Treg cells might have defects in suppression of Th1 responses [21]. Collectively, the findings obtained from B-TRAF3$^{-/-}$, T-TRAF3$^{-/-}$, and Treg-TRAF3$^{-/-}$ mice indicate that TRAF3 is a highly versatile regulator of different lymphocyte subpopulations in the adaptive immune system and thus adaptive immune responses.

Different from adaptive immune responses, inflammation and innate immunity are mainly mediated by myeloid cells, including granulocytes, monocytes, macrophages and dendritic cells (DCs) [22]. These cells constitutively or inducibly express a number of receptors of the TNF-R, TLR, NLR, and RLR families as well as cytokine receptors, whose signals are regulated by TRAF3 [10,21-25]. In particular, macrophages represent a major type of innate immune cell that initiate inflammatory responses and host defense against infections by producing pro-inflammatory cytokines and type I IFN [23]. Although *in vitro* evidence indicates that TRAF3 regulates pro-inflammatory cytokine and type I IFN production in macrophages and DCs [26,27] almost a decade ago, the *in vivo* functions of

TRAF3 in the innate immune system has remained elusive. Here I present *in vivo* functions of TRAF3 in myeloid cells as obtained from our investigation of mice where TRAF3 is specifically deleted from myeloid cells (M-TRAF3$^{-/-}$ mice).

TRAF3 IN TOLL-LIKE RECEPTOR (TLR) SIGNALING

A wide variety of pathogens can lead to production of cytokines and chemokines by macrophages as a result of activation of signaling receptors on these cells. TLRs are one of these receptors that are an ancient form of host defense system which can recognize pathogen associated molecular patterns (PAMPs) from different microbes including bacteria, viruses, parasites, protozoa and fungi [2,4]. There are a total of 13 TLRs in mammals that recognize a distinct set of molecular pattern [2,28-31]. Based on the type of pathogen encountered, TLR signaling can lead to the production of type I interferons (IFNα and IFNβ), pro-inflammatory cytokines (TNFα, IL-6, IL1β, IL-12, etc.), chemokines and other inflammatory mediators [4]. TRAF3 is known to play a negative role in signaling by receptors from TNF-R superfamily like CD40 and BAFF-R [8,32,33]. However, in TLR signaling it plays a dual role of positive and negative regulator based on the type of TLR, adaptors and its ubiquitination mode. TRAF3 is known to interact with TLR3, 4, 7, and 9 via different sets of adaptor molecules [1,4,5,34]. There are four different adaptors used by TLRs which include MyD88 (myeloid differentiation factor 88), MAL/TIRAP (MyD88 adaptor-like)/ TIR domain-containing adaptor protein), TRIF (TIR domain-containing adaptor protein inducing IFN-β), and TRAM (TRIF-related adaptor molecule) [2,4,5]. These adaptors have a Toll / IL-1 receptor (TIR) domain that interacts with the cytoplasmic TIR domains on the TLRs, which are dimerized or oligomerized upon ligand binding and leads to downstream signaling[4]. MyD88 is used by all TLR and IL-1R family members with the

exception of TLR3, whereas TRIF is only used by TLR3 and TLR4[4,5]. MAL/TIRAP and TRAM are co-adaptors of MyD88 and TRIF, respectively.

Since TLR4 uses all the adaptor molecules, I will use that as an example to illustrate differential use of TRAF3 in TLR signaling. TLR4 signaling occurs at two distinct membranes: plasma membrane (PM) and endosomal membrane. Upon binding of the TLR4 receptor at the PM to its ligand lipopolysaccharide (LPS), a component of gram-negative bacteria, a rapid assembly of a multi-protein complex involving MyD88 on the cytoplasmic side of the PM is seen [5] (Figure iiA). TRAF3, here, is poly-ubiquitinated at Lysine 48 (K48) and is rapidly degraded via proteasome, leading to expression of pro-inflammatory cytokines. Thus un-ubiquitinated TRAF3 acts as a negative regulator of MyD88-mediated pro-inflammatory pathway and this negative regulation is relieved by K48 ubiquitination of TRAF3. In contrast, K63-linked poly-ubiquitinated TRAF3 acts as a positive regulator of type I interferons downstream of TLR4-TRIF/TRAM adaptor molecules on the endosomal membrane. Thus, the ubiquitination mode of TRAF3 dictates its role in TLR signaling.

TLR3 also uses TRIF and TRAM adaptor molecules and TRAF3 plays a similar role as in TLR4-TRIF-TRAM complex for the induction of type I IFN response upon TLR3 stimulation which is triggered by dsRNA [1,4,11]. Interestingly, TLR9 uses TRAF3 in conjunction with MyD88 adaptor and unlike TLR4-MyD88 pathway, TRAF3 here plays a positive regulatory role and promotes the expression of type I IFNs via activation of IRF7 (interferon regulatory factor 7) [4,5]. Together these findings, shed light on the versatility and substantially distinct roles that TRAF3 can play based on the cell type, receptor and

adaptors in use [5,32]. Here we have investigated the role of myeloid cell TRAF3 downstream of TLR3 and TLR4 receptors and the results are presented in chapter I.

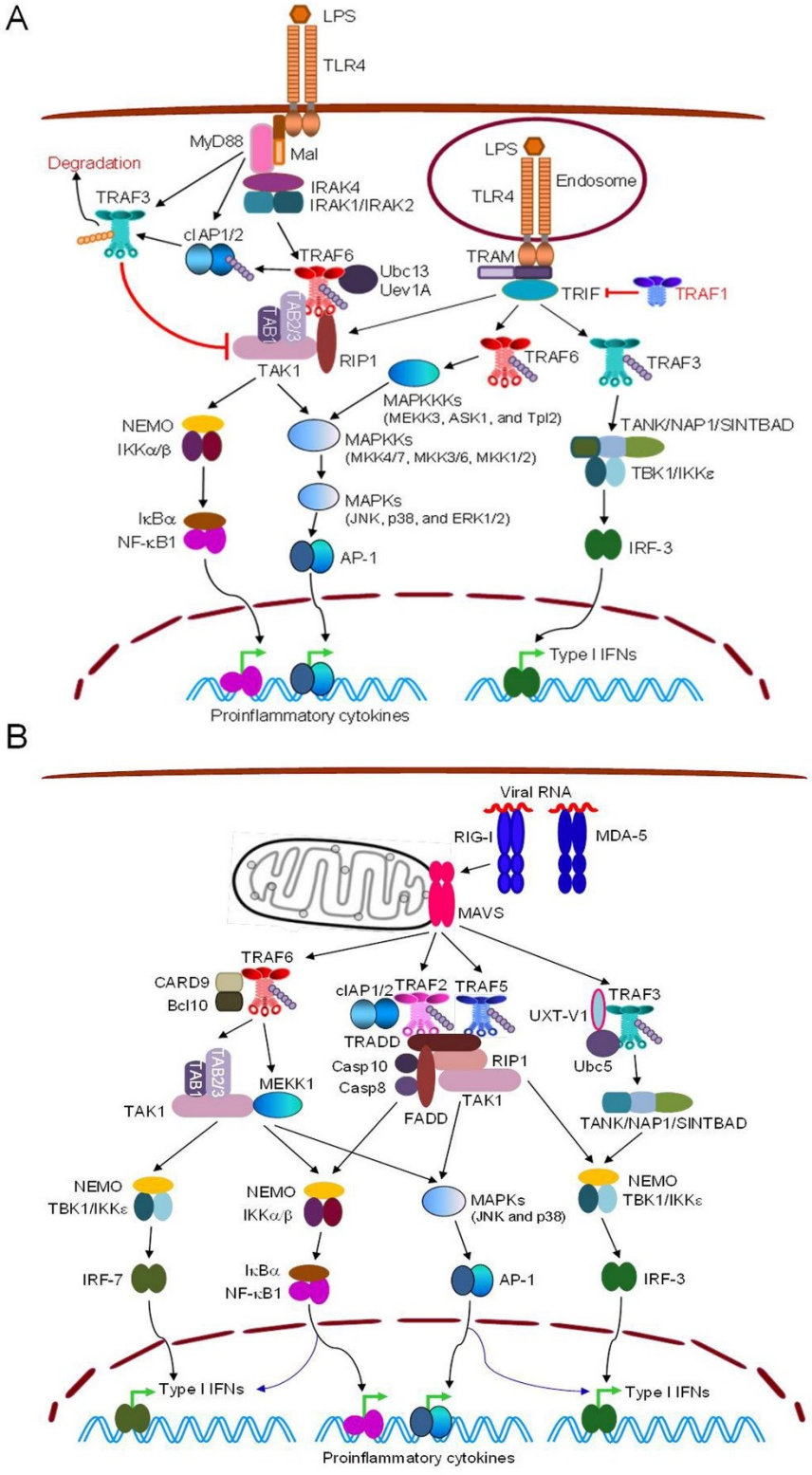

Figure ii: TRAF3 in signaling by TLR4 and RIG-I. (A) TLR4 signaling pathways: Upon LPS engagement on the plasma membrane, TLR4 recruits TRAF6 and TRAF3 via MyD88-IRAK1. Internalized TLR4 recruits TRAF3 and TRAF6 to endosomes via TRIF. (B) Upon ligand binding, RIG-I recruits TRAF3, TRAF6, TRAF2 and TRAF5 to mitochondria via MAVS. TRAF3 mediates RIG-I-induced IRF3 but not NF-κB1 activation. TRAF6 mediates RIG-I-induced IRF7 activation and also contributes to activation of NF-κB1, JNK, and p38. TRAF2 is important for p38 activation, and both TRAF2 and TRAF5 also contribute to activation of IRF3 and NF-κB1 in RIG-I signaling. Figure adapted from Xie, P. TRAF molecules in cell signaling and in human diseases[10].

TRAF3 IN RIG-I LIKE RECEPTOR (RLR) AND NOD-LIKE RECEPTOR (NLR) SIGNALING

RLRs and NLRs are cytoplasmic PRRs that recognize different forms of viral RNA and components of bacteria, respectively. They both lead to the production of type I IFNs and pro-inflammatory cytokines upon recognition of their respective PAMPs [1,4,5] (Figure ii, NLR signaling is not shown). RLRs, including RIG-I (retinoic acid inducible gene-1) and MDA-5 (melanoma differentiation-associated protein 5), recruit MAVS (mitochondrial anti-viral signaling protein; also known as CARDIF, VISA and IPS1) upon stimulation. TRAF3 then directly interacts with MAVS via the TRAF-interacting motif on MAVS and undergoes auto-ubiquitination at K63 residue [35,36]. This activates TRAF3 and leads to the recruitment and activation of TBK1 and IKKε, with subsequent phosphorylation, dimerization and nuclear translocation of IRF3 to trigger the production of type I IFNs [4,5,35]. This pathway is comparable to the one mediated by TRIF adaptor, as both involves the non-degradative (K-63 linked) phosphorylation of TRAF3 (Figure ii).

On the other hand, TRAF3 is used differently by different NLRs, including NOD1(Nucleotide-binding oligomerization domain-containing protein 1) and NOD2 (Nucleotide-binding oligomerization domain-containing protein 2), to induce the

production of type I IFNs [4]. Recognition of meso-diaminopimelic acid (DAP), found in bacterial peptidoglycan, leads to oligomerization of NOD1 and the recruitment of TRAF3 via RIP2 (Receptor-interacting protein 2; also known as RICK). TRAF3 in turn activates TBK1 and IKKε subsequently leading to activation of IRF7, which promotes the expression of type I IFNs [4,37]. Activation of NOD2 by its bacterial ligand, muramyl dipeptide (MDP) leads to transcription of pro-inflammatory cytokines via NF-kB and MAPK cascades. However, upon recognition of viral ssRNA, NOD2 instead leads to the production of type I IFNs in a MAVS dependent manner [4,38]. Weather TRAF3 is involved in MAVS dependent signaling downstream of NOD2 remains to be investigated. The integrity of NLR signaling pathways is important as loss of function mutations in NOD2 and insertion/deletion polymorphisms of NOD1 are associated with susceptibility to inflammatory bowel disease (IBD) [39].

Since TRAF3 is involved in signaling downstream of these cytoplasmic receptors, its deficiency in myeloid cells could lead to increased susceptibility to inflammation, infection or other abnormalities. Indeed, we found that M-TRAF3-/- mice are more prone to such abnormalities as discussed in chapter I.

MY DISSERTATION RESEARCH

The main goal of my dissertation research is to investigate the *in vivo* functions of TRAF3 in myeloid cell. In order to achieve that, our lab has created a conditional knockout mouse model where TRAF3 is specifically deleted from myeloid cells, thus allowing us to study its myeloid-cell specific function. In chapter I, I present results from our study of this mouse model. We found that deletion of TRAF3 from myeloid cells, leads to minor changes in young adult M-TRAF3-/- mice including enhanced pro-inflammatory cytokine production upon stimulation of TLR3 and TLR4 receptors and also enhanced antibody production of selected isotypes in response to T-cell independent and dependent antigens. However, we report that as M-TRAF3$^{-/-}$ age (15-22 months old) they are riddled with abnormalities ranging from chronic inflammation and infection to development of tumors in different cell types, leading to decreased life expectancy compared to control mice. They also show substantial expansion of immature and immune suppressive myeloid cells called myeloid derived suppressor cells (MDSC) and upregulation of several cytokines and chemokines that are implicated in chronic inflammation and tumor development. Thus, in chapter I we convincingly establish the *in vivo* role of myeloid cell TRAF3 as an inhibitor of chronic inflammation and tumor development.

In the later chapters, we have made an attempt to better understand the mechanism of tumor development and chronic inflammation in aging M-TRAF3$^{-/-}$ mice. In order to achieve that, we have developed a new model of chronic inflammation in young adult M-TRAF3-/- mice which highly resembles the phenotype observed in aging M-TRAF3-/- mice. Results from this chapter are presented in chapter II. This model allowed us to reassert the role of myeloid cell TRAF3 as an inhibitor of chronic inflammation by

suppression of MDSC expansion. In chapter III, we have characterized the TRAF3-sufficient B lymphomas observed in aging M-TRAF3-/- mice as arising from germinal center (GC) or post-GC B cells and show that they display significant upregulation of endogenous retroviruses. Moreover, we show that antibiotic treatment of aging M-TRAF3-/- mice prevents development of B lymphomas suggesting a requirement of commensal bacteria in B lymphomagenesis in these mice. However, antibiotic treatment leads to a greater incidence of TRAF3-deficient histiocytic sarcomas (HS) in the aging antibiotic treated M-TRAF3-/- mice, suggesting that TRAF3 acts as a tumor suppressor in histiocytes in a cell intrinsic manner. Finally, we have successfully established B lymphoma and HS cell lines which will serve as a new model system to investigate the role of TRAF3 in tumor immunity and surveillance and better understand the mechanism of tumor suppression in histiocytes by TRAF3.

Overall, the results from my dissertation research, have established myeloid cell TRAF3 as a critical regulator of innate and adaptive immune responses that is required to inhibit chronic inflammation, maintain tissue homeostasis, host-commensal mutualism and prevent tumor development via both cell-intrinsic (in histiocytes) and cell-extrinsic (B cells) mechanisms.

CHAPTER I: MYELOID CELL TRAF3 REGULATES IMMUNE RESPONSES AND INHIBITS INFLAMMATION AND TUMOR DEVELOPMENT IN MICE

ABSTRACT

Myeloid cells, including granulocytes, monocytes, macrophages and dendritic cells, are crucial players in innate immunity and inflammation. These cells constitutively or inducibly express a number of receptors of the TNF receptor and Toll-like receptor (TLR) families, whose signals are transduced by TRAF molecules. *In vitro* studies showed that TRAF3 is required for TLR-induced type I interferon production, but the *in vivo* function of TRAF3 in myeloid cells remains unknown. Here we report the generation and characterization of myeloid cell-specific TRAF3-deficient (M-TRAF3$^{-/-}$) mice, which allowed us to gain insights into the *in vivo* functions of TRAF3 in myeloid cells. We found that TRAF3 ablation did not affect the maturation or homeostasis of myeloid cells in young adult mice, even though TRAF3-deficient macrophages and neutrophils exhibited constitutive NF-κB2 activation. However, in response to injections with LPS (a bacterial mimic) or polyI:C (a viral mimic), M-TRAF3$^{-/-}$ mice exhibited an altered profile of cytokine production. M-TRAF3$^{-/-}$ mice immunized with T cell-independent (TI) and -dependent (TD) antigens displayed elevated TI IgG3 as well as TD IgG2b responses. Interestingly, 15-22 months old M-TRAF3$^{-/-}$ mice spontaneously developed chronic inflammation or tumors, often affecting multiple organs. Taken together, our findings indicate that TRAF3 expressed in myeloid cells regulates immune responses in myeloid cells and acts to inhibit inflammation and tumor development in mice.

1.1 BACKGROUND

Tumor necrosis factor receptor-associated factor 3 (TRAF3), a member of the TRAF family of cytoplasmic adaptor proteins, is employed in signaling by a variety of immune receptors, including the tumor necrosis factor receptor (TNF-R) superfamily, Toll-like receptors (TLRs), NOD-like receptors (NLRs), and RIG-I-like receptors (RLRs) [10,24]. TRAF3 binds directly to almost all members of the TNF-R superfamily that do not contain death domains, including CD40, BAFF-R, TACI, BCMA, LT-βR, CD27, CD30, RANK, HVEM, EDAR, XEDAR, 4-1BB (CD137), OX-40 (CD134), and GITR (TNFRSF18). TRAF3 is also indirectly recruited to the signaling complexes of pattern recognition receptors (PRRs) of the innate immune system through interactions with additional adaptor proteins, including MyD88 and TRIF for TLR signaling, RIP2 for NLR signaling, and MAVS for RLR signaling [40-42]. The shared usage of TRAF3 by such a variety of immune receptors is indicative of its broad functional roles in the immune system.

Mice made genetically deficient in TRAF3 ($TRAF3^{-/-}$) die within 10 days of birth with severe progressive runting, illustrating crucial developmental functions of TRAF3 [43]. To circumvent experimental limitations imposed by the early mortality of $TRAF3^{-/-}$ mice and to explore the *in vivo* functions of TRAF3 in various cell types of adult mice, we recently employed a conditional gene targeting strategy to generate conditional TRAF3-deficient ($TRAF3^{flox/flox}$) mice. This makes it possible to delete the *Traf3* gene in specific cell types or tissues [12]. Characterization of conditional TRAF3-deficient mouse models revealed that TRAF3 is critically involved in regulating multiple receptor signaling pathways in different immune cell types. We previously reported that specific ablation of TRAF3 in B lymphocytes results in marked peripheral B cell hyperplasia, due to

remarkably prolonged survival of mature B cells independent of the B cell survival factor BAFF, leading to the development of splenic marginal zone lymphomas (MZL) or B1 lymphomas by 18 months of age [12,14]. These findings indicated that a major homeostatic function of TRAF3 in peripheral B cells is the promotion of spontaneous apoptosis, a conclusion subsequently corroborated by Gardam and colleagues [13]. In contrast, specific deletion of TRAF3 from the T cell lineage leads to defective IgG1 responses to a T cell-dependent (TD) antigen (Ag) and impaired T cell-mediated immunity to infection with *Listeria monocytogenes* due to compromised T cell receptor (TCR)/CD28 signaling in both CD4 and CD8 T cells [16]. Additionally, recent evidence from other groups demonstrated that TRAF3 regulates the effector function of Treg cells [20] and that TRAF3 is required for the development of iNKT cells [18]. Thus, TRAF3 plays distinct and pivotal roles in regulating the development and function of different subsets of immune cells.

Myeloid cells, including granulocytes, monocytes, macrophages and dendritic cells (DCs), are crucial determinants of innate immunity and inflammation, and also play essential roles in antigen presentation as well as the effector phase of adaptive immunity. These cells constitutively or inducibly express a number of receptors of the TNF-R, TLR, NLR, and RLR families, whose signals are regulated by TRAF3 [10,24]. Although *in vitro* evidence indicates that TRAF3 is required for TLR-induced type I interferon (IFN) production [26,27] and for CD40-induced IL-12 production in macrophages [44], the *in vivo* functions of TRAF3 in myeloid cells remain unclear. In the present study, we generated $TRAF3^{flox/flox}LysM^{+/Cre}$ myeloid cell-specific TRAF3-deficient mice (M-$TRAF3^{-/-}$) to evaluate the functions of TRAF3 in innate immunity and inflammation mediated by myeloid cells. Cre expression driven by the lysozyme M promoter mediates deletion of

TRAF3 from neutrophils, eosinophils, basophils, monocytes, macrophages, and monocyte-derived DCs but not plasmacytoid DCs (pDC) [45,46]. We report here that deletion of TRAF3 in myeloid cells resulted in altered systemic responses to injections with LPS (an agonist of TLR4) or polyI:C (an agonist of TLR3), as well as TI and TD antigens. Furthermore, we found that M-TRAF3$^{-/-}$ mice spontaneously developed inflammation, infection, and tumors between 15 and 22 months of age. Taken together, our findings demonstrate obligatory and indispensable roles for myeloid cell TRAF3 in inhibiting inflammation and tumor development.

1.2 MATERIALS AND METHODS

1.2.1 GENERATION OF M-TRAF3$^{-/-}$ MICE

TRAF3$^{flox/flox}$ mice were generated as previously described [12]. The TRAF3$^{flox/flox}$ line was backcrossed with C57BL/6J (B6) mice (Jackson Laboratory) for >9 generations to generate TRAF3$^{flox/flox}$ mice on the B6 genetic background. These mice were subsequently bred with B6 mice transgenic for LysM-driven Cre expression (Jackson Laboratory, stock number: 4781). TRAF3$^{+/flox}$LysM$^{+/Cre}$ mice were backcrossed with TRAF3$^{flox/flox}$ B6 mice to generate TRAF3$^{flox/flox}$LysM$^{+/Cre}$ (M-TRAF3$^{-/-}$) mice. Mouse tails were screened by genomic PCR using primer sets (FC3 + BT6) [12], (Lys-Com + Lys-WT), and (Lys-Com + Lys-Cre) [45] as described. Deletion of exons 1 and 2 of the TRAF3 gene in peritoneal macrophages was detected by genomic PCR using primers U7 and BT6 as previously described [12]. All experimental mice for this study were subsequently produced by breeding of TRAF3$^{flox/flox}$ mice with TRAF3$^{flox/flox}$LysM$^{+/Cre}$ mice, and TRAF3$^{flox/flox}$ littermates (LMC) were used as controls for all experiments. All mice were kept in specific pathogen-free conditions in the Animal Facility at Rutgers University, and were used in

accordance with NIH guidelines and under an animal protocol (Protocol # 08-048) approved by the Animal Care and Use Committee of Rutgers University.

1.2.2 ANTIBODIES AND REAGENTS

Polyclonal rabbit Abs to TRAF1 (N19), TRAF3 (H122), TRAF6 (H274), and RelB were from Santa Cruz Biotechnology (Santa Cruz, CA). Polyclonal rabbit Ab to TRAF2 was from Medical and Biological Laboratories (Nagoya, Japan). Fluorescein isothiocyanate (FITC), phycoerythrin (PE), or Cy5 labeled Abs against mouse CD3, CD4, CD8, CD45R (B220), CD19, IgM, CD11b, Ly6C, Ly6G, CD115, F4/80, Siglec-F, CD68, CD11c, NK1.1, CD49b, CD21, CD23, CD5, CD44, CD62L, CD69, CD80, and MHC class II were purchased from eBioscience (San Diego, CA). Anti-mouse IL-6, IL-12, and TNF-α ELISA Ab pairs were also purchased from eBioscience. Anti-mouse IL-1β and IL-10 ELISA Ab pairs were also purchased from R&D (Minneapolis, MN). Polyclonal rabbit Abs against total or phosphorylated IRF3, p38, ERK, JNK, IκBα, Akt, and NF-κB2 were from Cell Signaling Technology (Beverly, MA). Anti-actin Ab was from Chemicon (Temecula, CA). HRP-labeled secondary Abs were from Jackson ImmunoResearch Laboratories, Inc. (West Grove, PA). Alkaline phosphatase (AP)-conjugated polyclonal goat Abs specific for mouse Ig isotypes were from Southern Biotechnology Associates (Birmingham, AL). Neutrophil purification kits were from Miltenyi Biotec Inc. (Auburn, CA). Tissue culture supplements including stock solutions of sodium pyruvate, L-glutamine, non-essential amino acids, and HEPES (pH 7.55) were from Invitrogen (Carlsbad, CA). DNA oligonucleotide primers were obtained from Integrated DNA

Technologies (Coralville, IA). AP substrates were purchased from Sigma-Aldrich Corp. (St. Louis, MO).

1.2.3 FLOW CYTOMETRY

Single cell suspensions were made from the spleen, bone marrow (BM), and peritoneal lavage. Immunofluorescence staining and FACS analyses were performed as previously described [12,14]. Erythrocytes from spleen were depleted with ACK lysis buffer. Cells (1 X 10^6) were blocked with rat serum and FcR blocking Ab (2.4G2), and incubated with various Abs conjugated to FITC, PE, PerCP, or Cy5 for multiple color fluorescence surface staining. Analyses of cell surface markers included antibodies to CD3, CD4, CD8, CD45R (B220), CD19, IgM, CD11b, Ly6C, Ly6G, CD115, F4/80, Siglec-F, CD68, CD11c, CD317, NK1.1, CD49b, CD21, CD23, CD5, CD44, CD62L, CD69, CD80, and MHC class II. Listmode data were acquired on a FACSCalibur (Becton Dickinson, Mountain View, CA) using Cell Quest software. The results were analyzed using FlowJo software (TreeStar, San Carlos, CA). FSC/SSC gating was used to identify live cells.

1.2.4 CULTURE OF BM-DERIVED MACROPHAGES (BMDMS) AND PERITONEAL EXUDATE MACROPHAGES (PEMS)

Bone marrow cells were harvested from 7-10 week old littermate control (LMC) or M-TRAF3$^{-/-}$ mice. BMDMs were prepared by culturing BM cells in complete RPMI-1640 medium (Invitrogen) supplemented with 20% conditioned medium from L929 cells overexpressing M-CSF for 7 days as described [47-49]. For preparation of PEMs, 7-10 week old LMC or M-TRAF3$^{-/-}$ mice were injected intraperitoneally (i.p.) with 3 ml of 4% thioglycollate (Becton Dickinson), and cells were harvested by peritoneal lavage on day 4

post injection as described [47]. The cells were washed, macrophages were allowed to adhere to the tissue culture plates for two hours, and non-adherent cells were removed.

1.2.5 PREPARATION OF THIOGLYCOLLATE-ELICITED PERITONEAL NEUTROPHILS

7-10 week old LMC or M-TRAF3$^{-/-}$ mice were injected i.p. with 3 ml of 4% thioglycollate (BD), and cells were harvested by peritoneal lavage at 18 h post injection. Neutrophils were purified from peritoneal cells using anti-Ly-6G-Biotin and anti-Biotin magnetic beads following the manufacturer's protocol (Miltenyi). Purified neutrophils were resuspended in RPMI-1640 medium containing 5% FCS, and aliquoted for stimulation.

1.2.6 TLR4 SIGNALING

Before stimulation with LPS, BMDMs or PEMs were cultured in 2.5% FCS medium for 2 hours. BMDMs, PEMs or neutrophils were stimulated with 100 ng/ml LPS. Total protein lysates were prepared at different time points as previously described [50] for measurements of early signaling events by immunoblot analysis. Total cellular RNA was extracted at different time points for measurement of cytokine transcript levels by quantitative real time PCR (RT-qPCR) using Taqman assay. Culture supernatants were collected at different time points for measurements of cytokine protein levels by ELISA.

1.2.7 TAQMAN ASSAYS OF IFNB, IFNA4, IL12A, IL6, AND TNFA TRANSCRIPTS

Total cellular RNA was extracted using TRIzol reagent (Invitrogen, Carlsbad, CA) according to the manufacturer's protocol. cDNA was prepared from RNA using the High Capacity cDNA Reverse Transcription Kit (Applied Biosystems, Foster City, CA). Quantitative real-time PCR (qPCR) was performed using TaqMan Gene Assay kit (Applied

Biosystems) as described [15]. TaqMan primers and probes (FAM-labeled) specific for individual mouse cytokines were used in the PCR reaction to detect Ifnb, Ifna4, Il12a, Il6, or Tnfa mRNA. Each reaction also included primers and a probe (VIC-labeled) specific for mouse Actb (b-actin) mRNA, which served as an endogenous control. Reactions were performed on a 7500 Fast Real-Time PCR System (Applied Biosystems). Relative mRNA expression levels of cytokines were analyzed using Sequencing Detection Software (Applied Biosystems) and the comparative Ct (ΔΔCt) method following the manufacturer's procedures.

ΔCt = Ct of cytokine – Ct of b-actin.

ΔΔCt = ΔCt of each sample – ΔCt of calibrator sample.

For each cytokine assay, the calibrator sample was the one with lowest detectable RNA level (highest Ct value). Duplicate PCR reactions were performed for each biological sample.

1.2.8 Cytokine ELISA

Concentrations of IL-6, IL-12, and TNFα in culture supernatants or mouse sera were determined by quantitative ELISA using cytokine-specific coating Abs and biotinylated detection Abs (eBioscience) as previously described [15,16]. Mouse serum levels of IL-10 and IL-1β were analyzed by ELISA using cytokine-specific coating Abs and biotinylated detection Abs (R&D) as previously described [15,16]. Levels of IFN-β in mouse sera were measured using the VeriKine-HS™ Mouse Interferon Beta Serum ELISA Kit (PBL Assay Science, Piscataway, NJ) following the manufacturer's protocol.

1.2.9 *IN VIVO* RESPONSES TO CHALLENGES WITH LPS OR POLYI:C

Age- and gender- matched 8-12 week old LMC and M-TRAF3$^{-/-}$ mice were injected *i.p.* with LPS (E. coli 0127:B8, Sigma; 300 μg LPS/20g body weight) or polyI:C (InvivoGen, 200 μg polyI:C/20g body weight). Sera were collected at 2 h and 6 h post injection, and cytokine levels in sera were analyzed by ELISA as described above.

1.2.10 IMMUNOBLOT ANALYSIS

Total protein lysates were prepared as described [50]. Proteins were separated by SDS-PAGE and immunoblotted with antibodies to phosphorylated (P-) or total IRF3, p38, ERK, JNK, Akt, IκBα, NF-κB2, RelB, TRAF3 and actin. Immunoblot analysis was performed using antibodies as previously described [14,50]. Images of immunoblots were acquired using a low-light imaging system (LAS-4000 mini, FUJIFILM Medical Systems USA, Inc., Stamford, CT) [14,50].

1.2.11 IMMUNIZATIONS AND IG ELISAS

Basal serum levels of various Ig isotypes in naïve 8-12 week old LMC and M-TRAF3$^{-/-}$ mice were analyzed by ELISA as previously described [12]. For TI antibody responses, age- and gender- matched 8-12 week old LMC and M-TRAF3$^{-/-}$ mice were immunized *i.p.* with 50 μg of trinitrophenyl (TNP)-Ficoll (Biosource Technologies, Vacaville, CA), and sera were collected on day 7 after immunization. For TD antibody responses, age- and gender- matched 8-12 week old LMC and M-TRAF3$^{-/-}$ mice were injected *i.p.* with 100 μg of TNP-KLH (Biosource Technologies) in an equal volume of Imject Alum (Thermo scientific, Rockford, IL), and sera were collected on day 7 after immunization. Serum TNP-specific Ig isotypes were measured by ELISA as previously

described [12]. Plates were read on a Versamax plate reader (Molecular Devices, Sunnyvale, CA) and results analyzed by using SoftMax Pro 4.0 software as described [12].

1.2.12 MOUSE DISEASE MONITORING AND HISTOLOGY

Mice were monitored daily for signs of illness including weight loss, labored breathing, hunched posture, and paralysis or spontaneous tumor formation indicated by enlarged lymph nodes or abdomen [14]. Necropsy and hematoxylin-eosin staining of formalin-fixed paraffin embedded tissues were performed to assess the presence of phenotypic abnormalities as described [12,14,51-56]. Bright field micrographs of stained sections were taken using a microscope (Olympus BX-51, Olympus America Inc., Center Valley, PA).

1.2.13 MOUSE CYTOKINE PROTEIN ARRAY ANALYSES

Sera were collected from 15-22 month old LMC and diseased M-TRAF3$^{-/-}$ mice. Serum levels of cytokines and chemokines were measured using a Mouse Cytokine Array Panel A kit (R&D, Minneapolis, MN) following the manufacturer's instructions. Images of the blots were acquired, and quantitative analyses of cytokine or chemokine spots were performed using a low-light imaging system (LAS-4000 mini, FUJIFILM Medical Systems USA, Inc., Stamford, CT) [14,50].

1.2.14 STATISTICS

Statistical analyses were performed using Prism software (GraphPad, La Jolla, CA). Survival curves were generated using the Kaplan-Meier method, and were compared using a log-rank (Mantel-Cox) test to determine whether differences are significant. For direct comparison of cytokine or Ig isotype levels between LMC and M-TRAF3$^{-/-}$ mice, statistical significance was determined with the unpaired t test for two-tailed data. P values

less than 0.05 are considered significant, and P values less than 0.001 are considered highly significant.

1.3 RESULTS

1.3.1 VALIDATION OF M-TRAF3$^{-/-}$ MICE

Previous *in vitro* studies indicated that TRAF3 regulates type I IFN and pro-inflammatory cytokine production in myeloid cells [26,27]. However, the *in vivo* functions of TRAF3 in myeloid cells had not been determined. To address this issue, we generated myeloid cell-specific TRAF3-deficient mice by crossing TRAF3$^{flox/flox}$ mice with mice that express Cre under the control of endogenous lysozyme M regulatory elements (LysM-Cre mice), which allows the specific deletion of floxed genes in myeloid cells [45]. Progeny were born at expected Mendelian frequencies with no developmental abnormalities noted, and matured and bred normally.

LysM-driven Cre expression has been shown to induce specific and highly efficient deletion of loxP-flanked gene segments in mature neutrophils and macrophages with a higher deletion efficiency in neutrophils [45,46,57]. In contrast, LysM-Cre-mediated deletion does not occur in T cells, B cells, NK cells, and pDCs, despite the presence of LysM activity in a small population of the hematopoietic stem cells [58]. Consistent with previous studies, we verified highly efficient deletion of the *Traf3* gene and a corresponding loss of TRAF3 protein (80~90% reduction) in peritoneal macrophages and BMDMs prepared from M-TRAF3$^{-/-}$ mice as determined by genomic PCR and Western blot analysis (Figure 1A and data not shown). No deletion of *Traf3* was observed in splenic T and B cells of M-TRAF3$^{-/-}$ mice (data not shown). Interestingly, we found that TRAF1 and TRAF2 protein

levels were modestly increased in TRAF3-deficient macrophages (Figure 1A). In contrast, TRAF6 protein levels were unchanged. We previously had observed modestly increased TRAF1 and TRAF2 protein levels in TRAF3$^{-/-}$ B cells and T cells [12,16]. These findings raise the possibility that increased TRAF1 and TRAF2 may partially compensate for the loss of TRAF3 in these cell types. Together, these data validated TRAF3$^{flox/flox}$LysM$^{+/Cre}$ mice as myeloid cell-specific TRAF3-deficient (M-TRAF3$^{-/-}$) mice.

1.3.2 YOUNG ADULT M-TRAF3$^{-/-}$ MICE HAVE NORMAL POPULATIONS OF LYMPHOID AND MYELOID CELLS

We previously reported that TRAF3 regulates mature B cell homeostasis in secondary lymphoid organs [12]. To investigate whether TRAF3 is involved in the maturation and homeostasis of myeloid cells, we first examined the size and cell numbers of lymphoid organs of 8-12 weeks old M-TRAF3$^{-/-}$ and TRAF3-sufficient littermate control mice (TRAF3$^{flox/flox}$, LMC). We found that M-TRAF3$^{-/-}$ mice had normal sized spleens, lymph nodes, and thymi, and also had normal numbers of cells in the BM and peritoneum (Table I and data not shown). We next used flow cytometry to characterize lymphocyte and myeloid cell populations in the BM, spleen, and peritoneum. Our data demonstrated that M-TRAF3$^{-/-}$ and LMC mice had similar proportions and numbers of splenic follicular and marginal zone B cell subsets and CD4 and CD8 T cells. This was also true for comparisons of granulocytes, monocytes and macrophages in the BM, spleen, and peritoneal lavage (Figure 1B, 1C, and Table I). Interestingly, TRAF3$^{-/-}$ and LMC CD11b^{+}F4/80^{+} macrophages in the spleen and peritoneal cavity also expressed comparable levels of MHC class II, CD80 and CD86, suggesting that macrophages were not activated as a result of TRAF3 deficiency in mice of this age (data not shown). In addition, following *i.p.* injection

of thioglycollate, the numbers of neutrophils (analyzed at 2, 4, 6, 12 or 18 h post injection) and macrophages (analyzed at day 3 or day 4 post injection) recruited to the peritoneal cavity were also comparable between M-TRAF3$^{-/-}$ and LMC mice (data not shown). Collectively, our findings indicate that specific ablation of TRAF3 in myeloid cells did not affect maturation, homeostasis or migration of macrophages and neutrophils and, as expected, had no effects on T and B cells.

Table I: Summary of lymphocyte and myeloid cell populations of M-TRAF3-/- mice analyzed by FACS

Organ	FACS markers	LMC	M-TRAF3-/-	Fold
Bone marrow (x 10^6 cells)		27.32 ± 2.11	27.80 ± 4.61	1.02
B cell lineage	B220+CD19+	7.13 ± 0.59	6.64 ± 1.03	0.93
immature B cells	B220+CD19+IgM+IgD-	1.37 ± 0.13	1.16 ± 0.21	0.84
mature B cells	B220+CD19+IgMloIgD+	1.31 ± 0.34	1.09 ± 0.22	0.83
T cell lineage	CD3+	0.66 ± 0.11	0.69 ± 0.25	1.04
Granulocyte lineage	CD11b+Ly6G+	9.43 ± 0.62	10.58 ± 2.15	1.12
neutrophils	CD11b+Ly6G+Siglec-F-SSCint	8.00 ± 0.95	8.67 ± 1.78	1.08
eosinophils	CD11b+Ly6GintSiglec-F+SSChigh	0.28 ± 0.07	0.29 ± 0.05	1.05
basophils	CD11bdullCD49b+FcsRIα+	0.21 ± 0.03	0.25 ± 0.07	1.19
Monocyte lineage	CD11b+Ly6C+Ly6G-	3.21 ± 0.61	3.28 ± 0.73	1.02
monocytes	CD11b+CD115(CSF1-R)+Ly6C+/loSSClo	0.64 ± 0.27	0.71 ± 0.11	1.10
Macrophages	CD11b+F4/80+CD68+	0.24 ± 0.10	0.24 ± 0.11	0.98
cDCs	CD11c+MHC ClassII+	0.42 ± 0.06	0.75 ± 0.30	1.77
NK cells	CD3-NK1.1+CD49b+	0.22 ± 0.03	0.28 ± 0.12	1.30
Spleen (x 10^6 cells)		97.84 ± 21.74	99.84 ± 14.16	1.02
B cell lineage	B220+CD19+	55.45 ± 14.27	56.84 ± 9.87	1.03
MZ B cells	B220+CD21+CD23int	5.29 ± 1.40	5.29 ± 0.93	1.00
Follicular B cells	B220+CD21intCD23+	52.91 ± 4.26	49.02 ± 4.28	0.93
T cell lineage	CD3+	32.96 ± 7.37	32.86 ± 6.41	1.00
CD4 T cells	CD3+CD4+CD8-	21.35 ± 5.09	20.58 ± 4.86	0.96
CD8 T cells	CD3+CD4-CD8+	13.63 ± 3.53	14.61 ± 3.67	1.07
Neutrophils	CD11b+Ly6G+Siglec-F-SSCint	1.63 ± 1.12	1.22 ± 0.77	0.75
Monocytes	CD11b+CD115+Ly6C+/loSSClo	0.30 ± 0.33	0.34 ± 0.43	1.12
Red pulp macrophages	CD11b+F4/80+CD68+	1.56 ± 1.13	1.36 ± 1.03	0.87
cDCs	CD11c+MHC ClassII+	1.66 ± 0.17	2.48 ± 0.57	1.49
NK cells	CD3-NK1.1+CD49b+	2.26 ± 0.65	2.14 ± 0.48	0.95
Peritoneal cavity (x 10^6 cells)		1.74 ± 0.59	1.72 ± 0.56	0.99
Macrophages	CD11b+F4/80+CD68+	0.35 ± 0.14	0.34 ± 0.11	0.97
B cells	B220+CD19+	1.20 ± 0.41	1.18 ± 0.42	0.98
B1a	B220+CD19+CD11b+CD5+	0.46 ± 0.22	0.35 ± 0.09	0.78
B1b	B220+CD19+CD11b+CD5-	0.27 ± 0.11	0.29 ± 0.14	1.08

Mice analyzed were 8 to 12 weeks old. Data shown are the results of five independent experiments (mean ± STDEV)

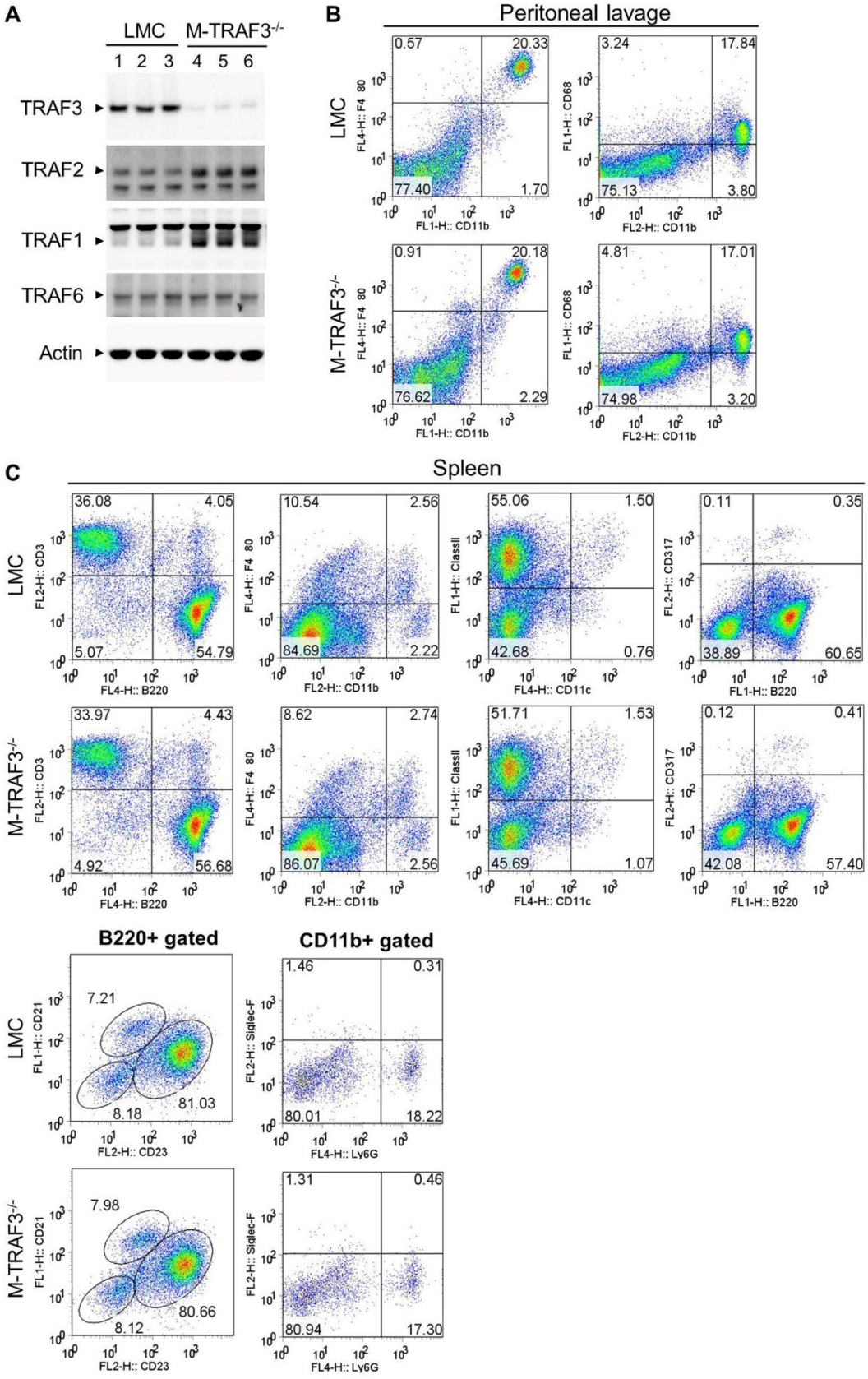
A
LMC
M-TRAF3-/-
1 2 3 4 5 6
TRAF3
TRAF2
TRAF1
TRAF6
Actin
B
Peritoneal lavage
LMC
M-TRAF3-/-
FL4-H:: F4 80
FL1-H:: CD11b
FL1-H:: CD68
FL2-H:: CD11b
0.57
20.33
77.40
1.70
3.24
17.84
75.13
3.80
0.91
20.18
76.62
2.29
4.81
17.01
74.98
3.20
C
Spleen
LMC
M-TRAF3-/-
FL2-H:: CD3
FL4-H:: B220
FL4-H:: F4 80
FL2-H:: CD11b
FL1-H:: ClassII
FL4-H:: CD11c
FL2-H:: CD317
FL1-H:: B220
36.08
4.05
5.07
54.79
10.54
2.56
84.69
2.22
55.06
1.50
42.68
0.76
0.11
0.35
38.89
60.65
33.97
4.43
4.92
56.68
8.62
2.74
86.07
2.56
51.71
1.53
45.69
1.07
0.12
0.41
42.08
57.40
B220+ gated
CD11b+ gated
FL1-H:: CD21
FL2-H:: CD23
FL2-H:: Siglec-F
FL4-H:: Ly6G
7.21
81.03
8.18
1.46
0.31
80.01
18.22
7.98
80.66
8.12
1.31
0.46
80.94
17.30

Figure 1:Normal lymphocyte and myeloid cell populations in M-TRAF3-/- mice.
TRAF3$^{flox/flox}$ littermate control (LMC) and M-TRAF3-/- mice analyzed were 8 to 12 weeks old. (A) Verification of TRAF3 deletion in BMDMs by Western blot analysis. Total cellular proteins were prepared from BMDMs derived from 3 pairs of LMC and M-TRAF3-/- mice. Proteins were immunoblotted for TRAF3, followed by TRAF2, TRAF1, TRAF6 and actin. (B) Representative FACS profiles of splenocytes prepared from LMC and M-TRAF3-/- mice. Cells were stained with fluorochrome-conjugated antibodies specific for B220, CD3, F4/80, CD68, CD21, and CD23, and then analyzed by a FACSCalibur. FACS profiles were scatter-gated on live cells. Similar results were observed in 4 additional experiments.

1.3.3 ALTERED CYTOKINE PRODUCTION IN TRAF3$^{-/-}$ BMDMS AND PEMS IN RESPONSE TO LPS STIMULATION

It was shown previously that LPS-induced type I IFN production is abolished but IL-12 production is enhanced in BMDMs derived from chimeric mice reconstituted with TRAF3$^{-/-}$ fetal liver cells [26,27]. We therefore analyzed LPS-induced cytokine production in BMDMs and PEMs derived from M-TRAF3$^{-/-}$ mice by RT-qPCR and ELISA. Consistent with published studies, we found that LPS-induced expression of *Ifnb* and *Ifna4* was almost abolished in BMDMs and PEMs derived from M-TRAF3$^{-/-}$ mice (Figure 2A and 2B). Interestingly, production of IL-12 was enhanced by TRAF3 deficiency at both the transcript and protein levels (Figure 2A-2D). In addition, although transcription of *Il6* was not changed (Figure 2A and 2B), secretion of IL-6 was significantly increased in TRAF3$^{-/-}$ BMDMs and PEMs (Figure 2C and 2D). In contrast, LPS-induced production of TNF-α in either cell population was not affected by TRAF3 deletion (Figure 2A-2D). Taken together, our results showed that in response to LPS stimulation, TRAF3-deficient macrophages exhibited alterations in expression of some cytokines but not others. These studies validated M-TRAF3$^{-/-}$ mice as a suitable model to explore the in *vivo* functions of myeloid cell TRAF3.

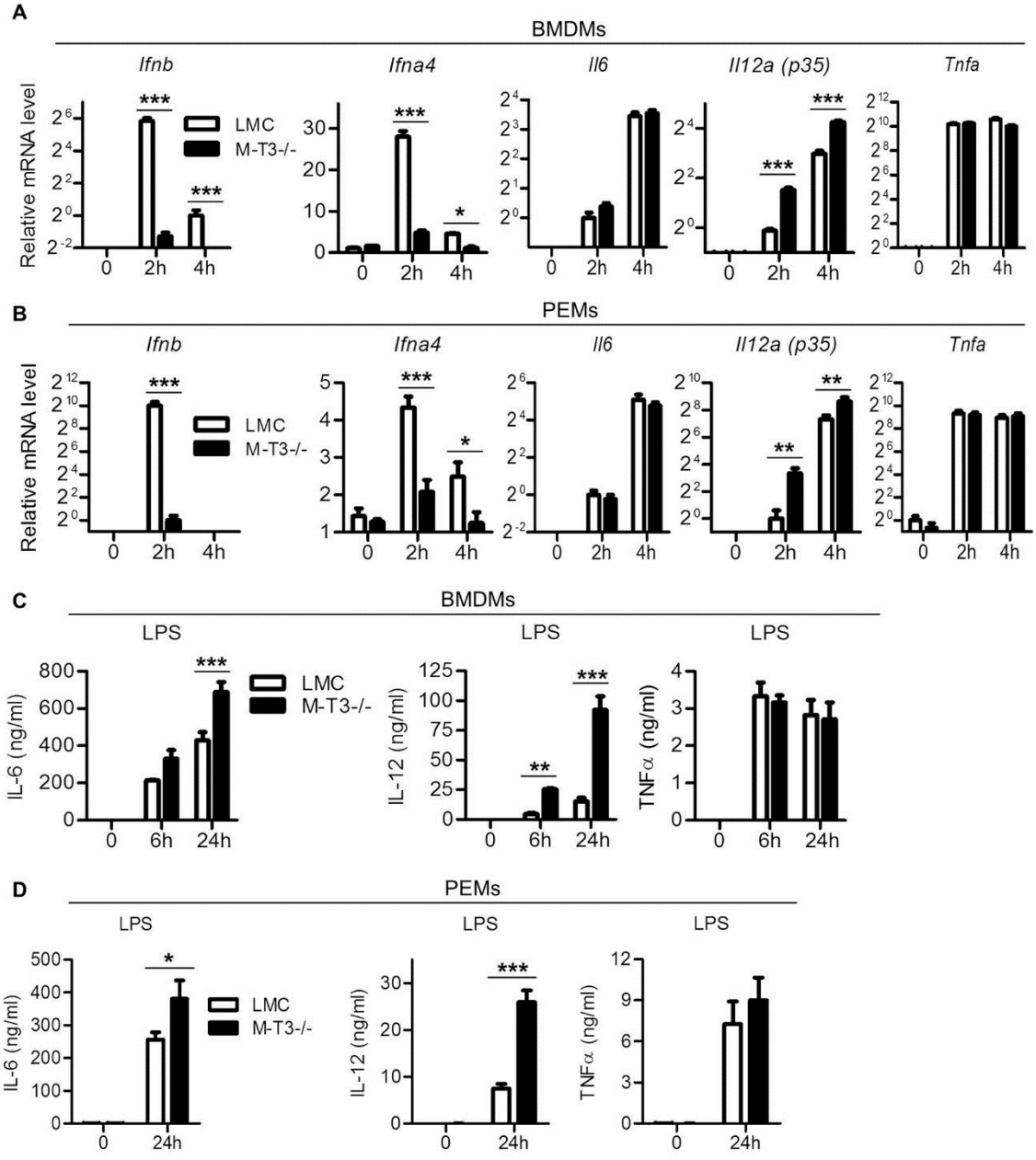
A
BMDMs
Ifnb
Ifna4
Il6
Il12a (p35)
Tnfa
Relative mRNA level
LMC
M-T3-/-
0
2h
4h
B
PEMs
C
BMDMs
LPS
IL-6 (ng/ml)
IL-12 (ng/ml)
TNFα (ng/ml)
0
6h
24h
D
PEMs

Figure 2: Impaired type I IFN but enhanced IL-6 and IL-12 production in TRAF3-/- macrophages in response to LPS stimulation.
(**A** and **B**) LPS-induced mRNA expression of cytokines in macrophages. BMDMs (A) or PEMs (B) derived from M-TRAF3$^{-/-}$ and LMC mice (7-10 week-old) were cultured in the absence or presence of 100 ng/ml of LPS for 2 or 4 hours. RNA was extracted, and real-time PCR was performed using TaqMan primers and probes specific for *Ifnb*, *Ifna4*, *Il6*, *Il12a (p35)*, and *Tnfa*. Each reaction also included the probe (VIC-labeled) and primers for *b-actin* mRNA, which served as an endogenous control. Relative mRNA expression levels of each cytokine were analyzed using the Sequence Detection Software (Applied Biosystems) and the comparative Ct method. Graphs depict the results of three independent experiments with duplicate reactions in each experiment (mean ± S.D.). (**C** and **D**) LPS-induced secretion of cytokines in macrophages. BMDMs (C) or PEMs (D) derived from M-TRAF3$^{-/-}$ and LMC mice (7-10 week-old) were cultured in the absence or presence of 100 ng/ml of LPS for indicated time periods. The levels of IL-6, IL-12 and TNFα in culture supernatants were analyzed by ELISA. Graphs depict the results of three independent experiments with duplicate samples in each experiment (mean ± S.D.). *, significantly different between LMC and M-TRAF3$^{-/-}$ (*t* test, $p < 0.05$); **, very significantly different between LMC and M-TRAF3$^{-/-}$ (*t* test, $p < 0.01$); ***, highly significantly different between LMC and M-TRAF3$^{-/-}$ (*t* test, $p < 0.001$).

1.3.4 ENHANCED PRO-INFLAMMATORY RESPONSES IN M-TRAF3$^{-/-}$ MICE CHALLENGED WITH LPS OR POLYI:C

Myeloid cells provide the first line of defense against bacterial and viral infections by producing type I IFN and pro-inflammatory cytokines. In light of our *in vitro* evidence for TRAF3 regulation of cytokine production in BMDMs and PEMs, we investigated the *in vivo* responses of M-TRAF3$^{-/-}$ mice inoculated with LPS or PolyI:C, which mimic aspects of bacterial and viral infections, respectively. We measured serum levels of IFN-β as well as pro-inflammatory and anti-inflammatory cytokines at different times after injection. Our results demonstrated that in response to LPS, serum levels of the pro-inflammatory cytokines TNFα and IL-1β were comparable in M-TRAF3$^{-/-}$ and LMC mice (Figure 3A). In contrast to the reduced *in vitro* inducibility of *Ifnb* observed in LPS-simulated BMDMs and PEMs of M-TRAF3$^{-/-}$ mice, serum levels of IFN-β were not decreased in M-TRAF3$^{-/-}$ mice inoculated with LPS or polyI:C (Figure 3A). The normal *in vivo* production of IFN-β may reflect the lack of TRAF3 deletion in pDCs, which are the

most potent producers of type I IFN following TLR ligation. Interestingly, levels of the pro-inflammatory cytokines IL-6 and IL-12 in sera of M-TRAF3$^{-/-}$ mice were elevated at 2 h, and IL-12 levels were also increased at 6 h post LPS injection (Figure 3A). Similarly, serum levels of IL-12 were also significantly elevated in M-TRAF3$^{-/-}$ mice at 2 h post injection with polyI:C (Figure 3B). In contrast, serum levels of the anti-inflammatory cytokine IL-10 were markedly decreased in M-TRAF3$^{-/-}$ mice compared to LMC mice at 2 and 6 h post LPS injection (Figure 3A). These results suggest that TRAF3 inactivation in myeloid cells alters cytokine production profiles to favor pro-inflammatory responses following *in vivo* challenges with LPS or polyI:C.

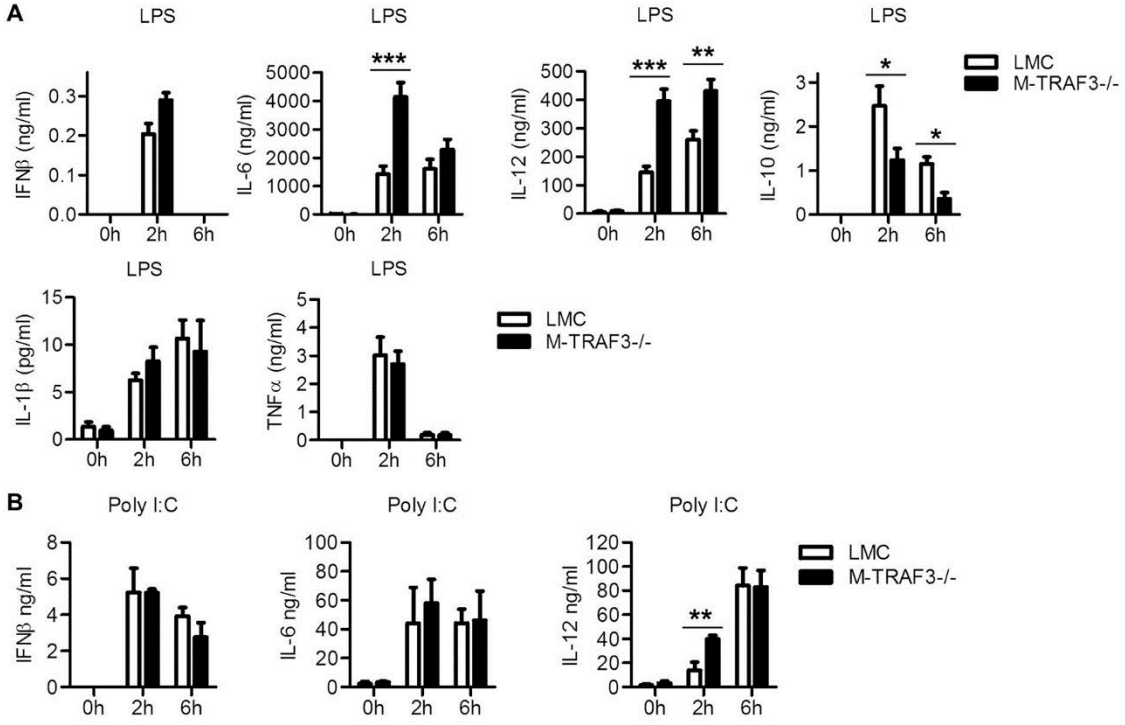

Figure 3: In vivo cytokine production in response to injection with LPS or polyI:C.
Gender and age-matched M-TRAF3$^{-/-}$ and LMC mice (8-12 week-old) were *i.p.* injected with LPS (300 μg LPS/20g body weight, n=9 for each group, **A**) or polyI:C (200 μg polyI:C/20g body weight, n=4 for each group, **B**), and sera were collected at 2 and 6 h post-injection. Serum levels of IFN-β, IL-6, IL-12, IL-10, IL-1β, and TNFα were measured by ELISA. *, significantly different between LMC and M-TRAF3$^{-/-}$ (*t* test, $p < 0.05$); **, very significantly different between LMC and M-TRAF3$^{-/-}$ (*t* test, $p < 0.01$); ***, highly significantly different between LMC and M-TRAF3$^{-/-}$ (*t* test, $p < 0.001$).

1.3.5 PROXIMAL SIGNALING EVENTS DOWNSTREAM OF LPS/TLR4 ENGAGEMENT IN TRAF3-DEFICIENT BMDMS AND NEUTROPHILS

To understand how TRAF3 deficiency affects LPS-induced cytokine production in myeloid cells, we investigated proximal signaling events following TLR4 engagement by LPS in TRAF3-deficient BMDMs and neutrophils. Purified thioglycollate-elicited neutrophils and BMDMs were stimulated with LPS, and total cellular proteins were prepared from both cell types at different time points. Phosphorylation of proximal signaling components of TLR4 including IRF3, p38, ERK, JNK, Akt, and IκBα were examined by immunoblot analyses. We found that LPS-induced phosphorylation of IRF3, the key transcription factor driving type I IFN expression, was markedly reduced in TRAF3$^{-/-}$ BMDMs (Figure 4A). We did not detect any induction of IRF3 phosphorylation by LPS in LMC or TRAF3$^{-/-}$ neutrophils (data not shown). We found that LPS-induced phosphorylation of p38, ERK, JNK, and Akt was normal in TRAF3$^{-/-}$ BMDMs and neutrophils (Figure 4A and 4B). Similarly, activation of the classical NF-κB1 pathway was not affected by TRAF3 deletion in either cell type as measured by phosphorylation and degradation of IκBα after stimulation with LPS (Figure 4A and 4B). We previously found that TRAF3 deficiency resulted in constitutive NF-κB2 activation in B cells, leading to prolonged B cell survival [12,14]. We therefore compared NF-κB2 processing in TRAF3$^{-/-}$ and LMC BMDMs and neutrophils. Interestingly, in the absence of stimulation, TRAF3-

deficient cells exhibited constitutive processing of NF-κB2 from the inactive precursor p100 to the active p52, which was as robust as that observed in LMC cells after stimulation with LPS (Figure 4A and 4B). However, in contrast to TRAF3-deficient B cells, constitutive NF-κB2 processing did not result in prolonged survival or decreased apoptosis in TRAF3$^{-/-}$ BMDMs or neutrophils (data not shown). Collectively, our findings indicate that TRAF3 deficiency leads to constitutive activation of NF-κB2 in both BMDMs and neutrophils, and specifically impairs LPS-induced activation of IRF3 in BMDMs, thereby modulating their cytokine production.

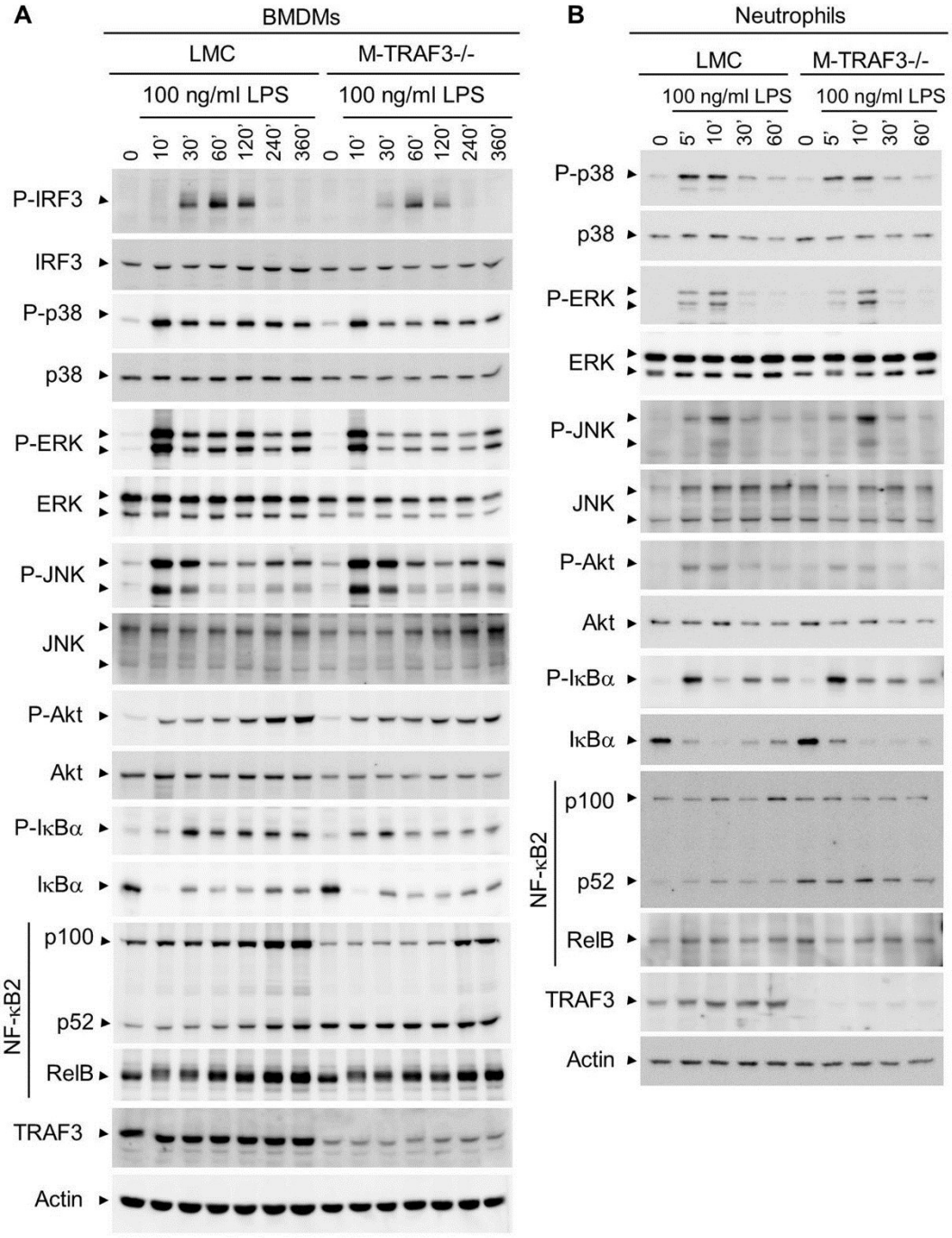

Figure 4: Altered signaling events in TRAF3-/- BMDMs and neutrophils in response to LPS stimulation.

BMDMs (**A**) or thioglycollate elicited peritoneal neutrophils (**B**) prepared from M-TRAF3$^{-/-}$ and LMC mice (8-12 week-old) were stimulated with 100 ng/ml of LPS for indicated time periods. Total protein lysates were prepared, and signaling events of TLR4 were analyzed by immunoblot analysis. Proteins were immunoblotted for phosphorylated (P-) or total IRF-3, p38, ERK, JNK, Akt, IκBα, followed by NF-κB2 (p100 and p52), RelB, TRAF3 and actin. Results shown are representative of 3 independent experiments.

1.3.6 ENHANCED TI AND TD IGG RESPONSES IN M-TRAF3$^{-/-}$ MICE

In addition to serving as primary players in innate immunity and inflammation, myeloid cells also play important roles in antigen presentation to activate adaptive immunity. We therefore measured basal Ig isotype levels in sera from 8-12 week old M-TRAF3$^{-/-}$ and LMC mice, and found that the levels of IgM, IgG1, IgG2b, IgG3, IgA and IgE were similar in both cohorts (Figure 5A). Following immunization with the TI Ag, TNP-Ficoll, M-TRAF3$^{-/-}$ mice tended to have slightly higher levels of all TNP-specific isotypes than LMC mice although only IgG3 differences were significant (Figure 5B). In contrast, following immunization with the TD Ag, TNP-KLH, only TNP-specific IgG2b levels were significantly increased in sera of M-TRAF3$^{-/-}$ as compared to LMC mice (Figure 5C). Collectively, these results indicate that while baseline levels of serum immunoglobulins were similar in M-TRAF3$^{-/-}$ and LMC mice, the responses to TI and TD antigens were altered in M-TRAF3$^{-/-}$ mice.

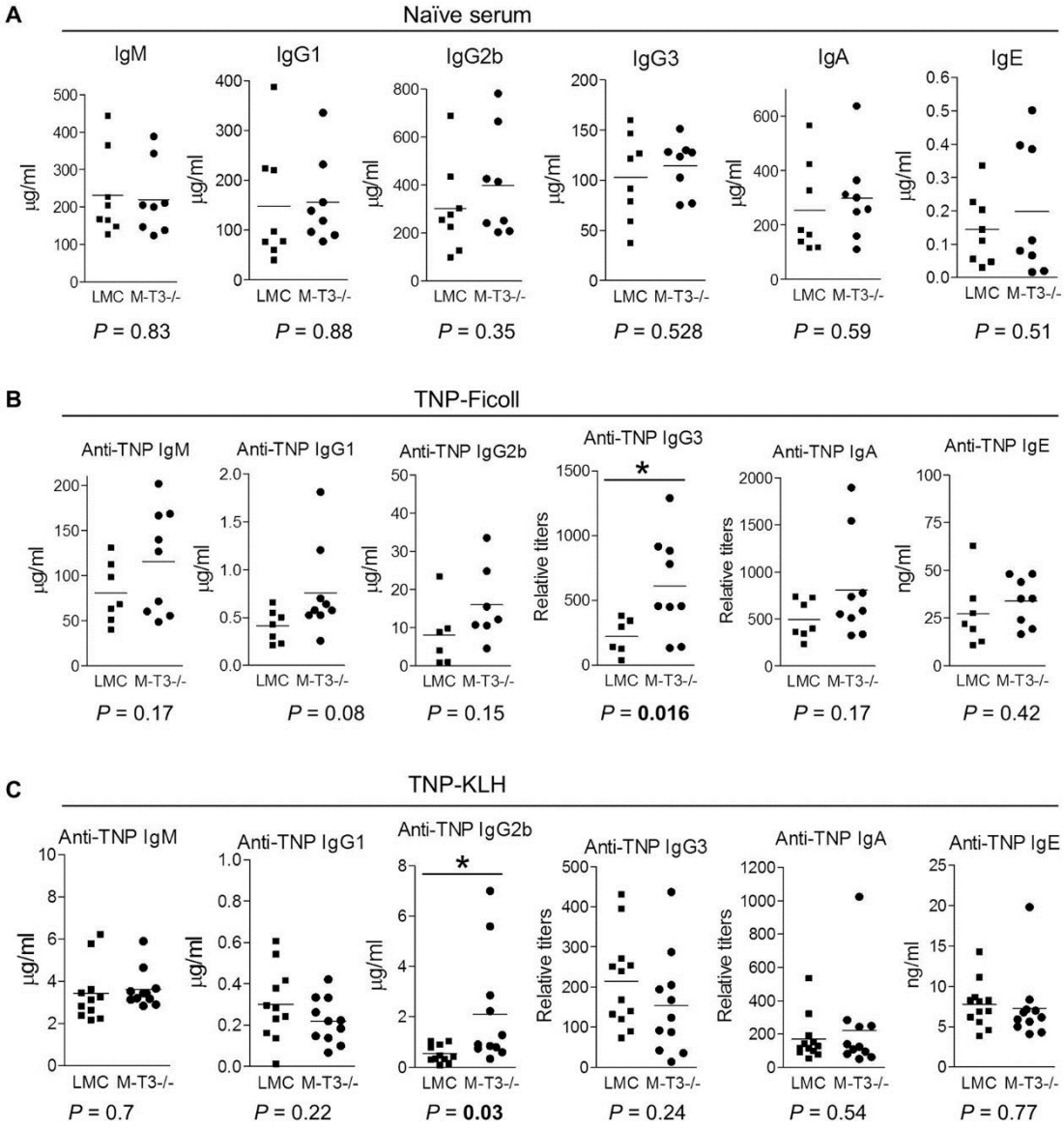

Figure 5: Altered antibody responses in M-TRAF3-/- mice.
LMC and M-TRAF3$^{-/-}$ mice analyzed were 8 to 12 weeks old. (**A**) Basal serum titers of Ig isotypes. Sera from naïve LMC and M-TRAF3$^{-/-}$ mice (n=8 for each group) were tested for IgM, IgG1, IgG2b, IgG3, IgA, and IgE levels by ELISA. (**B**) TI antibody responses. LMC and M-TRAF3$^{-/-}$ mice (n=9 for each group) were immunized with the TI Ag TNP-Ficoll, and sera were collected on day 7 after immunization. Serum titers of anti-TNP IgM, IgG1, IgG2b, IgG3, IgA, and IgE were analyzed by ELISA. (**C**) TD antibody responses. LMC and M-TRAF3$^{-/-}$ mice (n=12 for each group) were immunized with the TD Ag TNP-KLH in Alum. Sera were collected on day 7 after immunization. Serum titers of anti-TNP IgM, IgG1, IgG2b, IgG3, IgA, and IgE were measured by ELISA. Multiple serial dilutions of each serum sample were tested to ensure that the readout is within the linear range of the assay. *, significantly different from LMC (*t*-test, $P < 0.05$).

1.3.7 SPONTANEOUS INFLAMMATION, INFECTION, AND TUMOR DEVELOPMENT IN AGING M-TRAF3$^{-/-}$ MICE

In light of understandings that elevated pro-inflammatory cytokines contribute to inflammatory diseases, we hypothesized that M-TRAF3$^{-/-}$ mice should be predisposed to inflammation. We thus monitored the health of aging M-TRAF3$^{-/-}$ and LMC mice. We first noticed that beginning around 10 months of age, mortality of M-TRAF3$^{-/-}$ mice was greatly accelerated over that of LMC (Figure 6A). Histopathological studies were performed on 22 M-TRAF3$^{-/-}$ mice of 15-22 months old. We found that 15 out of the 22 (68.2%) mice displayed inflammation, infection, or tumors involving multiple organs, features that were not observed in age-matched LMC mice (Table II and Figure 6B). Twelve mice developed tumors, including two cases of histiocytic sarcomas (histiocytic neoplasms, tumors of a type of tissue-resident macrophages), one hepatocellular adenoma, and nine B cell lymphomas (Table II). Lymphomas observed in M-TRAF3$^{-/-}$ mice were diffuse large B cell lymphomas (DLBCLs) or follicular lymphomas (FLs). Six M-TRAF3$^{-/-}$ mice displayed inflammation involving multiple organs, including the liver, gastrointestinal tract (GI tract), lung, kidney, pancreas, and heart (Table II). Three M-TRAF3$^{-/-}$ mice had infections in the intestine/colon, liver, and lung (Table II). Notably, seven M-TRAF3$^{-/-}$ mice had internal hemorrhages and two had blistering (Table II). Interestingly, individual M-TRAF3$^{-/-}$ mice often had more than one type of pathology. Examples include B cell lymphoma and lung inflammation, pancreatitis and hepatocellular adenoma, bacterial infection and hemorrhagic liver. Together, our findings indicate that specific ablation of TRAF3 in myeloid cells contributed to spontaneous development of different types of tumors, inflammation, and infection.

Table II: Summary of histological observations of M-TRAF3-/- mice at the age of 15-22 months

Mice Examined ($N = 22$)	n	Organs Involved
Tumor		
Histiocytic sarcoma	2	Spleen, liver
Hepatocellular adenoma	1	Liver
B cell lymphoma (DLBCL or FL)	9	Spleen, cervical LNs, mesenteric LN, liver
Inflammation	6	Liver, GI tract, lung, kidney, pancreas, heart
Infection	3	GI tract, liver, lung
Unknown		
Hemorrhage	7	
Blister	2	
Normal	7	

Histologic diagnoses were made based on established criteria (23-28). Mice with DLBCL and FL were diagnosed histologically using criteria outlined in a consensus nomenclature of mouse lymphoid neoplasms (23). Malignancies of histiocytes (histiocytic sarcoma) were diagnosed histologically as described (24). Inflammation was diagnosed histologically using criteria of myeloid cell/lymphocyte infiltration in tissues as described (25). Cases diagnosed with inflammatory conditions exhibited expansions of immature myeloid cells, monocytes and granulocytes in tissues outside the bone marrow and often in spleen or liver. Infections were diagnosed with evidence for bacterial or parasitic infection in different tissues, including visualization of bacteria and entamoeba as described (26-28). Individual mice could have more than one type of pathology. Examples include B cell lymphoma and lung inflammation, pancreatitis and hepatocellular adenoma, bacterial infection and hemorrhagic liver.

1.3.8 HISTOPATHOLOGIC FEATURES OF M-TRAF3$^{-/-}$ MICE WITH SPONTANEOUS INFLAMMATION, INFECTION OR TUMOR DEVELOPMENT

Histologically, affected spleens of M-TRAF3$^{-/-}$ mice with spontaneous inflammation, infection or tumor development were most often characterized by a near complete loss of normal architecture (Figure 6C). In mice with histiocytic sarcomas, tumor cells were identified as the major cell type in the spleen, and nodal areas of pure histiocytosis were also observed in the liver (Figure 6C). In the mouse with hepatocellular adenoma, the liver was massively occupied by liver cancer cells in association with large cytoplasmic vacuoles (Figure 7). In mice with DLBCL, lymphoma cells were responsible for marked expansion of the splenic white pulp and infiltration of the liver (Figure 6C). In mice with inflammation, the majority of splenic lymphocytes were replaced with myeloid

cells, and granulocyte infiltration was observed in multiple organs, including the liver, intestine, lung, and pancreas (Figure 8 and data not shown). In addition, glomerular damage was observed in the kidneys of mice with inflammation (Figure 8). In mice with infection and inflammation, the splenic architecture was also disrupted by myeloid cells, and the liver contained clustered inflammatory cells, including histiocytes and necrotic areas (Figure 6C). We observed two cases of bacterial abscesses (Figure 6B), in which bacteria were clearly identified in micrographs (Figure 9a and 9b). Interestingly, we also detected one case of infection by *Entamoeba muris*, a strain of commensal protozoan parasite, in cecum (Figure 9c). Taken together, the splenic red pulp and white pulp were disrupted in mice with histiocytic sarcoma, DLBCL, inflammation, or infection, and other affected organs also exhibited infiltration with tumor or myeloid cells.

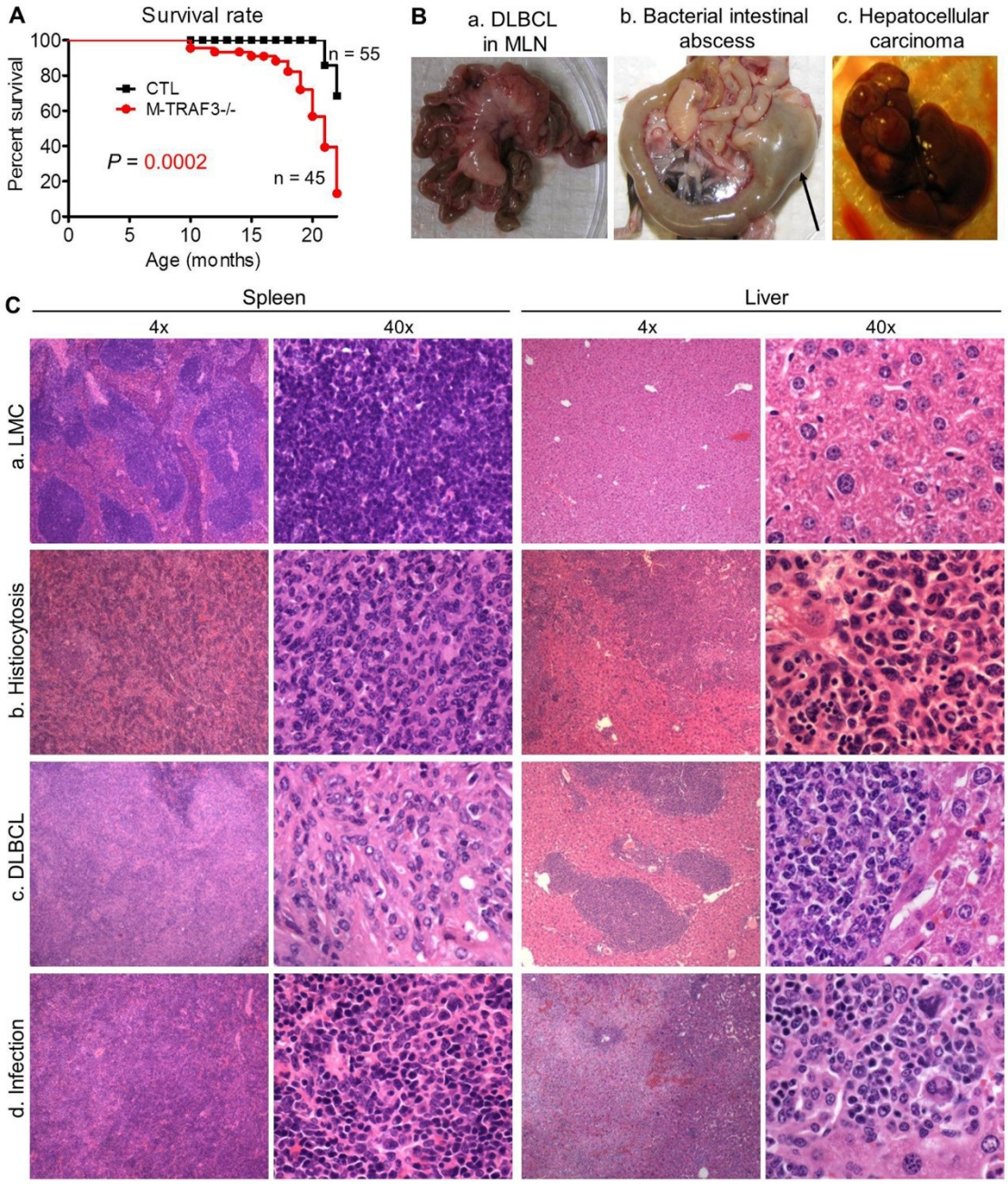
A
Survival rate
Percent survival
100
80
60
40
20
0
0
5
10
15
20
Age (months)
CTL
M-TRAF3-/-
P = 0.0002
n = 55
n = 45
B
a. DLBCL in MLN
b. Bacterial intestinal abscess
c. Hepatocellular carcinoma
C
Spleen
Liver
4x
40x
4x
40x
a. LMC
b. Histiocytosis
c. DLBCL
d. Infection

Figure 6: Gross and histopathological features of M-TRAF3-/- mice with spontaneous tumor, inflammation or infection.

(**A**) Accelerated mortality of M-TRAF3$^{-/-}$ mice. Survival curves of LMC and M-TRAF3$^{-/-}$ mice were generated using the Kaplan-Meier method. $P<0.001$ as determined by the Mantel-Cox log-rank test. (**B**) Representative images of affected organs in diseased M-TRAF3$^{-/-}$ mice. **a**, Massively enlarged mesenteric lymph node (MLN) in a mouse with DLBCL (mouse ID: 237-2). **b**, GI tract and MLN of a mouse with bacterial infection and inflammation (mouse ID: 228-5). Arrow indicates the large bacterial intestinal abscess. **c**, Liver of a mouse with hepatocellular adenoma (mouse ID: 237-4). (**C**) Representative micrographs of the spleen and liver of diseased M-TRAF3$^{-/-}$ mice. Sections of the spleen and liver were stained with hematoxylin and eosin, and representative micrographs of LMC and M-TRAF3$^{-/-}$ mice are shown for comparison. **a**, Normal tissues from a LMC mouse. **b**, Mouse (ID: 237-5) with extensive histiocytosis and increased erythroid activity in the spleen and areas of pure histiocytosis in the liver. **c**, Mouse (ID: 233-5) with DLBCL showing marked enlargement of the splenic white pulp by tumor cells and large perivascular infiltrates with tumor cells in the liver. **d**, Mouse (ID: 274-12) with infection showing inflammation and necrotic areas in the liver and marked red pulp hyperplasia of myeloid and erythroid elements in the spleen.

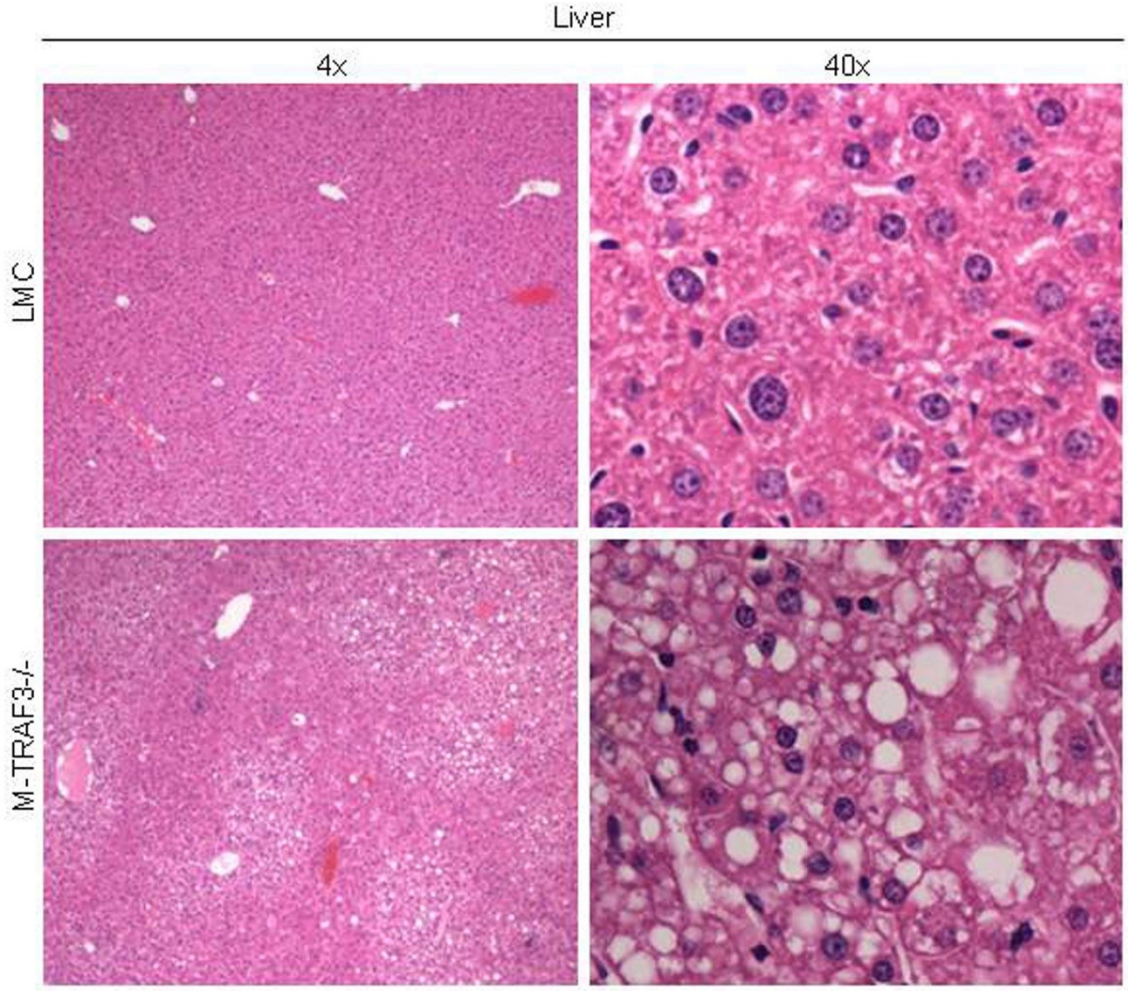

Figure 7: Hepatocellular adenoma observed in one M-TRAF3-/- mouse.
Sections of the liver were stained with hematoxylin and eosin, and representative micrographs of LMC (normal liver) and the M-TRAF3-/- mouse with hepatocellular adenoma are shown.

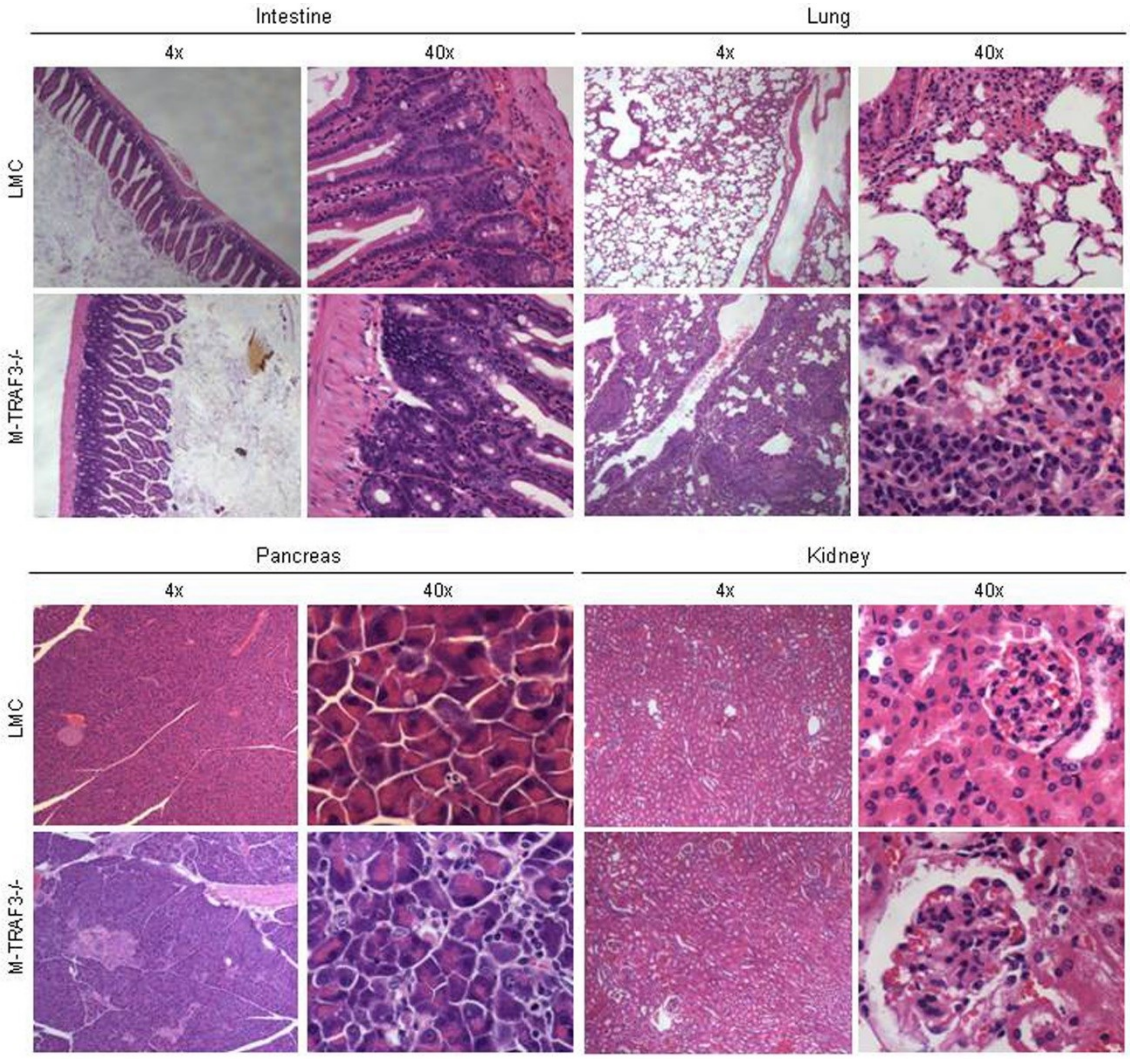

Figure 8: Spontaneous development of inflammation in M-TRAF3-/- mice at the age of 15 – 22 months.
Sections of the intestine, lung, pancreas, and kidney were stained with hematoxylin and eosin, and representative micrographs of LMC (normal tissues) and diseased M-TRAF3-/- mice are shown for comparison.

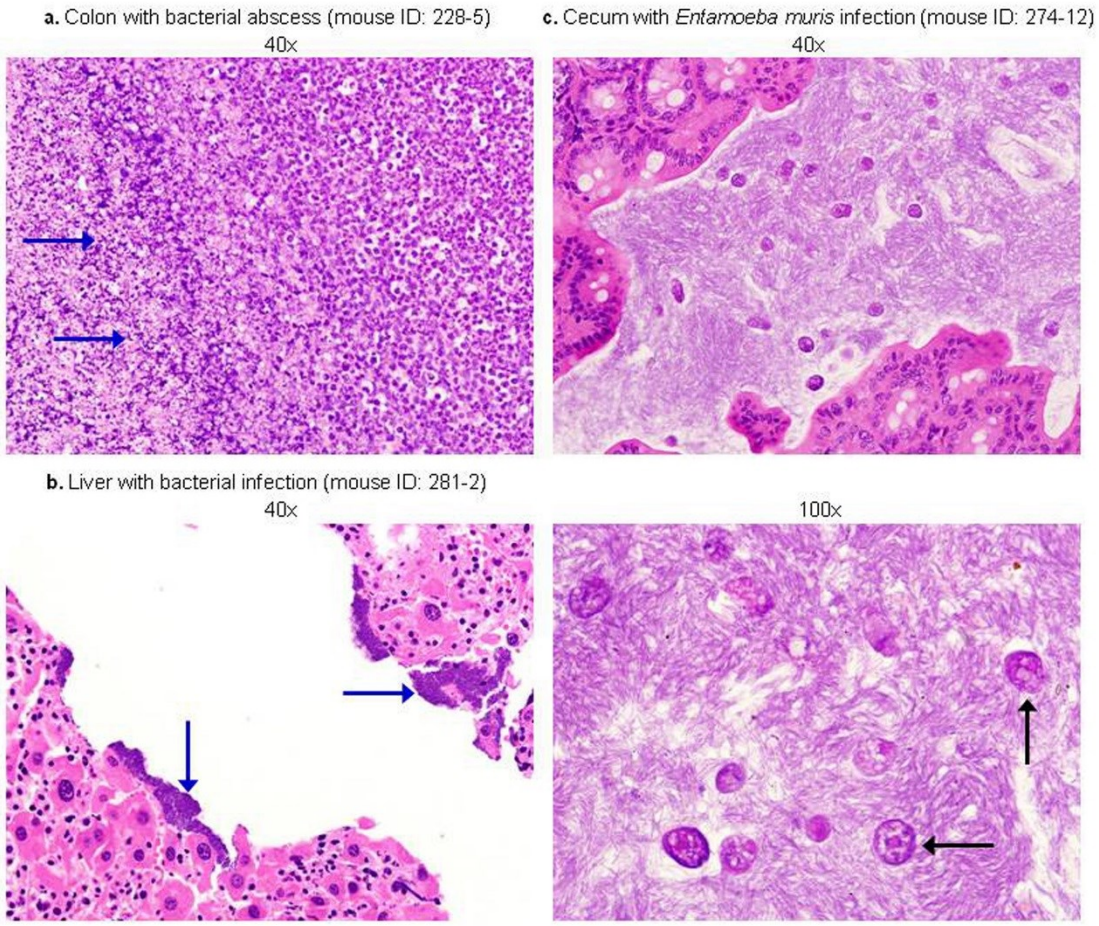

Figure 9: Spontaneous development of bacterial and parasitic infections in M-TRAF3-/- mice at the age of 15 – 22 months.
Sections of the colon, liver, and cecum were stained with hematoxylin and eosin, and representative micrographs of M-TRAF3$^{-/-}$ mice with infections are shown. Numerous bacteria (left panel) and *Entamoeba muris* (right panel) were clearly identified in the micrographs. Blue arrows indicate representative bacteria, and black arrows indicate representative *Entamoeba muris*.

1.3.8 FLOW CYTOMETRY REVEALS DRASTICALLY ALTERED LYMPHOCYTE AND MYELOID CELL POPULATIONS IN M-TRAF3$^{-/-}$ MICE WITH SPONTANEOUS INFLAMMATION, INFECTION OR TUMORS

To detect potential alterations of lymphocyte and myeloid cell populations underlying the above disease conditions, we performed immunophenotypic analyses using flow cytometry. In sharp contrast to the normal spleen size observed in young 8-12 week old M-TRAF3$^{-/-}$ mice or old LMC mice, diseased M-TRAF3$^{-/-}$ mice had greatly enlarged spleens as evidenced by significantly increased spleen weights (Figure 10A). Similarly, the splenic cell populations in M-TRAF3$^{-/-}$ mice with spontaneous inflammation, infection or tumor development were altered with increased populations of B220-CD3-CD11b$^{+/low}$Gr-1$^{+/low}$ myeloid cells (Figure 10B). Consistent with the histological diagnoses, the frequencies of normal B and T cells observed in LMC mice were often diminished in diseased M-TRAF3$^{-/-}$ mice. In mice with histiocytic sarcomas, splenic lymphocytes were mainly replaced by histiocytic tumor cells (B220-CD3-CD11b^{low}Gr-1^{low}) (Figure 10B). In mice with inflammation, most lymphocytes were replaced with a major population of Gr-1+CD11b+ myeloid cells in the spleen (Figure 10B). In mice with infections, splenic lymphocytes were also replaced with CD11b+Gr-1+ myeloid cells or B220-CD3-CD11b^{low}Gr-1^{low} histiocytes (Figure 10B). In summary, common features of altered cell populations observed in spleens of different individual M-TRAF3$^{-/-}$ mice with spontaneous inflammation, infection or tumor development include increased percentages of CD11b+Gr-1+ myeloid cells and decreased percentages of CD3+B220- T lymphocytes (Figure 10C). In mice with DLBCL, splenic B lymphoma cells were B220^{+}CD21^{-}CD23^{-} (Figure 10D). These results suggest that TRAF3 deficiency in myeloid cells promotes

inflammation but also greatly compromises the ability of mice to resist infections or control development of hematopoietic and solid tumors.

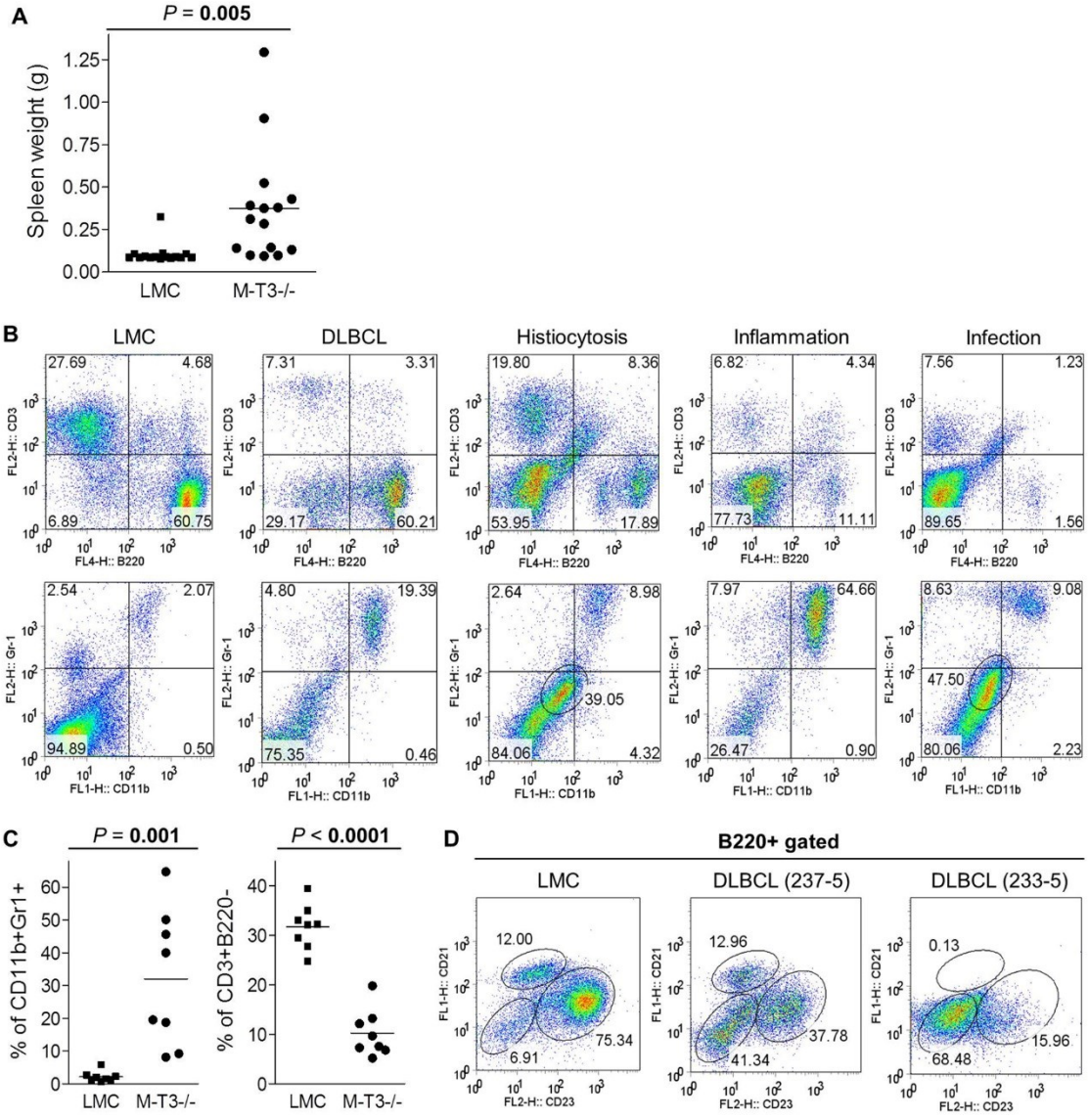

Figure 10: Abnormal lymphocyte and myeloid cell populations in the spleen of diseased M-TRAF3-/- mice.

(**A**) Enlarged spleens of M-TRAF3$^{-/-}$ mice (age: 15-22 month-old). The graph depicts spleen weights of age-matched LMC and M-TRAF3$^{-/-}$ mice (n=15 for each group of mice). (**B**) Representative FACS profiles of splenocytes of age-matched LMC and diseased M-TRAF3$^{-/-}$ mice. Splenocytes were stained with fluorochrome-conjugated B220, CD3, CD11b, Gr-1, CD21 and CD23 Abs, and then analyzed by a FACSCalibur. FACS profiles were scatter-gated on live cells. Gated cell populations include: B cells, B220+CD3-; T cells, CD3+B220-; myeloid cells, CD11b+Gr-1+; a distinct population of histiocytes (gated with a circle in the 3rd and 5th panel): CD11b^{low}Gr-1^{low}. M-TRAF3$^{-/-}$ mice shown include: 237-2, DLBCL; 237-5, histiocytosis; 237-1, inflammation; 274-12, infection and inflammation. FACS profiles shown are representative of 2 cases of DLBCL, 2 cases of histiocytosis, 2 cases of inflammation, and 2 cases of infection, respectively. (**C**) Increased percentage of CD11b+Gr-1+ myeloid cells and decreased percentage of CD3+B220- T cells in diseased M-TRAF3$^{-/-}$ mice. The graphs depict the percentages of CD11b+Gr-1+ myeloid cells or CD3+B220- T cells of age-matched LMC and diseased M-TRAF3$^{-/-}$ mice (n=8 for each group of mice) analyzed by FACS. *P* values (*t*-test) between LMC and M-TRAF3$^{-/-}$ mice are shown. (**D**) Representative FACS profiles of B220+ splenic B cells of M-TRAF3$^{-/-}$ mice with DLBCL. Follicular (FO) B cells are identified as B220+CD21^{Int}CD23+, and marginal zone (MZ) B cells are identified as B220+CD21+CD23^{Int}. The small population (6.91%) of B220+CD21-CD23- observed in LMC are immature and activated B cells, and the major population (41.34% in mouse ID 237-5 and 68.48% in mouse ID 233-5) of B220+CD21-CD23- observed in M-TRAF3$^{-/-}$ mice are predominantly DLBCL cells.

1.3.9 ABERRANT PRODUCTION OF CYTOKINES AND CHEMOKINES IN DISEASED M-TRAF3-/- MICE

To gain deeper understandings of diseased M-TRAF3$^{-/-}$ mice, we measured the serum levels of 40 cytokines and chemokines using a Mouse Cytokine Array assay kit. Our results demonstrated that M-TRAF3$^{-/-}$ mice with spontaneous tumor development or inflammation/infection exhibited strikingly elevated serum levels of a number of chemokines and cytokines, including CXCL-13, G-CSF, CCL1, IL-16, IL-17, IP-10, MCP-1, MCP-5, CXCL9, TIMP-1, and TREM-1 (Figure 11). Among these, G-CSF stimulates the bone marrow to produce granulocytes and release them into the blood stream, and also promotes the survival, proliferation, differentiation, and function of neutrophil precursors and mature neutrophils [59,60]. IL-17 is potent in inducing and mediating pro-inflammatory responses [61]. Four chemokines, including CCL1, MCP-1 (CCL2), MCP-5 (CCL12), and IP-10 (CXCL10), all act as chemoattractants to recruit monocytes/macrophages, dendritic cells, and lymphocytes to the sites of inflammation [62-68]. Interestingly, TREM-1, a triggering receptor expressed on myeloid cells, plays a role in promoting inflammatory responses mediated by monocytes/macrophages and neutrophils [69,70]. These cytokines and chemokines are also implicated in the pathogenesis of various inflammatory diseases and tumor development (26-37), consistent with the phenotypes observed in our M-TRAF3$^{-/-}$ mice. Thus, aberrantly elevated serum levels of these cytokines and chemokines suggest that dysregulation of myeloid cells actively contributes to the pathogenesis of spontaneous inflammation, infection and tumor development observed in aging M-TRAF3$^{-/-}$ mice.

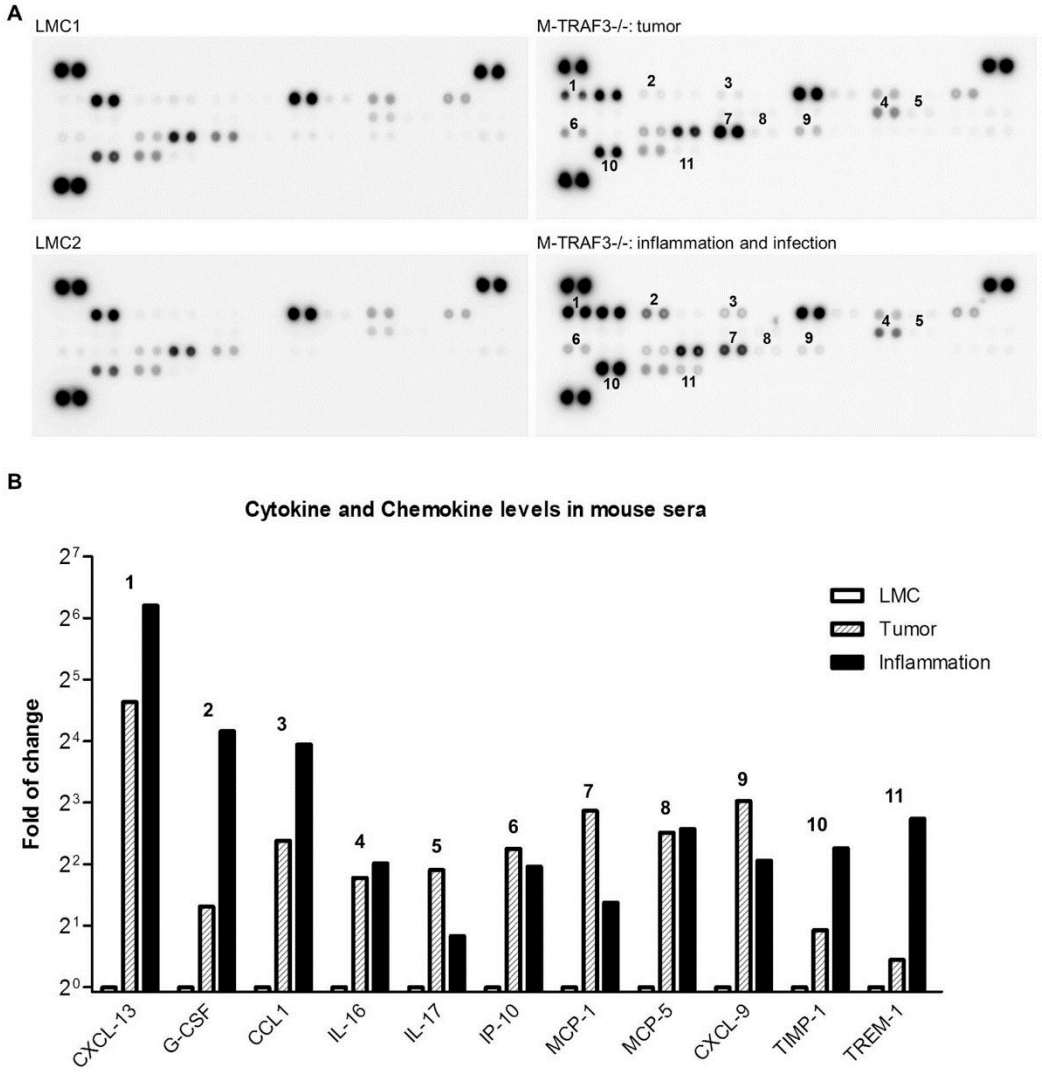

Figure 11:Aberrant serum cytokine and chemokine levels of diseased M-TRAF3-/- mice.
(**A**) Cytokine and chemokine protein array blots of age-matched LMC and diseased M-TRAF3$^{-/-}$ mice. Cytokines and chemokines in mouse sera were detected using the Mouse Cytokine Array Assay kit (R&D) following the manufacturer's protocol. In each blot, combined sera of three mice (70 µl serum of each mouse) were used for the cytokine array assay. Sera of M-TRAF3$^{-/-}$ mice with tumor examined include 237-5 (histiocytosis), 228-7 (DLBCL), and 274-11 (FL). Sera of M-TRAF3$^{-/-}$ mice with inflammation and infection examined include 228-5, 237-1, and 274-12. (**B**) Quantification of cytokine and chemokine levels of diseased M-TRAF3$^{-/-}$ mice measured by the cytokine protein array analyses. Each cytokine or chemokine spots on the blots in (A) were quantitated using a low-light imaging system, and the results presented graphically. The amount of each cytokine or chemokine in diseased M-TRAF3$^{-/-}$ mice (tumor or inflammation) was relative to the mean of the intensity of corresponding LMC1 and LMC2 spots. Each cytokine or chemokine has duplicate detection spots. The graph depicts the fold change (M-TRAF3$^{-/-}$/LMC) of each cytokine or chemokine (mean). Bold numeric labels indicate the spots that are strikingly different between M-TRAF3$^{-/-}$ mice with tumor or inflammation/infection and LMC in (A) and the corresponding cytokine/chemokine quantitation data in (B).

1.4 DISCUSSION AND CONCLUSIONS

In the present study, we generated and characterized M-TRAF3$^{-/-}$ mice to investigate the *in vivo* functions of TRAF3 in myeloid cells, central players in innate immunity and inflammation. Our results showed that 8-12 weeks old M-TRAF3$^{-/-}$ mice had normal lymphocyte and myeloid cell populations in various hematopoietic compartments, demonstrating that LysM-Cre-mediated TRAF3 ablation neither affects the development nor alters the homeostasis of myeloid cells in young adult mice. However, in response to challenge with LPS (a bacterial mimic) or polyI:C (a viral mimic), M-TRAF3$^{-/-}$ mice exhibited an altered profile of cytokine production. Following immunization, M-TRAF3$^{-/-}$ mice displayed elevated T-independent IgG3 as well as T-dependent IgG2b responses. Interestingly, 15-22 months old M-TRAF3$^{-/-}$ mice spontaneously developed chronic inflammation or tumors with some cases showing two pathologic conditions affecting multiple organs. Together, our findings indicate that myeloid cell TRAF3 regulates immune responses and is required for inhibiting inflammation and tumor development in mice.

It has been shown that TRAF3 regulates the homeostasis of multiple cell types through different mechanisms. Specific deletion of TRAF3 from B cells leads to vastly prolonged survival of mature B cells due to constitutive activation of the NIK-NF-κB2 pathway [12,13]. Although ablation of TRAF3 from T cells does not affect the homeostasis of CD4 or CD8 T cells [13,16], the frequency and number of regulatory T cells (Treg) are increased in T-TRAF3$^{-/-}$ mice and Treg-specific TRAF3$^{-/-}$ mice [16,20]. TRAF3 promotes IL-15-mediated survival and proliferation in invariant natural killer T cells [18]. TRAF3 also regulates the development of medullary thymic epithelial cells by affecting the LTβR-NF-

κB2 and CD40-NF-κB2 pathways [71]. In osteoclast precursor cells, TRAF3 inhibits osteoclast formation by suppressing RANK-NF-κB2 signaling [72]. In the present study, we also observed constitutive NF-κB2 activation in TRAF3-deficient macrophages and neutrophils. Interestingly, although the homeostasis of macrophages and neutrophils was normal in young adult M-TRAF3$^{-/-}$ mice, we detected malignant histiocytosis and frequent expansion of CD11b+Gr-1+ myeloid cells in aged M-TRAF3$^{-/-}$ mice. It would thus be interesting to investigate whether and how TRAF3 regulates the survival and/or proliferation of histiocytes and CD11b+Gr-1+ myeloid cells. We speculate that TRAF3 deficiency may gradually lead to prolonged survival or increased proliferation of CD11b+Gr-1+ myeloid cells, causing chronic inflammation in M-TRAF3$^{-/-}$ mice. However, increasing evidence indicates that both inflammation and tumors stimulate the expansion of CD11b+Gr-1+ myeloid-derived suppressor cells (MDSC) [73-76]. Therefore, it remains possible that the increased population of CD11b+Gr-1+ cells observed in our study consists mostly of expanded MDSC as a consequence of spontaneous inflammation and tumor development.

The importance of TRAF3 in innate immunity is highlighted by the evidence that a variety of viral and bacterial proteins target TRAF3 for inactivation. These include Lb(pro) of foot-and-mouth disease virus, X protein (HBx) of hepatitis B virus, UL36 of herpes simplex virus 1 (HSV-1), YopJ of the Gram- bacterium Yersinia pestis, Tat protein of HIV-1, Gn protein of NY-1 hantavirus, and M protein of severe acute respiratory syndrome coronavirus [10]. All these pathogen proteins target TRAF3 and thus inhibit IRF3 phosphorylation and type I IFN production [10]. Consistent with these findings, TRAF3 mediates type I IFN production and viral resistance in BMDMs, DCs, and TLR2-

reprogrammed macrophages [26,27,37,77,78]. In the present study, we verified previous observations that LPS-induced IRF3 phosphorylation and type I IFN production are impaired in TRAF3$^{-/-}$ BMDMs, and extended these findings to PEMs. Paradoxically, *in vivo* IFN-β production was not affected in young adult M-TRAF3$^{-/-}$ mice injected with LPS or polyI:C, which is likely due to compensation by TRAF3-sufficient plasmacytoid DCs, the most potent producers of type I IFN. Regardless of this, innate immunity is evidently altered by TRAF3 deletion in myeloid cells, as demonstrated by the spontaneous development of inflammation and infection in M-TRAF3$^{-/-}$ mice older than 15 months. Bacterial or entamoeba infections observed in aged M-TRAF3$^{-/-}$ mice are most likely caused by opportunistic strains of commensal microbiota (termed "pathobionts") [79-81], which may trigger TRAF3-dependent signaling pathways via TLRs or NLRs in macrophages, neutrophils and DCs. For example, lipopeptidophosphoglycan of entamoeba has been shown to induce signaling through TLR2 and TLR4, while DNA of entamoeba triggers signaling via TLR9 in macrophages [82]. Similarly, muramyl dipeptide and *meso*-diaminopimelic acid of commensal bacteria stimulate signaling through NOD1 and NOD2, respectively [83,84]. Defective type I IFN production in TRAF3$^{-/-}$ myeloid cells in response to TLR or NLR signaling may occasionally allow colonization of commensal bacteria or entamoeba following opportunistic penetration of protective mucosal and epithelial barriers in the gut. Thus, TRAF3 appears to be required for the proper control of commensal microbiota-triggered innate immune responses and inflammation in myeloid cells.

Myeloid cells not only mediate innate immunity and inflammation, but also act as antigen-presenting cells in adaptive immunity. Here we found that a TI Ag stimulated

increased IgG3 response while a TD Ag induced increased IgG2b response in M-TRAF3$^{-/-}$ mice, which may result from elevated levels of pro-inflammatory cytokines in myeloid cells. It has been previously shown that IL-12 enhances TI IgG3 responses [85]. IL-6 selectively promotes IgG2b production in germinal center (GC) B cells, and TD IgG2b responses are selectively impaired in IL-6$^{-/-}$ mice [86,87]. Additionally, IL-6 induces the differentiation, expansion, and maintenance of T follicular helper (T_{FH}) cells by inducing Bcl6 expression [88-90]. Decreased T_{FH} cell number has been shown to correlate with decreased TD IgG2b response [91]. Therefore, elevated levels of IL-12 and IL-6 likely mediate increased TI IgG3 and TD IgG2b responses, respectively. We previously reported that specific deletion of TRAF3 in B cells leads to hypergammaglobulinemia, increased IgM and IgG responses after immunization with a TI Ag, but normal IgG1 responses to a TD Ag [12]. In contrast, specific deletion of TRAF3 in T cells causes defective IgG1 responses to a TD Ag due to impaired CD4 helper T cell activation [16]. Interestingly, specific ablation of TRAF3 in Treg cells results in moderately enhanced IgG2b responses to a TI Ag and markedly increased IgG1 and IgG2b responses to a TD Ag, due to decreased induction of follicular regulatory CD4 T cells (T_{FR}) after immunization [20]. Therefore, TRAF3 deficiency in different immune cell types modulates antibody responses in distinct manners.

One particularly interesting finding of our study is spontaneous tumor development in older M-TRAF3$^{-/-}$ mice. Notably, malignant transformation was not only detected in TRAF3-deficient histiocytes, a type of tissue-resident macrophages, but was also observed in other cell types that are TRAF3-sufficient, including B cells and hepatocytes. In contrast, tumor development is limited to TRAF3-deficient B cells but is not observed in other

TRAF3-sufficient cell types in B-TRAF3$^{-/-}$ mice [14]. This suggests that TRAF3 signaling pathways in myeloid cells may contribute to tumor surveillance. In this regard, B cells are especially susceptible to genetic alterations due to the unique features of B cell formation and development, which includes V(D)J recombination, somatic hypermutation (SHM) and class switch recombination (CSR) of Ig genes. All of these processes produce double strand DNA breaks (DSBs), which increase the risk of genomic instability in B cells [92-94]. Indeed, unlike MZLs and B1 lymphomas observed in B-TRAF3$^{-/-}$ mice that do not involve SHM or CSR [14], the DLBCLs and FLs identified in M-TRAF3$^{-/-}$ mice originate from germinal center (GC) or post-GC B cells, which are undergoing or have gone through GC related events, including SHM and CSR. B cells that have acquired oncogenic alterations during GC passage may escape the compromised tumor surveillance and develop into malignant lymphomas in M-TRAF3$^{-/-}$ mice. Alternatively, the chronic inflammatory environment of M-TRAF3$^{-/-}$ mice, a strong risk factor for cancer, may induce mutations that facilitate malignant transformation of TRAF3-sufficient cells (e.g., hepatocytes and B cells), stimulate tumor growth, and promote angiogenesis to accelerate tumor progression, invasion, and metastasis [95-98]. Consistent with this notion, we did detect strikingly elevated levels of 11 cytokines and chemokines in M-TRAF3$^{-/-}$ mice with tumors. Furthermore, chronic inflammation may induce the generation and expansion of CD11b+Gr-1+ MDSC, which in turn suppress the anti-tumor immune responses mounted by natural killer (NK) cells and CD8 cytotoxic T cells [73-76]. MDSC can also recruit and activate Treg cells to further inhibit anti-tumor responses [73-76]. Taken together, the above evidence suggests that TRAF3 is a tumor suppressor gene not only in B cells but also in myeloid cells.

Considering that TRAF3 is employed in signaling by many immune receptors [10,24], it will be especially interesting to further decode the signaling pathways that lead to spontaneous inflammation and tumor development in M-TRAF3$^{-/-}$ mice. In the absence of infection with pathogens, TLRs and NLRs can be activated by commensal micro-organisms or danger-associated molecular patterns (DAMPs) derived from injured body cells or necrotic cancer cells [83,84,99-101]. TRAF3 regulates signaling of TLRs through direct interaction with two key adaptor proteins MyD88 and TRIF. Similarly, TRAF3 participates in NOD1 and NOD2 signaling via direct binding to the adaptor protein RIP2 [10,24]. Defective type I IFN production in TRAF3$^{-/-}$ myeloid cells in response to TLR-MyD88, TLR-TRIF, or NOD1-RIP2 signaling may result in compromised tumor surveillance or anti-tumor immunity [10,24,100,102]. Meanwhile, enhanced production of pro-inflammatory cytokines in TRAF3$^{-/-}$ myeloid cells mediated by TLR-MyD88 or NOD1/2-RIP2 signaling may exacerbate inflammation [10,24,102,103]. Of particular interest, TRAF3 also directly interacts with NLRP12, which inhibits NF-κB2 activation and inflammation [104]. Additionally, TRAF3 is a negative regulator of LT-βR signaling [10], which inhibits inflammatory responses by inducing cross-tolerance to TLR4 and TLR9 activation in macrophages [105]. Relevant to our mouse model, myeloid cell-specific deletion of MyD88 rescues the spontaneous colitis observed in IL-10$^{-/-}$ mice [106], and TLR4$^{-/-}$, NOD1$^{-/-}$, NOD2$^{-/-}$, RIP2$^{-/-}$, or NLRP12$^{-/-}$ mice are all more susceptible to colitis and colorectal cancer development when subjected to AOM-DSS treatment [102,104,107]. Thus, breeding of M-TRAF3$^{-/-}$ mice with conditional knockout mice of MyD88, TRIF, RIP2, or NF-κB2 will help to delineate the involvement of specific signaling pathways in the disease pathogenesis.

Findings obtained from different TRAF3-deficient mouse models generated in multiple laboratories strongly indicate that aberrant functions of TRAF3 may contribute to the pathogenesis of a variety of diseases, and have sparked interest in investigating *Traf3* genetic alterations in human patients. Published reports have mainly focused on *Traf3* mutations in B cell malignancies. Indeed, somatic biallelic deletions and inactivating mutations of *Traf3* have been documented in a variety of human B cell neoplasms, including multiple myeloma, MZL, B cell chronic lymphocytic leukemia, mantle cell lymphoma, Waldenström's macroglobulinemia and Hodgkin lymphoma [108-114]. To date, only one case of a heterozygous *Traf3* autosomal dominant mutation has been reported in a young adult with a history of herpes simplex virus-1 encephalitis in childhood, due to impaired TLR3-induced type I IFN production [115]. Interestingly, expression of TRAF3 is significantly decreased in peripheral blood mononuclear cells of patients chronically infected with hepatitis B virus as compared to healthy controls [116]. In the present study, we demonstrated that TRAF3 deletion leads to spontaneous inflammation and tumor development in mice. Future studies thus need to be directed at systematically determining the existence and frequency of somatic deletions, mutations, single nucleotide polymorphisms, or decreased expression of *traf3* in myeloid cells in human patients with chronic inflammation and tumors, including hepatitis, inflammatory bowel diseases, pneumonia, histiocytic sarcoma, DLBCL, and hepatocellular adenoma.

CHAPTER 2: INVESTIGATING THE ROLE OF TRAF3 IN MYELOID DERIVED SUPPRESSOR CELLS

2.0 ABSTRACT

Results obtained in the previous chapter showed that myeloid cell TRAF3 plays an anti-inflammatory and tumor suppressor role by preventing development of chronic inflammation and cancer in littermate control mice as opposed to M-TRAF3$^{-/-}$ mice. One major finding of that study was the significantly high numbers of Gr1^{+}CD11b^{+} myeloid cells observed in the spleen of M-TRAF3-/- mice affected with chronic inflammation and cancer. Here we show that Gr1^{+}CD11b^{+} myeloid cells are myeloid derived suppressor cells as they potently suppress proliferation of T cells and also show typical morphological characteristics of MDSC. In order to further investigate the role of TRAF3 in MDSC physiology, we have created a new model of chronic inflammation in young adult M-TRAF3$^{-/-}$ mice by repeated injections of Bacillus Calmette-Guérin (BCG) which closely resembles the phenotype observed in aging M-TRAF3$^{-/-}$ mice affected with chronic inflammation and leads to significant expansion of MDSC in spleen. Closer analysis in BCG inflamed mice showed that MDSC induction is directly proportional to the intensity of inflammation. Moreover, higher numbers of MDSC seen in M-TRAF3-/- mice could be attributed to greater *de novo* synthesis in spleen of these mice compared to LMC mice. Finally, our preliminary data suggest that differentiation of MDSC into their mature counterparts is not grossly affected by cell intrinsic TRAF3. However, TRAF3-deficient MDSC show enhanced STAT3 phosphorylation upon stimulation with GM-CSF. Overall, the results here further support the anti-inflammatory role of myeloid cell TRAF3 and establishes it as a suppressor of MDSC expansion.

2.1 INTRODUCTION

In chapter I we showed that deletion of TRAF3 in myeloid cells *in vivo* leads to altered signaling downstream of TLR3 and TLR4 receptors and also to an altered antibody response to T-dependent and T-independent antigens. More importantly, we reported that M-TRAF3$^{-/-}$ mice spontaneously develop inflammation, infection, and tumors between 15 and 22 months of age, pointing to critical roles of myeloid cell TRAF3 in controlling chronic inflammation and tumor development. One of the major findings in that study was the expansion of CD11b^{+}Gr1^{+} myeloid cells in the spleen of mice containing spontaneous cancer, inflammation and infection. We speculated these cells to be myeloid derived suppressor cells (MDSC), given the disease phenotype that they are expanded in.

MDSC are a heterogeneous group of immature myeloid cells that are normally present in the bone marrow of a healthy individual. They are precursors of dendritic cells (DC), macrophages, and granulocytes [76]. However, during pathological conditions like cancer, inflammation, infection and stress, an increase in the numbers of MDSC is evident in peripheral lymphoid organs and in circulation [117]. MDSC potently suppress both adaptive and innate immune responses against tumor cells, and also facilitate angiogenesis, invasion and metastasis of solid tumors, thereby promoting tumor progression [76,118,119]. In mice they are identified by the expression of CD11b^{+}Gr1^{+} markers. They are further divided into two major subsets: Granulocytic or polymorphonuclear (G-MDSC or PMN-MDSC) and Monocytic (M-MDSC) which are phenotypically similar to neutrophils and monocytes, respectively [120]. Due to differences in the mechanisms of immune-suppression and the half-life of immune-suppressive mediators secreted by these two cell types, M-MDSC is more suppressive as compared to G-MDSC on a per cell basis [121]. Therefore,

investigating their ratio is of significance and variability in their ratio has been found in different cancer types [121-123]. Research efforts in the past decade has led to a better understanding of the MDSC biology, however, the intrinsic role of TRAF3 remains unexplored.

Here we confirm that the $CD11b^{+}Gr1^{+}$ myeloid cells expanded in tumor-bearing and inflammation affected M-$TRAF3^{-/-}$ aging mice are indeed MDSC. Moreover, we report results from a new chronic inflammatory mouse model that closely mimics the phenotype observed in aging M-$TRAF3^{-/-}$ and confirms the role of TRAF3 as a suppressor of MDSC expansion. Finally, our preliminary data suggest that differentiation of MDSC into their mature counterparts is not grossly affected by cell intrinsic TRAF3.

2.2 MATERIALS AND METHODS

2.2.1 MICE

$TRAF3^{flox/flox}$ and $TRAF3^{flox/flox}LysM^{+/Cre}$ (M-$TRAF3^{-/-}$) mice were generated as previously described [12,124]. Mouse tails were screened by genomic PCR using primer sets (FC3 + BT6) [12], (Lys-Com + Lys-WT), and (Lys-Com + Lys-Cre) [45] as described. Deletion of exons 1 and 2 of the TRAF3 gene in peritoneal macrophages was detected by genomic PCR using primers U7 and BT6 as previously described [12]. All experimental mice for this study were subsequently produced by breeding of $TRAF3^{flox/flox}$ mice with $TRAF3^{flox/flox}LysM^{+/Cre}$ mice, and $TRAF3^{flox/flox}$ littermates (LMC) were used as controls for all experiments. All mice were kept in specific pathogen-free conditions in the Animal Facility at Rutgers University, and were used in accordance with NIH guidelines and under

an animal protocol (Protocol # 08-048) approved by the Animal Care and Use Committee of Rutgers University.

2.2.2 ANTIBODIES AND REAGENTS

FITC-, PE-, or Cy5-labeled Abs against mouse CD3, CD4, CD8, CD45R (B220), CD11b, Ly6C, Ly6G, F4/80, CD11c, and MHC class II were purchased from eBioscience (San Diego, CA). Tissue culture supplements including stock solutions of sodium pyruvate, L-glutamine, nonessential amino acids, and HEPES (pH 7.55) were from Invitrogen (Carlsbad, CA). DNA oligonucleotide primers were obtained from Integrated DNA Technologies (Coralville, IA).

2.2.3 FLOW CYTOMETRY

Single cell suspensions were made from the spleen, bone marrow (BM), and peritoneal lavage. Immunofluorescence staining and FACS analyses were performed as previously described [12,14]. Erythrocytes from spleen were depleted with ACK lysis buffer. Cells ($1x10^6$) were blocked with rat serum and FcR blocking Ab (2.4G2), and incubated with various Abs conjugated to FITC, PE, or Cy5 for multiple color fluorescence surface staining. Analyses of cell-surface markers included Abs to CD3, CD4, CD8, CD45R (B220), CD11b, Ly6C, Ly6G, F4/80, CD11c, and MHC class II. List-mode data were acquired on a FACSCalibur (Becton Dickinson, Mountain View, CA) using Cell Quest software. The results were analyzed using FlowJo software (Tree Star, San Carlos, CA). Forward light scatter/side light scatter gating was used to identify live cells.

2.2.4 THE *IN VIVO* MODEL SYSTEM FOR CHRONIC INFLAMMATION

Bacillus Calmette–Guérin was administered as previously described[125]. Briefly, heat-killed *Mycobacterium tuberculosis*-BCG (231141; Difco Laboratories) was administrated by three subcutaneous injections (100 μg per animal/dose) at 1 week intervals to induce chronic inflammation. One and two subcutaneous injections of BCG were performed to study the kinetics of MDSC expansion. The first two injections were administrated as a mixture of BCG and IFA (Sigma) at a 1:1 ratio emulsified by vortexing for 15 mins at highest speed, and the third BCG injection was with PBS only. Unless stated otherwise, cells were collected 2 days after each injection. Control mice were subjected to the same protocol.

2.2.5 ALEXA FLOUR670 LABELING AND EX VIVO T CELL PROLIFERATION ASSAY

Purified T cells (20 x 10^6) were incubated in 10 mls of HBSS 1x with Ca2+ and Mg2+, containing 0.5 μM of a proliferation dye Alexa Flour 670 (eBioscience) for 10 min at 37^o C. Cells were then chilled on ice for 5 mins and washed two times with HBSS. Non-tissue culture treated 24-well plates were coated with 10 μg/ml of CD3 antibody (Biolegend) at 37^0 C for 2 hours. Unbound antibody was then washed away with PBS. Labeled T cells were then plated in equal ratio with or without purified MDSC in the presence or absence of 2 μg of CD28 antibody (Biolegend). The percentage of proliferating $CD8^+$ T cells were determined by flow cytometry.

2.2.6 CELL ISOLATION AND PURIFICATION OF SPLENIC CD8+ T CELLS AND MDSC

CD8+ T cells were purified from control mice using CD8+ T cell purification kit from Miltenyi Biotec per manufacturer's instructions. MDSC were purified from

splenocytes by depleting B and T cells first using B220 and CD90.2 beads from Miltenyi Biotec, respectively, and the B220-CD90.2- fraction was subsequently used to purify $Gr1^+$ MDSC using anti-Gr1 followed by anti-PE beads from Miltenyi Biotec. The purity of cell populations was verified to be greater than 90% as determined by flow cytometry.

2.2.7 MDSC DIFFERENTIATION ASSAY

MDSC were isolated from inflamed mice and cultured in the presence or absence of 10 ng/ml of G-, M-, or GM-CSF (Biolegend) for 3 or 5 days or 1 μg/ml LPS (Sigma), 5 μg/ml R848 (Axxora LLCs), 1μM CpG (IDT) or 10μg/ml pIC (InvivoGen) for 20 hours in non-tissue culture treated plates. The cells were harvested by trypsinization if needed and phenotypes were determined by flow cytometry.

2.2.8 CELL MORPHOLOGICAL EXAMINATION

Morphological characterization of MDSC subtypes was performed on cytospin preparations of purified MDSC from aging M-$TRAF3^{-/-}$ mice using a Diff-Quick staining kit (VWR). Bright field micrographs of stained slides were taken using a microscope (Olympus BX-51, Olympus America Inc., Center Valley, PA).

2.2.9 *IN VIVO* BRDU LABELING

BrdU (BD Pharmingen™, San Diego, CA) 3 mg in 0.3 ml of Dulbecco's PBS was given to mice in two doses via *i.p.* route 16 and 19 h before sacrifice and cell harvest. The percentage of BrdU+ cells was determined by intracellular staining with an APC-conjugated anti-BrdU antibody using reagents from the BrdU flow kit (BD Pharmingen™).

2.2.10 STATISTICS

Statistical analyses were performed using Prism software (GraphPad, La Jolla, CA). For direct comparison of means between LMC and M-TRAF3$^{-/-}$ mice, statistical significance was determined with the unpaired *t* test for two-tailed data. For comparison of two independent variables as in time course analysis, two-way ANOVA was used. *P* values less than 0.05 are considered significant (*), and *P* values less than 0.0001 are considered highly significant (***).

2.3 RESULTS

2.3.1 CD11B^{+}GR1^{+} CELLS FROM SPLEEN OF TUMOR-BEARING AND INFLAMMATION AFFECTED AGING M-TRAF3-/- MICE ARE MDSC

As previously reported in chapter I, the percentage of CD11b^{+}Gr1^{+} cells in the spleen of M-TRAF3$^{-/-}$ aging mice with spontaneous chronic inflammation and tumor development are significantly higher than that observed in littermate control mice of similar age (Figure 12A). The CD11b and Gr1 markers are shared by neutrophils as well as MDSC in mice. However, MDSC can be distinguished from neutrophils morphologically by the shape of nucleus and functionally by the potent immunosuppressive effects toward T cells [126]. As mentioned earlier, there are two different subsets of cells within MDSC, G-MDSC and M-MDSC, which exhibit differential expression levels of the cell surface markers of granulocytes and monocytes such as Ly6G and Ly6C. We therefore used flow cytometry to identify these two subsets in the spleen of M-TRAF3$^{-/-}$ aging mice (Figure 12A). Indeed, we identified two subsets in the expanded CD11b^{+}Gr1^{+} cells, including Ly6G^{+}Ly6C^{Int} cells (likely represent G-MDSC or mature neutrophils) and Ly6G$^{lo/-}$Ly6C^{Hi} cells (likely represent M-CDSC or mature monocytes) (Figure 12B). Out of the total CD11b^{+}Gr1^{+} population, we found that Ly6G^{+}Ly6C^{Int} cells

were much higher in proportion than $Ly6G^{lo/-}Ly6C^{Hi}$ cells with the ratio of approximately 3:1, which is in line with what is reported in tumor-bearing mice and human patients with cancer [122,127] (Figure 12B). To further characterize the $CD11b^{+}Gr1^{+}$ cells, we purified these cells from the spleen of diseased M-TRAF3$^{-/-}$ aging mice using magnetic sorting. We next examined the morphology of purified $CD11b^{+}Gr1^{+}$ cells by doing Wright-Giemsa staining of cytospin slides using a Diff-Quick staining kit. The purified $CD11b^{+}Gr1^{+}$ cells exhibited a nuclear morphology distinct from mature neutrophils, and displayed ring-shaped or oval-shaped nuclear morphology (Figure 12C), which are characteristic of G-MDSC and M-MDSC, respectively. Thus the two subsets were confirmed immuno-phenotypically and morphologically.

Next, we looked at the immune-suppressive capacity of these cells by co-culturing them with splenic CD8 T cells purified from naïve LMC mice in equal ratio. We found that the vast majority of CD8 T cells (>80%) are proliferated cells after stimulation with CD3 and/or CD28 for 4 days in the absence of MDSC as demonstrated by the dilution of the proliferation dye eFluor 670 (Figure 12D). However, CD8 T cell proliferation was significantly reduced (<10%) after co-culture with $CD11b^{+}Gr1^{+}$ cells purified from aging M-TRAF3$^{-/-}$ mice for 4 days (Figure 12D). These data indicate that the purified $CD11b^{+}Gr1^{+}$ cells are highly immune-suppressive. Taken together, our results convincingly show that the $CD11b^{+}Gr1^{+}$ cells expanded in the spleen of tumor-bearing or inflammation affected aging M-TRAF3$^{-/-}$ mice are indeed MDSC and they will be referred as such going forward.

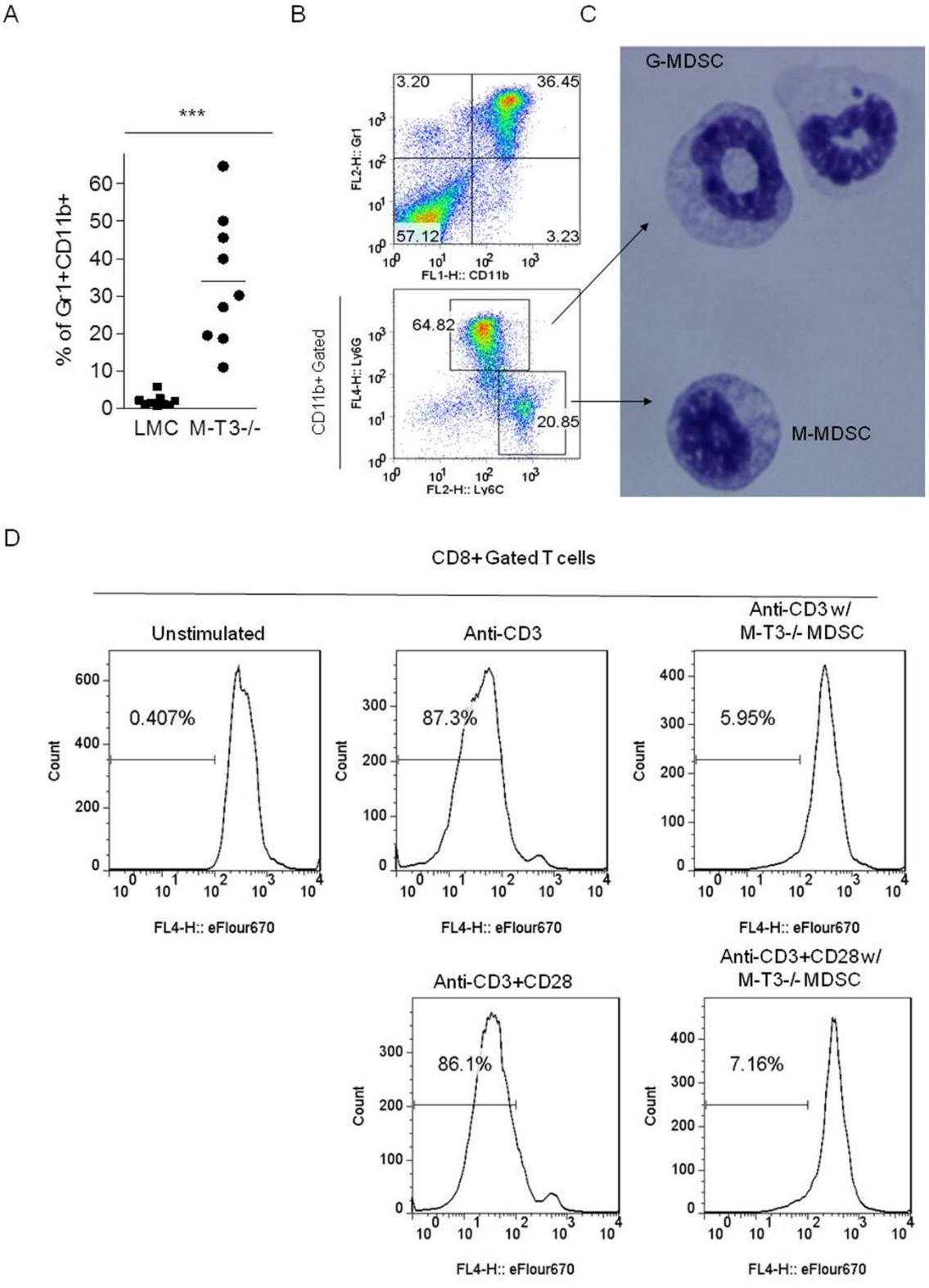
A
B
C
***
% of Gr1+CD11b+
LMC
M-T3-/-
3.20
36.45
57.12
3.23
FL2-H:: Gr1
FL1-H:: CD11b
CD11b+ Gated
64.82
20.85
FL4-H:: Ly6G
FL2-H:: Ly6C
G-MDSC
M-MDSC
D
CD8+ Gated T cells
Unstimulated
0.407%
Anti-CD3
87.3%
Anti-CD3 w/
M-T3-/- MDSC
5.95%
Count
FL4-H:: eFlour670
Anti-CD3+CD28
86.1%
Anti-CD3+CD28 w/
M-T3-/- MDSC
7.16%

Figure 12: CD11b+Gr1+ cells in diseased aging M-TRAF3-/- mice are MDSC.
M-TRAF3$^{-/-}$ mice analyzed were 15-22 months old (n=8 per group). **(A)** Increased percentage of CD11b+Gr-1+ myeloid cells in the spleen of diseased M-TRAF3-/- mice. Each data point depicts an individual mouse. (**B**) Representative FACS profiles of splenocytes. Cells were stained with fluorochrome-conjugated CD11b, Gr-1, Ly6G, and Ly6C Abs, and then analyzed by a FACSCalibur. Two subsets of CD11b+Gr1+ cells were identified, including G-MDSC (CD11b^{+} Ly6G^{+} Ly6C^{Int}) and M-MDSC (CD11b^{+} Ly6G$^{lo/-}$ Ly6C^{Hi}). (**C**) Representative micrographs of CD11b+Gr1+ cells purified from aging M-TRAF3-/- mice analyzed by cytospin and Wright-Giemsa staining. **(D)** Potent suppressive activities of CD11b+Gr-1+ cells purified from diseased M-TRAF3-/- mice on CD8 T cell proliferation in co-culture experiments. CD8 T cells were purified from naïve LMC mice, labeled with a cell proliferation dye eFluor 670, stimulated with anti-CD3 or anti-CD3+anti-CD28 in the absence or presence of purified CD11b+Gr-1+ cells (1:1 ratio) for 4 days, and then stained with fluorochrome-conjugated CD8 Ab followed by FACS analyses. Dilution of the proliferation dye eFluor 670 labeling was compared.

2.3.2 MYELOID CELL TRAF3 SUPPRESSES MDSC ACCUMULATION DURING CHRONIC INFLAMMATORY RESPONSE

Since it takes about 15 months for M-TRAF3$^{-/-}$ mice to spontaneously develop chronic inflammation and cancer with significant upregulation of MDSC in the spleen, we sought to establish an *in vivo* mouse model of chronic inflammation to induce MDSC in young adult mice. It has been previously reported that repeated and sustained exposure of mice to heat-killed pathogens or Toll-like receptor (TLR) ligands can lead to chronic inflammation and induction of MDSC [128,129]. We therefore administered three subcutaneous injections of heat-killed *Mycobacterium tuberculosis* - Bacillus Calmette-Guérin (BCG) in mice at 1 week intervals to induce chronic inflammation, modified from Sade-Feldman *et al.* [125]. Our results showed an enhanced inflammatory response in young adult M-TRAF3$^{-/-}$ as compared to age- and gender- matched littermate control (LMC) mice as indicated by the significantly increased spleen weight (Figure 13A). Moreover, immuno-phenotypic analysis revealed substantially elevated proportions of MDSC (2-fold higher) in the spleen of M-TRAF3$^{-/-}$ mice as compared to LMC mice (Figure 13B, top panel). The absolute numbers of total MDSC and G- and M-MDSC are approximately 3-fold higher in

M-TRAF3$^{-/-}$ mice compared to those detected in LMC mice (Figure 13C, bottom panel). In addition, the ratio of G-MDSC to M-MDSC in BCG inflamed M-TRAF3$^{-/-}$ young adult mice was similar (3:1) to that observed in tumor-bearing and chronically inflamed aging M-TRAF3$^{-/-}$ mice (Figure 13C and 12B). We also noticed a significant decrease in the percentages of B and T cells in M-TRAF3$^{-/-}$ compared to LMC mice (Figure 13C), which was also evident in the diseased aging M-TRAF3$^{-/-}$ mice (Figure 10B). In BCG-inflamed young adult M-TRAF3$^{-/-}$ mice, the decrease in the percentage of B and T cells appears to be an indirect result of the hyperexpansion of MDSC in the spleen, because the numbers of splenic B and T cells were not decreased as compared to those observed in LMC mice (Figure 13C, bottom panel). Overall, these results reaffirm the role of myeloid cell TRAF3 as an inhibitor of chronic inflammation and MDSC expansion.

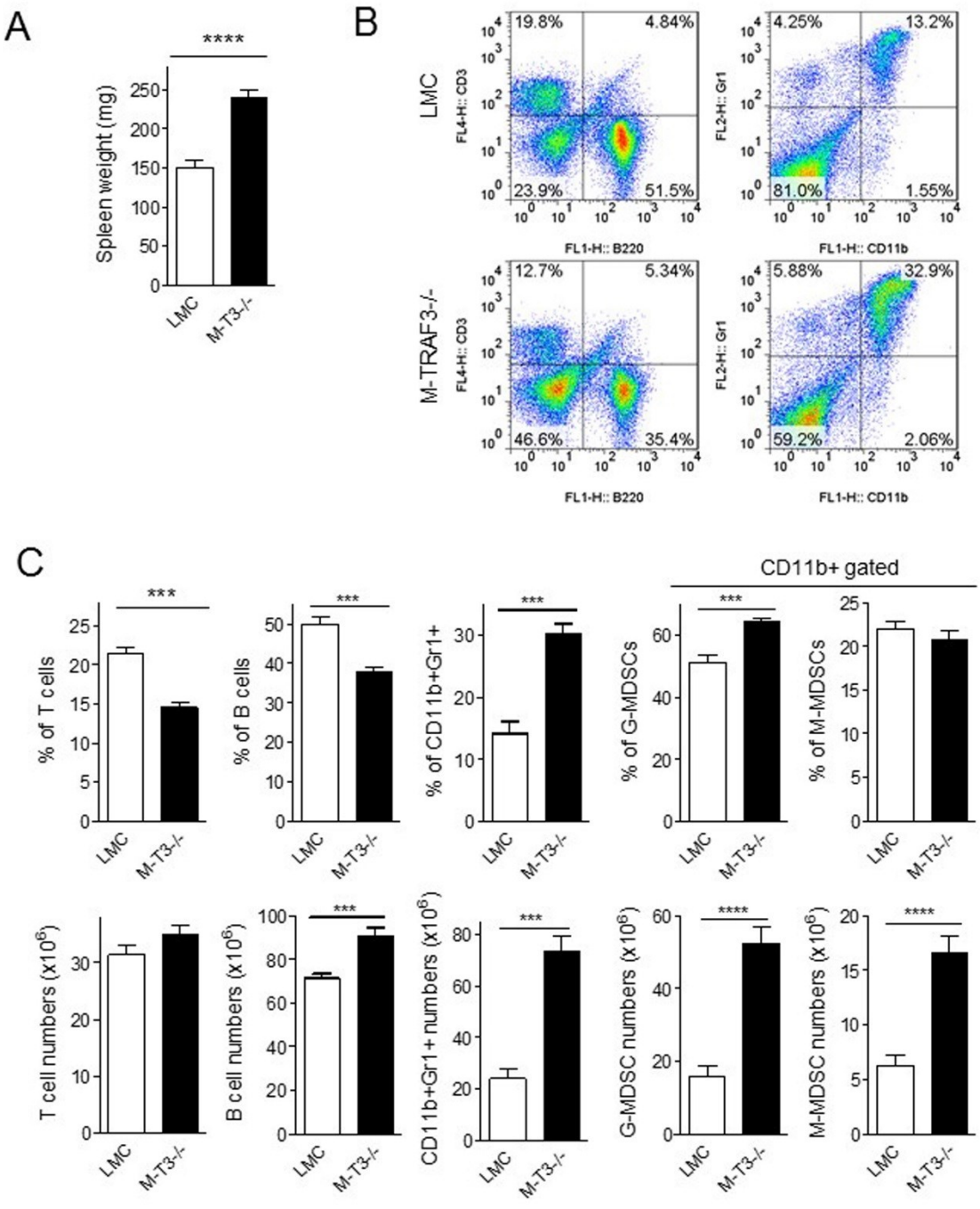
A
****
Spleen weight (mg)
250
200
150
100
50
0
LMC
M-T3-/-
B
LMC
M-TRAF3-/-
FL4-H:: CD3
FL1-H:: B220
FL2-H:: Gr1
FL1-H:: CD11b
19.8%
4.84%
23.9%
51.5%
4.25%
13.2%
81.0%
1.55%
12.7%
5.34%
46.6%
35.4%
5.88%
32.9%
59.2%
2.06%
C
CD11b+ gated
% of T cells
% of B cells
% of CD11b+Gr1+
% of G-MDSCs
% of M-MDSCs
T cell numbers (x10^6)
B cell numbers (x10^6)
CD11b+Gr1+ numbers (x10^6)
G-MDSC numbers (x10^6)
M-MDSC numbers (x10^6)
***
****
LMC
M-T3-/-

Figure 13: Myeloid cell TRAF3 suppresses MDSC induction during chronic inflammatory response induced by heat-killed BCG.
$TRAF3^{flox/flox}$ littermate control (LMC) (n=23) and M-$TRAF3^{-/-}$ mice (n=13) analyzed were 8 to 12 weeks old. Mice were s.c. injected with heat-killed BCG (100 ug/100 ul/mouse) at 1 week intervals. The first two injections were administrated as a mixture of BCG/PBS and incomplete Freud adjuvant (IFA) at a 1:1 ratio, and the third BCG injection was in PBS only. Spleens were harvested on day 2 after the third injection. **(A)** The graph depicts spleen weights of LMC and M-$TRAF3^{-/-}$ mice. **(B)** Representative FACS profiles of splenocytes from age- and gender- matched LMC and M-TRAF3-/- mice. FACS profiles were scatter-gated on live cells. The gated cell populations include: B cells, B220+CD3-; T cells, CD3+B220-; MDSC, CD11b+Gr-1+. **(C)** Frequency and numbers of B and T lymphocytes, total MDSC, and G- and M-MDSC within total MDSC population analyzed by FACS. * P value < 0.05; ** P value < 0.01; *** P value < 0.001. Error bars represent SEM.

2.3.3 MDSC FROM CHRONICALLY INFLAMED YOUNG M-$TRAF3^{-/-}$ MICE SHOW POTENT IMMUNOSUPPRESSIVE ACTIVITY

We further investigated if TRAF3 deficiency in MDSC affects their immune-suppressive capacity as compared to control TRAF3-sufficient MDSC. We purified MDSC from BCG-inflamed young adult M-$TRAF3^{-/-}$ and LMC mice, and performed co-culture experiments with splenic CD8 T cells purified from naïve LMC mice in the absence or presence of stimulation with anti-CD3 or anti-CD3 + anti-CD28. Our results showed that TRAF3-/- MDSC are equally suppressive as control MDSC as revealed by comparable suppression of T cell proliferation upon co-culture with MDSC at equal ratios (Figure 14). Together, the above results validate heat-killed BCG-induced chronic inflammation as a suitable model to further study the role of TRAF3 in MDSC physiology, especially in MDSC expansion, in young adult mice.

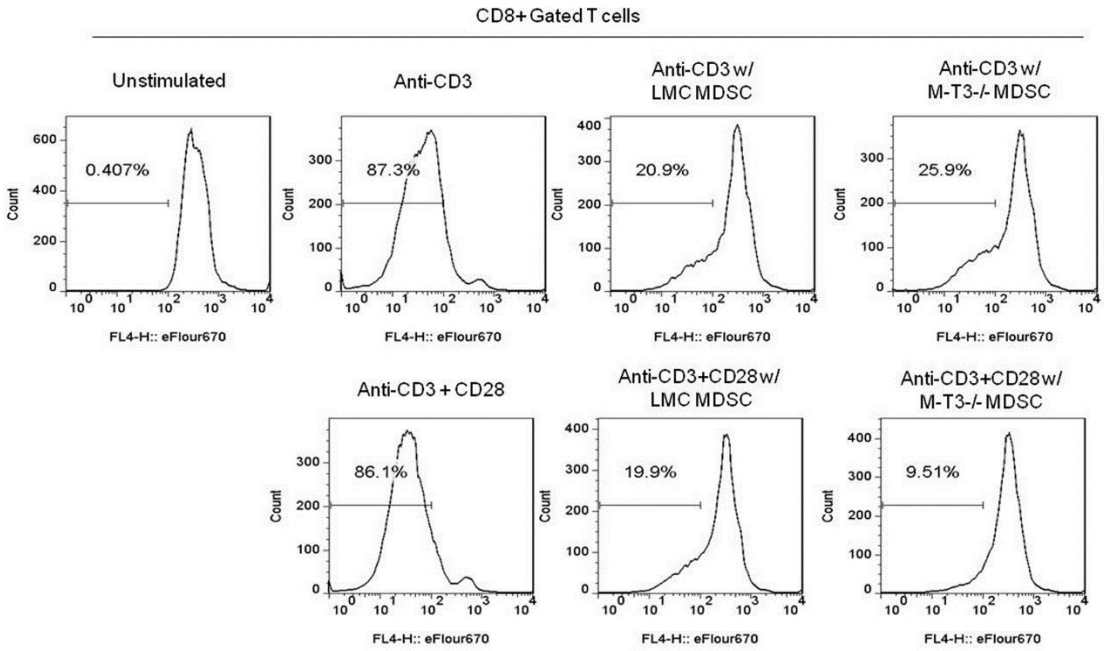

Figure 14: Potent immunosuppressive activity of MDSC induced by repeated BCG injections in young adult mice.
Mice were s.c. injected with heat-killed BCG (100 ug/100 ul/mouse) at 1 week intervals. The first two injections were administrated as a mixture of BCG/PBS and incomplete Freud adjuvant (IFA) at a 1:1 ratio, and the third BCG injection was in PBS only. Spleens were harvested on day 2 after the third injection. CD8 T cells were purified from naïve LMC mice, labeled with a cell proliferation dye eFluor 670, stimulated with anti-CD3 or anti-CD3+anti-CD28 in the absence or presence of purified CD11b+Gr-1+ cells (1:1 ratio) for 4 days, and then stained with fluorochrome-conjugated CD8 Ab followed by FACS analyses. Dilution of the proliferation dye eFluor 670 labeling was compared. Representative FACS profiles from 2 separate experiments are shown here.

2.3.4 TRAF3 DEFICIENCY LEADS TO ALTERED KINETICS OF MDSC INDUCTION DURING AN INFLAMMATORY RESPONSE

We next sought to investigate the kinetics of MDSC induction during the heat-killed BCG-induced chronic inflammatory response between the two genotypes as well as the ability of each genotype to resolve inflammation assessed by a reduction in the numbers of MDSC. We therefore looked at the spleen weight and percentage and absolute numbers of MDSC at day 2 after 1, 2, and 3 BCG injections (1 week apart) and also 4 weeks after

the 3rd BCG injection (Figure 15A). We noticed that the spleen weight and percentage and numbers of MDSC were higher in M-TRAF3$^{-/-}$ mice compared to LMC mice as early as day 2 after 1st injection (Figure 15B, 15C, and 15D). The differences keep getting wider as the number of BCG injections increase and it is most pronounced on day 2 after 3rd injection when the chronic inflammatory response is well established. At this time point, there is a highly significant difference in the spleen weight, percentage and numbers of MDSC between the two genotypes (Figure 15B, 15C, and 15D). However, both the genotypes are able to successfully reduce the percentage of MDSC in the spleen at 4 weeks after the 3rd injection, but M-TRAF3$^{-/-}$ mice continue to display higher numbers of MDSC due to significantly higher spleen weight (Figure 15B, 15C, and 15D). Taken together, these results show that myeloid cell TRAF3 suppresses MDSC induction during the acute and chronic inflammatory response to heat-killed BCG.

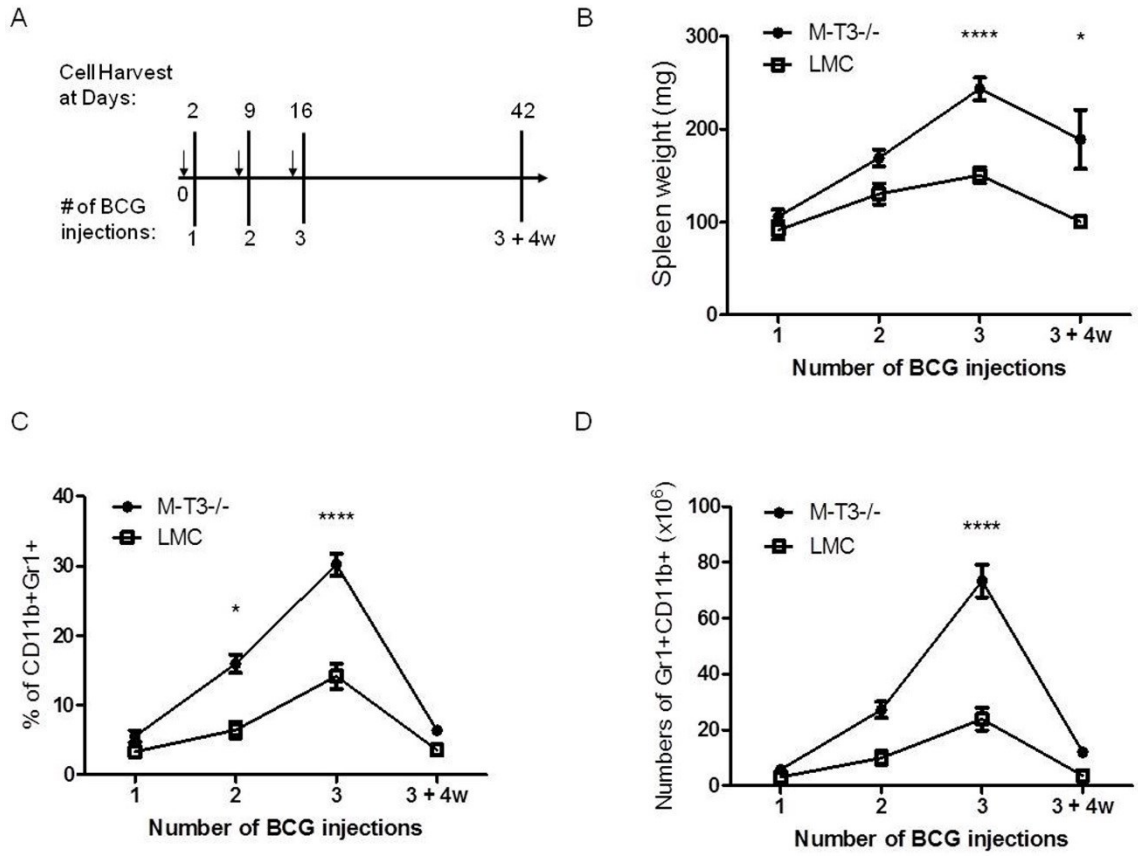

Figure 15: Kinetics of MDSC induction by BCG in young adult mice.
Kinetics of MDSC induction. **(A)** An *in vivo* model for chronic inflammation induced by BCG injections showing different timepoint when cells were harvested for analysis. Arrows indicate BCG injection given on day 0, 7 and 14, 2 days before the cell harvest time point. **(B)** The graph depicts spleen weights of age-matched LMC and M-TRAF3$^{-/-}$ mice at indicated time points. **(C)** The graph depicts percentage of MDSC in spleen of age-matched LMC and M-TRAF3$^{-/-}$ mice at indicated time points. **(D)** The graph depicts absolute numbers of MDSC in spleen of age-matched LMC and M-TRAF3$^{-/-}$ mice at indicated time points. * P value < 0.05; **** P value < 0.0001. P values were obtained by two-way ANOVA. Error bars represent SEM. n=3 to 23 for LMC and 3 to 13 for M-TRAF3$^{-/-}$.

2.3.5 TRAF3 DEFICIENCY LEADS TO ENHANCED PROLIFERATION OF MDSC IN THE SPLEEN

Myelopoiesis, including MDSC proliferation, is known to primarily occur in the BM. However, it can also occur in extramedullary sites such as the spleen especially during inflammation associated pathologies, including cancer, stress and infection [130-132]. We therefore examined the frequency and numbers of lymphocytes and MDSC in the BM and spleen using *in vivo* BrdU labeling in the context of chronic inflammation on day 2 after the 2nd BCG injection. We noticed no significant difference in the percentage of $BrdU^+$ B and T lymphocytes in the spleen between the two genotypes (Figure 16A and 16B). However, the percentage and absolute numbers of proliferating ($BrdU^+$) MDSC were remarkably higher in the spleen of M-TRAF3-/- mice as compared to the LMC mice (Figure 16A and 16B). In addition, the absolute number of non-proliferating ($BrdU^-$) MDSC was also higher in the spleen of M-TRAF3-/- mice although the percentage of these cells was decreased (Figure 16A and 16B). Furthermore, the number of proliferating MDSC were also significantly higher in the BM of M-TRAF3-/- mice compared to LMC mice but there was no significant difference in the frequency of proliferating MDSC in the BM between the two genotypes (Figure 16C and 16D). Whereas LMC mice showed higher numbers of $BrdU^+$ cycling MDSC in the BM than the spleen, the M-TRAF3-/- mice showed higher numbers of $BrdU^+$ cycling MDSC in the spleen than the BM (Figure 16A and 16C). Overall, our results indicate that the spleen and BM are both major sites of MDSC proliferation during a chronic inflammatory response and that the higher percentage and numbers of MDSC observed in the spleen of M-TRAF3-/- mice may be attributed to the higher MDSC proliferation in the spleen of these mice.

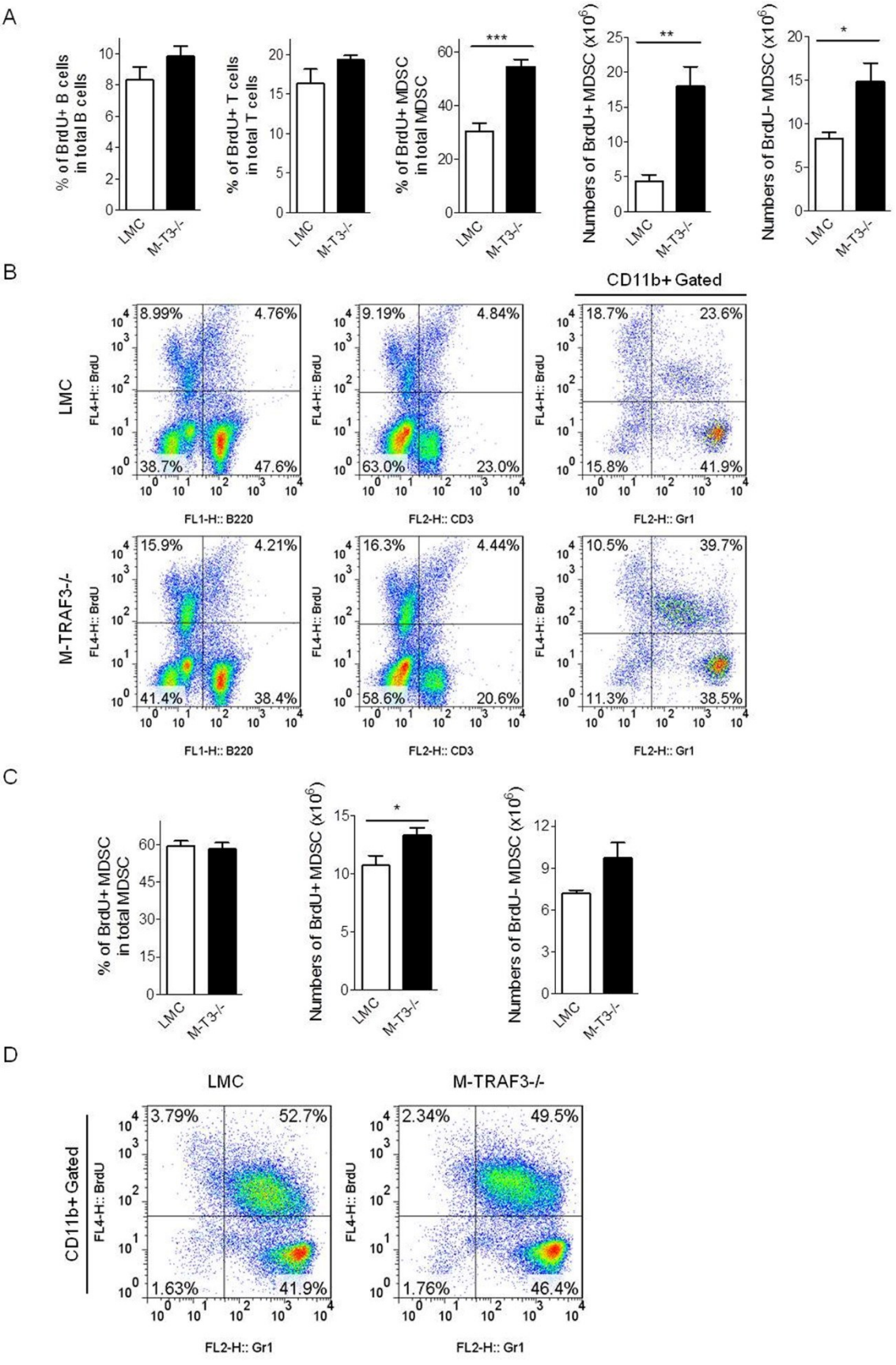
A
% of BrdU+ B cells in total B cells
% of BrdU+ T cells in total T cells
% of BrdU+ MDSC in total MDSC
Numbers of BrdU+ MDSC (x10^6)
Numbers of BrdU- MDSC (x10^6)
LMC
M-T3-/-
***
**
*
B
CD11b+ Gated
LMC
M-TRAF3-/-
FL4-H:: BrdU
FL1-H:: B220
FL2-H:: CD3
FL2-H:: Gr1
8.99%
4.76%
38.7%
47.6%
9.19%
4.84%
63.0%
23.0%
18.7%
23.6%
15.8%
41.9%
15.9%
4.21%
41.4%
38.4%
16.3%
4.44%
58.6%
20.6%
10.5%
39.7%
11.3%
38.5%
C
% of BrdU+ MDSC in total MDSC
Numbers of BrdU+ MDSC (x10^6)
Numbers of BrdU- MDSC (x10^6)
D
LMC
M-TRAF3-/-
CD11b+ Gated
FL4-H:: BrdU
FL2-H:: Gr1
3.79%
52.7%
1.63%
41.9%
2.34%
49.5%
1.76%
46.4%

Figure 16: In vivo proliferation of MDSC in the spleen and bone marrow after 2 BCG injections.

Gender-matched young adult mice were s.c. injected with heat-killed BCG (100 ug/100 ul/mouse) at 1week interval. The two injections were administrated as a mixture of BCG/PBS and incomplete Freud adjuvant (IFA) at a 1:1 ratio. Spleens and BM cells were harvested on day 2 after the second injection. **(A)** Graphs depict the percentage of $BrdU^+$ B and T lymphocytes and MDSC among each cell type in the spleen of inflamed mice. Numbers of proliferating ($BrdU^+$) and non-proliferating ($BrdU^-$) MDSC are also shown. **(B)** Representative FACS profiles of proliferating B cells (B220+ BrdU+), T cells (CD3+ BrdU+) and MDSC (Gr1+ CD11b+ BrdU+) in the spleen of inflamed mice. **(C)** Graphs show the percentage and numbers of proliferating MDSC as well as the numbers of non-proliferating MDSC in the BM of inflamed mice. **(D)** Representative FACS profiles of proliferating MDSC in the BM. * P value < 0.05; ** P value < 0.01; *** P value < 0.001. Error bars represent SEM. n=4 for LMC and 5 for M-TRAF3-/-.

2.3.6 TRAF3 DOES NOT GROSSLY AFFECT DIFFERENTIATION OF MDSC TO MATURE MYELOID CELLS

MDSC are a group of immature myeloid progenitor cells that can differentiate into their mature counterparts including neutrophils, macrophages and dendritic cells (DC) if given an appropriate stimuli [117,125]. We therefore stimulated control and $TRAF3^{-/-}$ MDSC purified from BCG-inflamed mice after 3 BCG injections with different Toll-like receptor (TLR) and colony-stimulating factor receptor (CSFR) ligands. Figure 17 shows representative FACS dot plots of MDSC from 2 such experiments. Our preliminary results suggest that upon stimulation with ligands for TLR7/8 (R848), TLR4 (LPS), TLR9 (CpG) and TLR3 (pIC) for 20 hours, TRAF3 deficient MDSC are slightly less capable of differentiating to mature macrophages ($CD11b^+$ $F4/80^+$) (Figure 17A). We also compared the percentage of mature macrophages upon incubation of MDSC with CSFR ligands macrophage-colony stimulating factor (M-CSF) and granulocyte-macrophage colony stimulating factor (GM-CSF) for 3 and 5 days. As expected, M-CSF leads to highest percentage of macrophages and their percentages were found to be similar between the two genotypes on day 3 and day 5 (Figure 17B and 17D). Also, M-CSF did not promote differentiation of MDSC to mature DC (ClassII+ CD11c+), on day 3 and 5 time points for

either genotypes (Figure 17C and 17E). But, GM-CSF promoted differentiation of MDSC of both genotypes almost equally to mature DC on day 3 and 5 (Figure 17C and 17E) but not to mature macrophages (Figure 17B and 17D). We also did not find any obvious differences between the two genotypes in the percentage of apoptotic cells (Annexin V+) upon stimulation with the above mentioned TLR and CSFR ligands (data not shown). However, these results are preliminary and further repetition is required for conclusive remarks.

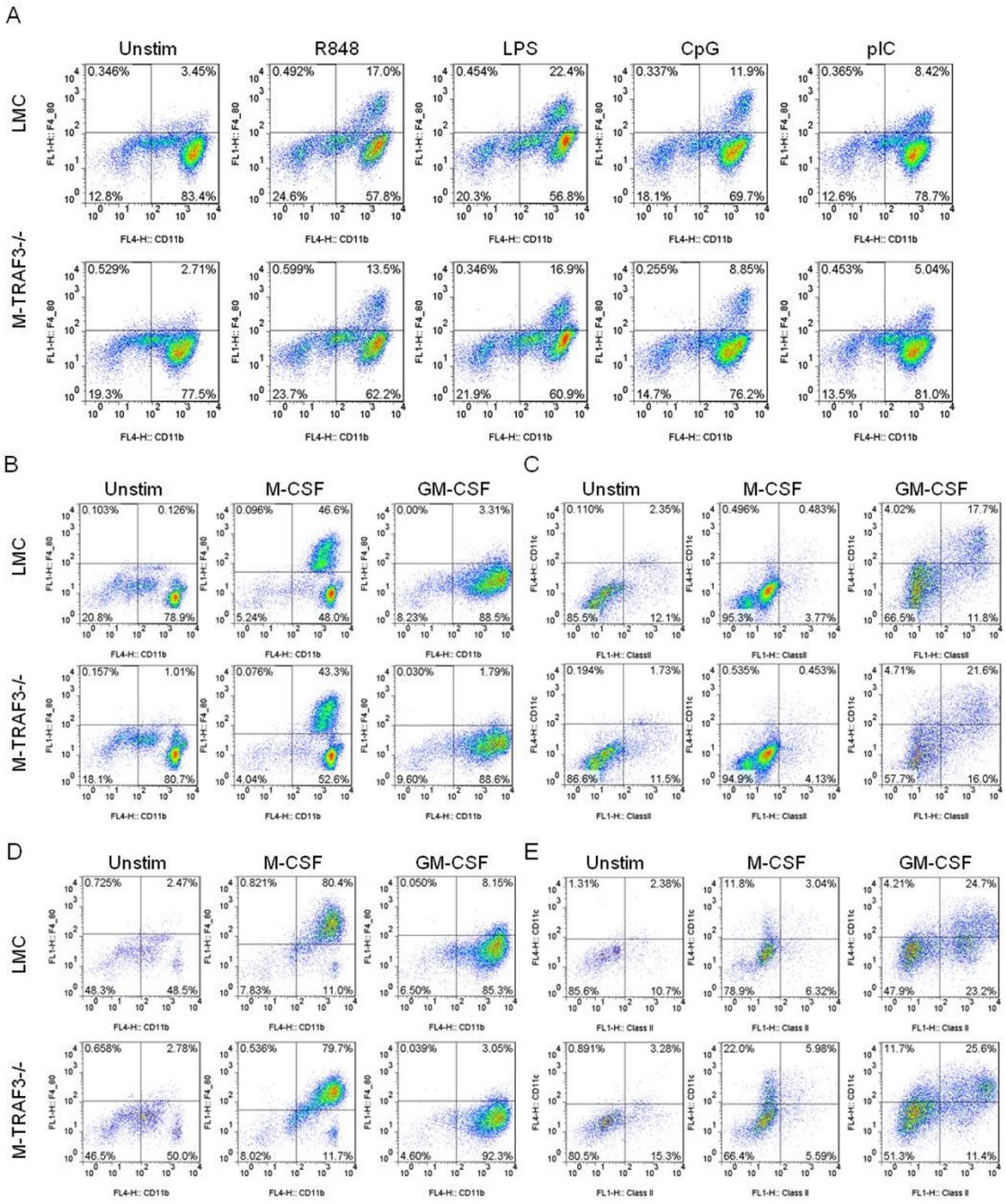
A
Unstim
R848
LPS
CpG
pIC
LMC
M-TRAF3-/-
0.346%
3.45%
12.8%
83.4%
0.492%
17.0%
24.6%
57.8%
0.454%
22.4%
20.3%
56.8%
0.337%
11.9%
18.1%
69.7%
0.365%
8.42%
12.6%
78.7%
0.529%
2.71%
19.3%
77.5%
0.599%
13.5%
23.7%
62.2%
0.346%
16.9%
21.9%
60.9%
0.255%
8.85%
14.7%
76.2%
0.453%
5.04%
13.5%
81.0%
FL1-H:: F4_80
FL4-H:: CD11b
B
Unstim
M-CSF
GM-CSF
LMC
M-TRAF3-/-
0.103%
0.126%
20.8%
78.9%
0.096%
46.6%
5.24%
48.0%
0.00%
3.31%
8.23%
88.5%
0.157%
1.01%
18.1%
80.7%
0.076%
43.3%
4.04%
52.6%
0.030%
1.79%
9.60%
88.6%
C
Unstim
M-CSF
GM-CSF
0.110%
2.35%
85.5%
12.1%
0.496%
0.483%
95.3%
3.77%
4.02%
17.7%
66.5%
11.8%
0.194%
1.73%
86.6%
11.5%
0.535%
0.453%
94.9%
4.13%
4.71%
21.6%
57.7%
16.0%
FL4-H:: CD11c
FL1-H:: ClassII
D
Unstim
M-CSF
GM-CSF
LMC
M-TRAF3-/-
0.725%
2.47%
48.3%
48.5%
0.821%
80.4%
7.83%
11.0%
0.050%
8.15%
6.50%
85.3%
0.658%
2.78%
46.5%
50.0%
0.536%
79.7%
8.02%
11.7%
0.039%
3.05%
4.60%
92.3%
E
Unstim
M-CSF
GM-CSF
1.31%
2.38%
85.6%
10.7%
11.8%
3.04%
78.9%
6.32%
4.21%
24.7%
47.9%
23.2%
0.891%
3.28%
80.5%
15.3%
22.0%
5.98%
66.4%
5.59%
11.7%
25.6%
51.3%
11.4%
FL4-H:: CD11c
FL1-H:: Class II

Figure 17: In vitro differentiation of MDSC in response to TLR and CSF ligands.
MDSC were purified from mice on day 2 after the 3rd BCG injection. **(A)** Purified MDSC were incubated in the presence or absence of 1 μg/ml LPS, 5 μg/ml R848, 1μM CpG or 10μg/ml pIC for 20 hours in non-tissue culture treated plates. **(B, C, D** and **E)** MDSC were also separately cultured in the presence or absence of 10 ng/ml of M-CSF or GM-CSF for 3 days **(B** and **C)** or 5 days **(D** and **E)** in non-tissue culture treated plates. Cells were then harvested and analyzed for mature macrophage markers (F4/80+ CD11b+) (Panel B and D) or DC markers (CD11c+ MHC class II+) (Panel C and E) via flow cytometry using FACSCalibur and FlowJo software. FACS profiles were scatter gated on live cells.

2.3.7 ENHANCED STAT3 PHOSPHORYLATION IN RESPONSE TO SIGNALING BY GM-CSF IN TRAF3-/- MDSC

Colony stimulating factors (CSF) are critical factors that have been demonstrated to regulate the expansion and activation of MDSC in different tumor mouse models as well as in human tumor samples [117]. These factors along with others trigger signaling pathways that lead to activation of Janus kinase (JAK) protein family members and signal transducer and activation of transcription (STAT) proteins, which promotes cell survival, proliferation, and differentiation [117]. Upon preliminary investigation, we found that, TRAF3-/- MDSC show enhanced activation of STAT3 at 5, 10, 30, 60 mins and 20 hours after stimulation with GM-CSF as compared to LMC MDSC (Figure 18). We also detected slightly higher levels of STAT1 phosphorylation (P-STAT1) at 30 and 60 mins after GM-CSF stimulation (Figure 18A). However, no difference was observed between the two genotypes in the levels of arginase I, an enzyme secreted by MDSC that leads to suppression of T cell activation (Figure 18B). Taken together, these results suggest that the higher percentage and numbers of MDSC seen in chronically inflamed M-TRAF3-/- mice could be at least partially due to enhanced GM-CSF-STAT3 signaling.

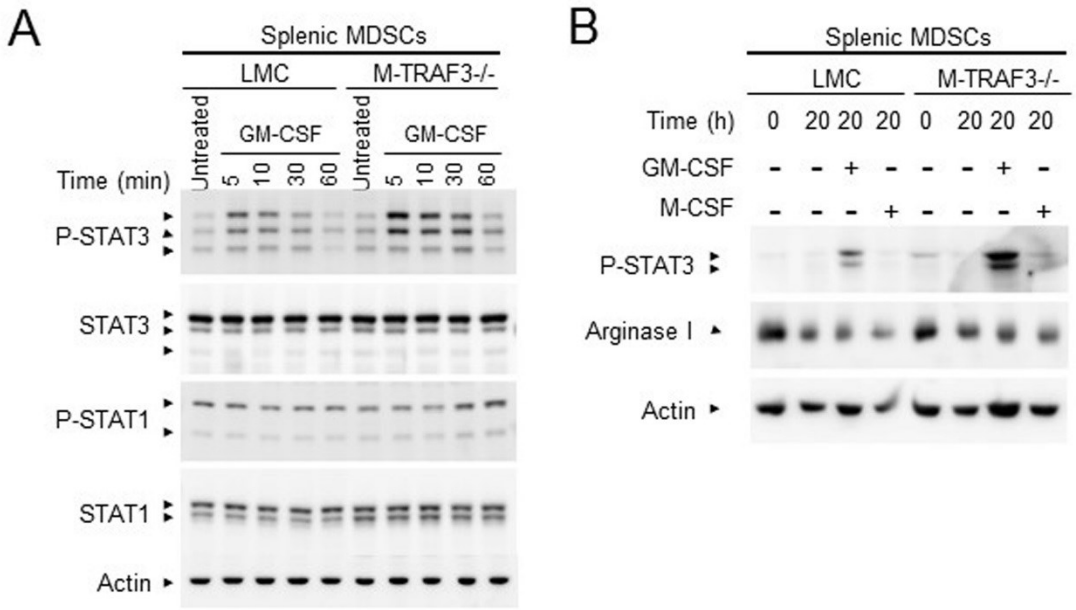

Figure 18: Enhanced STAT3 signaling downstream of GM-CSF receptors in M-TRAF3-/- MDSC.

Splenic MDSC were harvested from mice on day 2 after 3 BCG injections. **(A)** 6 x 10^6 MDSC were starved for 2 hours in 2.5% media before stimulation with or without 10 ng/ml of GM-CSF for indicated time periods. **(B)** 10 x 10^6 MDSC were stimulated with or without 10 ng/ml of GM- or M-CSF for indicated time points. Total protein lysates were subsequently prepared, and signaling events were analyzed by immunoblotting analysis. Proteins were immunoblotted for phosphorylated (P-) or total STAT3, STAT1 or Arginase I followed by actin.

2.4 DISCUSSION AND CONCLUSIONS

We have previously reported that deletion of TRAF3 specifically in myeloid cells leads to significant expansion of splenic $CD11b^+$ $Gr1^+$ myeloid cells in the context of chronic inflammation and cancer as the mice age [124](Chapter 1). In this study, we report that these splenic $CD11b^+$ $Gr1^+$ myeloid cells are myeloid-derived suppressor cells (MDSC) as indicated by their ability to significantly block the proliferation and activation of CD8 T cells. We have further established an *in vivo* mouse model of chronic inflammation by repeated injections of heat-killed BCG bacteria. We have shown that this model is highly comparable to the phenotype of aging M-TRAF3$^{-/-}$ mice with spontaneous chronic inflammation, as it leads to hyper expansion of MDSC in the spleen with similar ratio of G- to M-MDSC but significant reduction in the percentage of T and B lymphocytes. Furthermore, TRAF3 deficiency leads to higher expansion of MDSC not only during the chronic phase but also during acute phase of the inflammatory response to heat-killed BCG. Interestingly, M-TRAF3$^{-/-}$ mice as compared to LMC mice show significantly higher proliferation of MDSC in the spleen than in the BM. Finally, our preliminary results suggest that TRAF3 deficiency does not grossly affect the differentiation response of MDSC induced by several ligands of TLRs or CSF-Rs. However, stimulation with GM-CSF leads to enhanced phosphorylation of STAT3, suggesting a potential involvement of this pathway in the hyper expansion of TRAF3-deficient MDSC. Taken together, our results suggest that TRAF3 is required for suppressing MDSC expansion in a chronic inflammatory milieu *in vivo*.

Repeated exposure of mice to inactivated pathogens is known to induce an inflammatory response and lead to chronic inflammation [128,129]. Such a response is mainly

mediated by TLRs and other pathogen recognition receptors (PRRs) upon recognition of their respective ligands where TRAF3 is known to play a critical role in regulation of signaling downstream of these receptors as discussed in the Introduction Chapter (Figure ii). A major characteristic of chronic inflammation is the induction and activation of MDSC, which leads to suppression of innate and adaptive immune responses [73]. As a result, MDSC expansion is associated with several pathologies characterized by inflammation including bacterial and parasitic infections, sepsis, autoimmune diseases and inflammatory bowel diseases [117]. For example, MDSC numbers are increased in the spleen and blood in a mouse model of multiple sclerosis, where they enter the central nervous system during the inflammatory phase of the disease [133]. MDSC expansion is also seen during chronic infection with helminths [134], *Leishmania major* [135] and *Candida albicans* [136,137]. We believe that sustained release of BCG in the chronically inflamed young M-TRAF3-/- mice and the opportunistic pathogens of commensal microbiota termed "pathobionts" in the aging M-TRAF3$^{-/-}$ mice provide constant stimulation of PRRs and lead to expansion and accumulation of MDSC. Consistent with this notion, we did find bacterial infection in liver and colon and protozoan infection of *Entamoeba muris* in the caecum of aging M-TRAF3$^{-/-}$ mice with expanded MDSC (chapter I). Overall, these data suggest that activation and accumulation of MDSC in response to pathogens expressing TLR ligands is an inherent innate immune response by the host, possibly to restrict the damage caused by a prolonged active immune response [117].

Why TRAF3 deficiency in myeloid cells lead to an enhanced expansion of MDSC as compared to control mice in BCG-induced chronic inflammation as well as in spontaneously inflamed aging M-TRAF3-/- mice could be explained by enhanced pro-

inflammatory cytokine production by TRAF3 deficient myeloid cells upon PRR stimulation. We have reported increased production of pro-inflammatory cytokines IL-6 and IL-12 from TRAF3-deficient bone-marrow derived macrophages (BMDMs) and increased expression of these genes *in vivo* in M-TRAF3-/- mice upon stimulation or immunization with TLR4 and TLR3 ligands, respectively (Chapter I; Figure 2 and 3). In support of this, MDSC accumulation and suppressive functions are regulated by a complex mix of factors associated with inflammation. These factors include pro-inflammatory cytokines like IL-1β, IL-6, TNF-α and IFN-γ and inflammatory mediators like complement factors (C5a), endogenous ligands of TLRs such as HMGB1, chemoattractants (S100A8, S100A9) and prostaglandins (PGE_2) [73,138]. These inflammatory factors regulate different aspects of MDSC functions including prevention of MDSC differentiation to their mature counterparts – macrophages, dendritic cells and neutrophils, increasing resistance to Fas-mediated apoptosis by T cells and enhancing suppressive activity by increased production of reactive oxygen and nitrogen species [73]. Among these, IL-6 is an important cytokine that leads to increase in suppressive activity and accumulation of MDSC in tumor setting by acting downstream of IL-1β signaling [139,140]. Moreover, bacterial products like LPS, which is a ligand for TRAF3-dependent TLR4 receptor, and other cytokines like IL-1β and IFN-γ, all induce expression of COX-2 in monocytes, which prevents their differentiation into DCs and rather promote differentiation to MDSC by expression of IDO1, iNOS, IL-10, IL-4Rα and PGE_2 endogenously [117]. Given the pivotal roles played by these inflammatory cytokines and mediators in MDSC physiology, it would be critical to check their expression levels endogenously in TRAF3-deficient MDSC and also systemically in M-TRAF3$^{-/-}$ mice

after induction of chronic inflammation to better understand the mechanism of MDSC suppression by TRAF3.

Colony stimulating factors like GM-CSF, M-CSF and G-CSF are among the other factors that govern MDSC development and accumulation [141]. Our preliminary results show that TRAF3 deficiency in MDSC from BCG-inflamed M-TRAF3-/- mice does not grossly affect their differentiation into mature myeloid cells following stimulation with M-CSF or GM-CSF (Figure 17). However, these cells show enhanced activation of phosphorylated STAT3 upon GM-CSF stimulation, indicating a different mechanism of MDSC accumulation (Figure 18). STAT3 is considered as one of the most important transcription factors that controls the expansion of MDSC. STAT3 regulates MDSC in several different ways [117,142]: 1) STAT3 upregulates the expression of anti-apoptotic genes Bcl-xL, c-myc and cyclin D1, which leads to an increase in the half-life and proliferation of MDSC in humans and mice [143,144]. 2) It induces expression of S100A8 and S100A9 proteins, which prevents the differentiation of myeloid progenitor cells resulting in expansion of MDSC in the spleen [145]. 3) It activates another key transcription factor called C/EBPβ which promotes cell proliferation by induction of c-myc. 4) STAT3 is also necessary for the immunosuppressive program in both murine and human MDSC [146]. STAT3 activation leads to increased reactive oxygen species (ROS) production by upregulation of p47 and gp91, which are part of the ROS generating complex called NAD(P)H oxidase enzyme complex (NOX) [147]. STAT3 is also activated by GM-CSF and IL-6, and IL-6 is upregulated in TRAF3-deficient BMDMs upon TLR stimulation. Moreover, a combination of GM-CSF and IL-6 is sufficient to induce MDSC generation from human and murine bone marrow cells *in vitro*, which were able to inhibit the

proliferation of both mitogen and alloantigen-activated T cells [123,146]. These findings underscore the importance of STAT3 signaling in the regulation of MDSC functions and might represent the dominant mechanism used by TRAF3-deficient MDSC upon stimulation by a myriad signaling molecules encountered in the complex *in vivo* inflammatory environment.

Increasing evidence also suggests that myeloid cell TRAF3 may control tumor development by inhibiting the expansion of $CD11b^{+}Gr\text{-}1^{+}$ myeloid derived suppressor cells (MDSC), which in turn suppress the anti-tumor immunity mounted by natural killer (NK) cells and CD8 cytotoxic T cells. This might provide an explanation for the higher incidence of tumors observed in M-TRAF3-/- mice. We have consistently observed that aging M-$TRAF3^{-/-}$ mice with spontaneous tumors or chronic inflammation also display striking expansion of MDSC [124]. Although the increased population of MDSC may be a consequence of spontaneous inflammation and tumor development [73-76], emerging new evidence suggests that TRAF3 may directly or indirectly regulate the expansion and function of MDSC. First, Parker et al. found that an endogenous agonist of the TRAF3-dependent receptor TLR4, HMGB1, is commonly present in the tumor microenvironment and potently promotes the generation and suppressive activity of MDSC [148]. Second, Jin et al. demonstrated that upon ligand stimulation, TRAF3 is recruited to M-CSFR and GM-CSFR, which are known to play essential roles in regulating the development and differentiation of MDSC [25,149,150]. Signaling by M-CSFR or GM-CSFR induces the degradation of TRAF3 and subsequent accumulation of c-Rel and p52 NF-κB2 [25,151]. Third, Yu et al. reported that c-Rel and p52 NF-κB2 cooperatively bind to the promoter region of the *Csf2* gene to induce the production of GM-CSF in Th17 cells, raising the interesting

possibility that this may also occur in certain myeloid cell populations [152]. Increased GM-CSF production has been shown to cause the expansion of MDSC [153]. Finally, constitutive activation of NF-κB2 has been shown to promote the immuno-suppressive activity of MDSC by mediating the expression of IDO, an enzyme that catalyzes the degradation of tryptophan through the kynurenine pathway to suppress T cell proliferation and activation [154]. Consistent with this, we have noticed constitutive activation of NF-κB2 in bone marrow derived macrophages and neutrophils from M-TRAF3$^{-/-}$ mice in the absence of any stimulation and this could very well be the case in MDSC, however it needs to be investigated. Collectively, the above evidence obtained by other groups supports the conclusion reported in this Chapter that TRAF3 is a novel critical regulator of the expansion of MDSC, which are recognized as crucial drivers of tumor progression and chronic inflammation in the tumor microenvironment [73,74,76,118,119].

CHAPTER 3: CHARACTERIZATION OF B LYMPHOMA AND HISTIOCYTIC SARCOMA OBSERVED IN AGING M-TRAF3$^{-/-}$ MICE

3.0 ABSTRACT

As reported in chapter I, specific deletion of TRAF3 from myeloid cells leads to spontaneous development of tumor in TRAF3-sufficient B cells and also in TRAF3-deficient tissue resident macrophages called histiocytes in aging mice. Here we have characterized these B lymphomas using V(D)J sequencing of Ig heavy chain gene. We found that these malignant B cells have undergone isotype switching and somatic hypermutation, and preferentially use two major IgV families indicating activation by similar endogenous antigens. Southern blot analysis of B lymphomas showed that they are monoclonal or oligoclonal and further examination revealed significant upregulation of reactivated and native endogenous retroviruses (ERV). Treatment of mice with broad-spectrum antibiotics prevented development of B lymphomas in aging M-TRAF3-/- mice, indicating the requirement of commensal bacteria in B lymphoma development. However, antibiotic treatment did not affect the development of histiocytic sarcomas (HS) in M-TRAF3-/-, indicating that TRAF3 functions as a tumor suppressor in tissue-resident macrophages in a cell intrinsic manner. Immunophenotypic analysis of HS revealed their positivity for Mac2 and CD68 markers, which are typical macrophage lineage markers. B lymphomas and HS observed in M-TRAF3-/- mice were both transplantable, verifying their malignant states. Furthermore, we have successfully developed B lymphoma and HS cell lines from these tumor cells. Collectively, the results presented here provide support for the requirement of myeloid cell TRAF3 in the maintenance of innate immune responses

to commensal bacteria and prevention of ERV reactivation as well as in inhibiting tumor development in B cells and histiocytes.

3.1 BACKGROUND

A very interesting finding obtained from our characterization of aging M-TRAF3-/- mice was the spontaneous development of tumors that affected multiple organs at the age of 15-22 months [124](Chapter I). Tumors observed in M-TRAF3$^{-/-}$ mice include histiocytic sarcomas, B cell lymphomas, and hepatocellular adenoma [124]. Development of tumor in B cells and hepatocytes in M-TRAF3-/- mice was of surprise to us since these cells are not affected by the LysM-Cre mediated deletion of TRAF3. Also, this finding was in sharp contrast to that observed in B-TRAF3$^{-/-}$ mice, in which tumor development is limited to TRAF3-deficient B cells but is not observed in other TRAF3-sufficient cell types [14]. However, unlike the B1 lymphomas and maginal zone lymphomas (MZLs) observed in B-TRAF3-/- mice, the B lymphomas from M-TRAF3-/- mice appeared to be diffuse large B cell lymphomas (DLBCLs) and follicular lymphomas (FLs) based on their histopathological features. B1 lymphomas and MZLs of B-TRAF3-/- mice are derived from naïve B cells, whereas DLBCLs and FLs are known to derive from germinal center (GC) or post-GC B cells [124]. B cells normally undergo somatic hypermutation (SHM) and class switch recombination (CSR) of Ig genes as they pass through GC reactions [71-73]. In order to verify these GC reactions and determine the clonality of B lymphoma cells from M-TRAF3-/- mice, we have performed V(D)J sequencing analysis of the Ig heavy chain (IgH) gene. Here, we report that these B lymphoma cells show significant SHM and have undergone isotype switching with majority of the examined lymphomas preferentially utilizing two major IgV gene families during V(D)J recombination.

The above results prompted us to hypothesize that B cells in M-TRAF3-/- mice could be activated by an endogenous antigen leading to utilization of similar IgV gene families during V(D)J recombination. We therefore, first checked for reactivation of endogenous retroviruses (ERV), as they could be a potential source of endogenous antigens and also their reactivation has been reported to cause lymphoma and leukemia in mice [155]. Indeed, we found significant upregulation of replication-defective ERV transcripts and potentially replication-competent ERV transcripts in B lymphomas harvested from aging M-TRAF3-/- mice. Moreover, commensal bacteria serve as another potential source of endogenous antigens for B cells and their products are known to induce the expression of ERV, we therefore sought to investigate their involvement in B lymphoma development. We discovered that B lymphoma development along with other abnormalities observed in aging M-TRAF3-/- mice can be prevented upon treatment of mice with broad-spectrum antibiotics. Interestingly, antibiotics treatment of mice led to a greater incidence of TRAF3-deficient histiocytic sarcomas than that observed in aging M-TRAF3-/- mice, indicating that TRAF3 functions as a tumor suppressor in histiocytes in a cell intrinsic manner. Here, we also report results from further characterization of these histiocytic sarcomas that are spontaneously developed in antibiotics-treated M-TRAF3-/- mice using immunophenotypic and morphological analyses. Overall, our results hint towards a critical function of myeloid TRAF3 in fine-tuning of innate immune responses to maintain host-commensal mutualism and prevent tumor development via both cell-intrinsic (in histiocytes) and cell-extrinsic (B cells) mechanisms.

3.2 MATERIALS AND METHODS

3.2.1 MICE AND DISEASE MONITORING

TRAF3$^{flox/flox}$ and TRAF3$^{flox/flox}$ LysM$^{+/Cre}$ (M-TRAF3$^{-/-}$) mice were generated as previously described [12,124]. NOD SCID mice (Jackson Laboratory, stock number: 001303, strain name: NOD.CB17-Prkdc^{scid}/J) were used as recipients in B lymphoma and histiocytic sarcoma transplantation experiments. All mice were kept in specific pathogen-free conditions in the Animal Facility at Rutgers University, and were used in accordance with NIH guidelines and under an animal protocol (Protocol # 08-048) approved by the Animal Care and Use Committee of Rutgers University. Mice were monitored daily for spontaneous tumor formation, or signs of illness or discomfort, including weight loss, enlarged lymph nodes or abdomen, labored breathing, hunched posture, and paralysis [51].

3.2.2 ANTIBODIES AND REAGENTS

FITC-, PE-, or Cy5-labeled Abs against mouse CD45R (B220), IgM, IgG, CD11b, Gr1, F4/80, CD68, CD14 and Mac2 were purchased from eBioscience (San Diego, CA) and BioLegend (San Diego, CA). Tissue culture supplements including stock solutions of sodium pyruvate, L-glutamine, nonessential amino acids, and HEPES (pH 7.55) were from Invitrogen (Carlsbad, CA). DNA oligonucleotide primers were obtained from Integrated DNA Technologies (Coralville, IA).

3.2.3 FLOW CYTOMETRY

Single cell suspensions were made from the spleen, liver and intestinal tumors. Immunofluorescence staining and FACS analyses were performed as previously described [12,14]. Erythrocytes from spleen were depleted with ACK lysis buffer. Cells ($1x10^6$) were blocked with rat serum and FcR blocking Ab (2.4G2), and incubated with various Abs

conjugated to FITC, PE, or Cy5 for multiple color fluorescence surface staining. Intracellular markers were stained after fixation and permeabilization of cells using an Intracellular Staining kit (BD Biosciences, San Jose, CA). Cell-surface and intracellular markers analyzed include CD45R (B220), IgM, IgG, CD11b, Gr1, F4/80, CD68, CD14 and Mac2. List-mode data were acquired on a FACSCalibur (Becton Dickinson, Mountain View, CA) using Cell Quest software. The results were analyzed using FlowJo software (Tree Star, San Carlos, CA). Forward light scatter/side light scatter gating was used to identify live cells.

3.2.4 SOUTHERN BLOT ANALYSIS OF THE IGH GENE OF B LYMPHOMAS

Genomic DNA was prepared from the spleen or ascites of M-TRAF3$^{-/-}$ mice as described [12,51]. DNA was digested with EcoRI, separated on a 0.7% agarose gel, and blotted onto a Zeta-Probe GT membrane (Bio-Rad, Hercules, CA). Blots were hybridized with a J_H4 probe of the mouse IgH locus. The J_H4 probe was generated by PCR using LMC genomic DNA as template, and primers J_H4-F (5'-TAC TAT GCT ATG GAC TAC TGG-3') and InE-R (5'-CTC TCC AGT TTC GGC TGA ATC-3') [156]. The purified J_H4 probe has been confirmed by DNA sequencing. Southern blot hybridization was performed as described [156].

3.2.5 CLONING AND SEQUENCING OF THE VDJ REGIONS OF THE IGH GENE OF B LYMPHOMAS

Total cellular RNA was prepared from the spleen, ascites, liver or mesenteric lymph node (MLN) of M-TRAF3$^{-/-}$ mice with B lymphomas using TRIzol reagent (Invitrogen) according to the manufacturer's protocol. cDNA was prepared from RNA using High Capacity cDNA Reverse Transcription Kit (Applied Biosystems, Foster City, CA). The IgH VDJ regions were amplified from cDNA by PCR using common forward primer V_H

consensus (5'-GTG CAG CTG GTG GAG TCT GG-3') and isotype specific reverse primer C-μ4 (5'-CCT GGA TGA CTT CAG TGT TGT TCT G-3') for IgM isotype, C-G1 (5'-AGA TGG GGG TGT CGT TTT GG-3') for IgG1 isotype, C-G2b (5'-GCC AGT GGA TAG ACT GAT G-3') for IgG2b isotype, and C-G3 (5'-GAC CAA GGG ATA GAC AGA TG-3') for IgG3 isotype. The high fidelity polymerase, Pfu UltraII, was used in the amplification reaction. PCR products were subsequently subcloned into pBlueScript vector. Mini-prep DNAs of about 20 clones of each B lymphoma sample were sequenced from both orientation using the primers T7 and T3 of the pBlueScript vector, respectively. Each VDJ sequence was aligned with mouse germline IgH database at the following website: http://www.ncbi.nlm.nih.gov/igblast/ to determine whether it contains somatic hypermutation (SHM).

3.2.6 TRANSPLANTATION IN NOD SCID MICE

Spleen cells, ascites or liver cells (20 x 10^6) from representative M-TRAF3$^{-/-}$ mice with B lymphomas or histiocytic sarcomas (HS) were i.p. injected into immunocompromised NOD SCID recipient mice. Lymphoma or HS growth and progression were monitored in the recipient mice daily. 6-16 weeks post-transplantation, spleens, ascites and liver were harvested from recipient mice for immunophenotypic analysis using flow cytometry and for culture to generate immortalized cell lines.

3.2.7 TREATMENT OF MICE WITH ANTIBIOTICS

Age- and gender- matched LMC and M-TRAF3$^{-/-}$ mice were treated with broad spectrum antibiotics continuously for 4 months starting from the age of 8-10 months. Antibiotic treatment was administered *ad libitum* in drinking water using a cocktail of three broad spectrum antibiotics: ampicillin (1 mg/ml, Henry Schein, Melville, NY) and

sulfamethoxazole-trimethoprim (1.6 mg/ml : 0.32 mg/ml, prescribed and obtained from local pharmacy) in amber bottles. Antibiotic water was refreshed twice weekly. Mice were monitored daily for any abnormalities or discomfort daily until 22 months of age or when moribund. Organs were collected for histopathological and immunophenotypic analysis.

3.2.8 GENERATION OF IMMORTALIZED B LYMPHOMA AND HISTIOCYTIC SARCOMA CELL LINES

Cell lines were generated from TRAF3 sufficient primary B lymphomas harvested from aging M-TRAF3-/- mice and also from histiocytic sarcomas from antibiotics-treated M-TRAF3-/- mice as previously described [157]. Briefly, primary tumor cells were harvested from the diseased mouse and were passaged in NOD SCID mice once. Tumor cells harvested from transplanted NOD SCID mice were plated in 24-well plates in mouse media [12] containing 10% FCS. After culture for 1 month, several actively proliferating clones were expanded and passaged successively. The cell lines were derived after continuous culture for 4-5 months and frozen for future use.

3.2.9 QUANTITATIVE REAL-TIME PCR ANALYSIS

Total cellular RNA was extracted using TRIzol reagent (Invitrogen, Carlsbad, CA) according to the manufacturer's protocol. cDNA was prepared from RNA using the High Capacity cDNA Reverse Transcription Kit (Applied Biosystems, Foster City, CA). cDNA was then used as a template for the amplification of target gene transcripts with SYBR green PCR master mix (Applied Biosystems). *Hprt* was used as an endogenous control gene. Reactions were performed on a 7500 Fast Real-Time PCR System (Applied Biosystems). Relative mRNA expression levels of target genes were analyzed using

Sequencing Detection Software (Applied Biosystems) and the comparative Ct (ΔΔCt) method following the manufacturer's procedures.

ΔCt = Ct of *sample* – Ct of *Hprt*.

ΔΔCt = ΔCt of each sample – ΔCt of litter mate control (LMC).

Fold change = $2^{-\Delta\Delta Ct}$

Duplicate PCR reactions and triplicate experiments were performed for each biological sample. Primers used to detect native and reactivated endogenous retroviruses (including eMLV, MMTV, and RARV) as well as the gene encoding the envelope protein ecotropic gp70 were previously described [155].

3.2.10 CELL MORPHOLOGY

Morphological characterization of histiocytic sarcoma cells was performed on cytospin preparations of dissociated HS cells derived from aging M-TRAF3$^{-/-}$ mice using a Diff-Quick staining kit (VWR). Bright field micrographs of stained HS cells were taken using a microscope (Olympus BX-51, Olympus America Inc., Center Valley, PA).

3.2.11 STATISTICAL ANALYSIS

Statistical analyses were performed using the Prism software (GraphPad, La Jolla, CA). Survival curves were generated using the Kaplan-Meier method, and were compared using a log-rank (Mantel-Cox) test to determine whether differences are significant.

3. 3 RESULTS

3.3.1 B LYMPHOMAS DEVELOPED IN AGING M-TRAF3-/- MICE HAVE UNDERGONE ISOTYPE SWITCHING AND SOMATIC HYPERMUTATION

To determine the clonality of B lymphomas spontaneously developed in aging M-TRAF3$^{-/-}$ mice, we performed Southern blot analysis of the IgH gene of primary B lymphoma samples harvested from the spleen, ascites, liver and mesenteric lymph node (MLN) of diseased M-TRAF3-/- mice. Our results of Southern blot analyses revealed that one or more non-germline bands were present in most of the genomic DNA samples examined, indicating monoclonal or oligoclonal expansion of malignant B cells in these aging M-TRAF3$^{-/-}$ mice (Figure 19). To gain information about the origin, history and partitioning of malignant B cells, we further cloned and sequenced the IgH V(D)J regions of B lymphomas spontaneously developed in 9 individual M-TRAF3$^{-/-}$ mice. The V(D)J regions of IgG isotypes were also cloned and sequenced since the B lymphomas were histopathologically characterized as arising from germinal center (GC) or post-germinal center (GC) B cells (Chapter I). Our initial analysis revealed that 8 out of 9 examined mice show somatic hypermutations (SHM) and all of them showed clonality of isotype switched B cell, thus confirming the GC or post-GC status of these B cells (Table III). Interestingly, the IgV families identified in the examined mice were mainly dominated by two specific IgV clones, namely IGHV5-9-3*01 and IGHV5-17*02 (Table III). These results suggest that two common endogenous antigens drive the GC reaction of two specific clones of B cells across all the 9 examined mice, eventually leading to B lymphoma development in the immunocompromised context of M-TRAF3-/- mice. Taken together, the results from both Southern blot analyses and V(D)J sequencing confirmed our original

histopathological classification of these B lymphomas as DLBCLs or FLs, which were derived from GC or post-GC B cells.

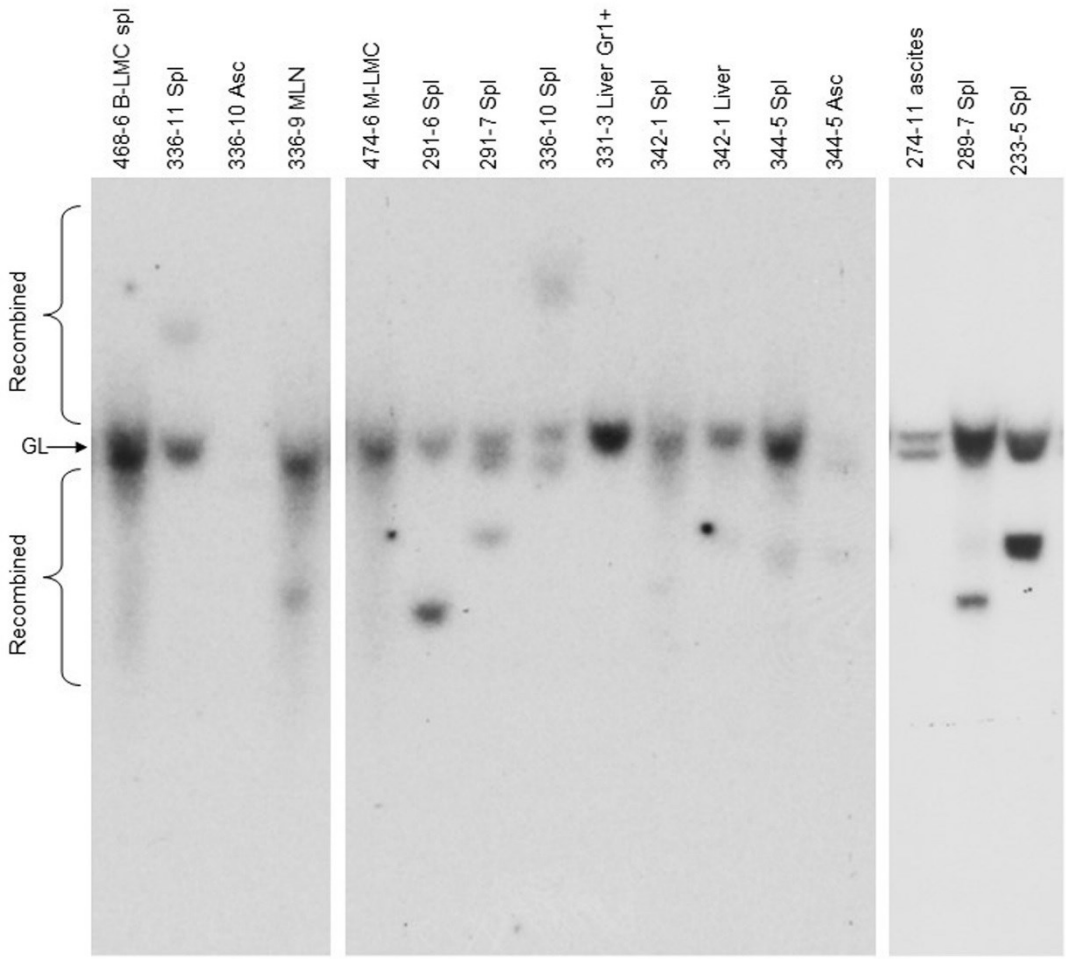

Figure 19: Clonality of the IgH gene of B lymphomas characterized by Southern blot analysis.
Representative Southern blots of the IgH gene rearrangement of B lymphomas from aging M-TRAF3$^{-/-}$ mice are shown. Genomic DNA was prepared from the spleen (SP), ascites (AS), mesenteric LN (MLN), liver, or Gr1+ cells purified from the liver. DNA was digested with EcoRI, and hybridized with a J_H4 probe. Germline bands (GL) of the IgH gene are indicated by arrowheads. All bands of sizes different from the germline band are recombined IgH bands, representing clonal expansion of B lymphoma cells.

Table III: Sequencing of the V(D)J regions of the IgH gene of B lymphomas

Mouse		IgG1		IgG2b		IgG3		Somatic
ID	Tissue	IgV clone	Frequency	IgV clone	Frequency	IgV clone	Frequency	hypermutation
274-11	Ascites	IGHV5-9-3*01	100% (20/20)	IGHV5-9-3*01	93% (14/15)	-	-	Yes
291-6	Spleen	IGHV5-9-3*01	17% (2/12)	IGHV5-9-3*01	95% (21/22)	IGHV5-9-3*01	96% (24/25)	Yes
291-7	Spleen	IGHV5-9-3*01	100% (23/23)	IGHV5-9-3*01	100% (22/22)	IGHV5-9-3*01	95% (20/21)	Yes
336-11	Spleen	IGHV5-9-3*01	21% (4/19)	IGHV5-9-3*01	32% (6/19)	IGHV5-9-3*01	16% (3/19)	No
336-10	Ascites	IGHV5-9-3*01	94% (17/18)	-	-	-	-	Yes
336-9	MLN	IGHV5-9-3*01	32% (6/19)	IGHV5-9-3*01	5% (1/18)	IGHV5-9-3*01	29% (4/14)	Yes
342-1	Liver	IGHV5-9-3*01	15% (3/20)	IGHV5-17*02	25% (5/20)	IGHV5-17*02	6% (2/33)	Yes
	Spleen	IGHV5-17*02	67% (10/15)	IGHV5-17*02	73% (16/22)	IGHV5-17*02	94% (15/16)	Yes
342-3	Spleen	IGHV5-17*02	50% (10/20)	IGHV5-17*02	22% (4/18)	IGHV5-17*02	5% (1/20)	Yes
344-5	Spleen	IGHV5-17*02	10% (2/20)	IGHV5-17*02	41% (7/17)	IGHV5-17*02	65% (11/17)	Yes
	Ascites	IGHV5-9-3*01	72% (13/18)	IGHV5-9-3*01	25% (5/20)	IGHV5-9-3*01	55% (6/11)	Yes

IgH V(D)J regions of primary B lymphomas harvested from aging M-TRAF3$^{-/-}$ mice were cloned and sequenced as described in the methods section. This table summarizes the most frequently occurring IgV clone of each IgG isotype from each sample.

3.3.2 B LYMPHOMAS FROM AGING M-TRAF3$^{-/-}$ MICE ARE TRANSPLANTABLE IN IMMUNODEFICIENT RECIPIENT MICE

To verify the malignant nature of the B lymphomas spontaneously developed in aging M-TRAF3-/- mice, we transplanted primary tumor cells via intraperitoneal (*i.p.*) route to immunodeficient NOD SCID mice, which are highly receptive to foreign cells as they lack T and B cells along with other immune deficiencies [158]. At 6-7 weeks after tumor transplantation, multiple organs were found to have lymphoma infiltrates in the recipient mice including spleen, liver and numerous nodules of peritoneal B lymphomas associated with the intestine (data not shown). Some transplanted NOD SCID mice also had ascites in the peritoneal cavity. Immunophenotypic analysis of these tumors using flow cytometry revealed that both the primary B lymphomas of M-TRAF3-/- mice and the secondary splenic B lymphomas of NOD SCID mice are B220+ IgG^{+} (Figure 20A). These immunophenotypic data also confirmed the Ig isotype switching to IgG as revealed by the

V(D)J sequencing analysis (Table III). Thus these results of transplantation experiments proved that the B lymphomas spontaneously developed in aging M-TRAF3-/- mice are indeed malignant and transplantable in NOD SCID mice.

3.3.3 GENERATION OF CELL LINES FROM TRANSPLANTED B LYMPHOMAS DERIVED FROM AGING M-TRAF3$^{-/-}$ MICE

In order to create new model systems to study tumor immunity and tumor immune surveillance in M-TRAF3$^{-/-}$ mice, we generated cell lines from primary B lymphomas spontaneously developed in two aging M-TRAF3$^{-/-}$ mice (291-6 and 291-7). The primary tumor B cells were passed once through NOD SCID mice and the affected organs with transplanted B lymphomas were harvested and dissociated into single cell suspensions. These cells were cultured *in vitro* in 24-well plates for 4 weeks and malignant clones were identified, which eventually developed into cell lines that are able to propagate via successive passages in culture. Four clones from each original mouse (291-6 and 291-7) were successfully developed into cell lines. These cell lines have been cultured for 5 months without obvious changes in morphology or growth rate. We confirmed the transplantation potential of 291-6 and 291-7 cell lines using NOD SCID mice, in which rapid lymphoma growth killed the recipient mice within 3 weeks (data not shown). We also performed flow cytometric analysis to characterize these B lymphoma cell lines, and representative FACS data from 2 such clones are shown in Figure 20B. Both 291-6 and 291-7 B lymphoma cell lines were immunophenotypically characterized as B220^{+} IgG^{+} (Figure 20B). These B lymphoma cell lines will serve as useful model systems in future *in vivo* experiments to study the role of myeloid cell TRAF3 in tumor immunity and tumor surveillance.

A

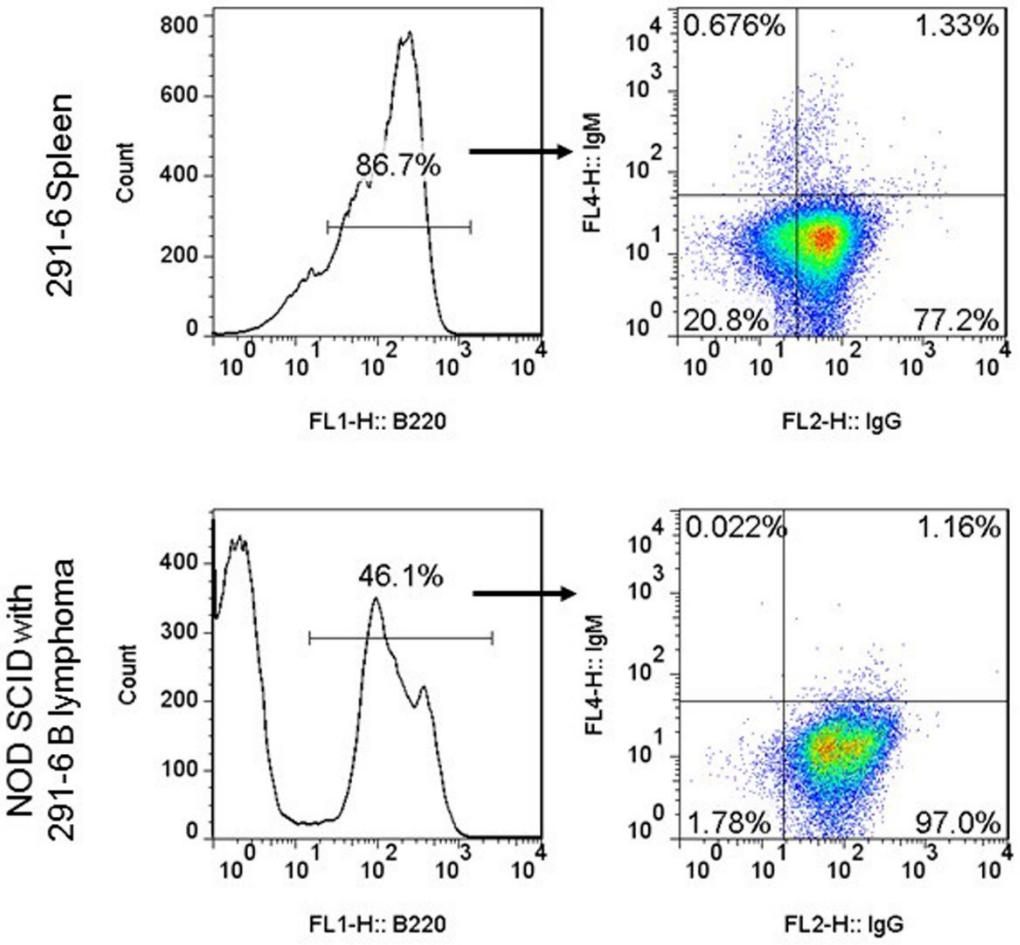
291-6 Spleen
Count
86.7%
FL1-H:: B220
FL4-H:: IgM
0.676%
1.33%
20.8%
77.2%
FL2-H:: IgG
NOD SCID with
291-6 B lymphoma
Count
46.1%
FL1-H:: B220
FL4-H:: IgM
0.022%
1.16%
1.78%
97.0%
FL2-H:: IgG

B

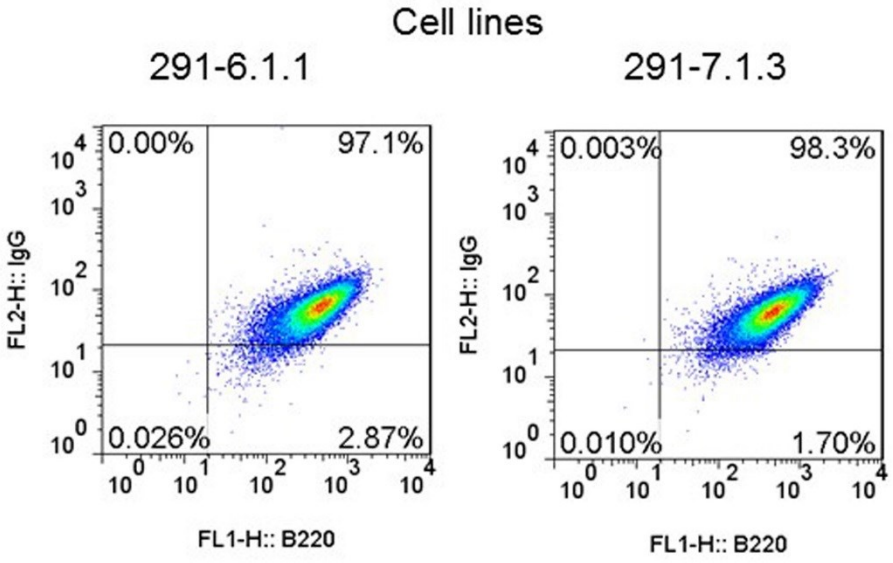
Cell lines
291-6.1.1
291-7.1.3
FL2-H:: IgG
0.00%
97.1%
0.026%
2.87%
FL1-H:: B220
FL2-H:: IgG
0.003%
98.3%
0.010%
1.70%
FL1-H:: B220

Figure 20: Immunophenotypic characterization of B lymphoma cells developed in M-TRAF3 -/- mice.
Splenocytes or B lymphoma cells were stained with Abs to B220 IgM and IgG, and then analyzed by a FACSCalibur. Representative FACS profiles of splenocytes from primary B lymphoma from aging M-TRAF3$^{-/-}$ mouse 291-6 **(A, top panel)**, secondary B lymphoma from NOD SCID mouse transplanted with 291-6 B lymphoma cells **(A, bottom panel),** and B lymphoma cell lines derived from secondary lymphomas from NOD SCID mice transplanted with 291-6 and 291-7 B lymphoma cells **(B)**. B lymphoma cells were identified as B220+ IgG+.

3.3.4 ENDOGENOUS RETROVIRUSES WERE REACTIVATED IN B LYMPHOMAS SPONTANEOUSLY DEVELOPED IN AGING M-TRAF3-/- MICE

To understand the pathological mechanisms underlying B lymphomagenesis observed in M-TRAF3-/- mice, we explored the potential involvement of reactivation of endogenous retroviruses, an oncogenic event commonly observed in immunocompromised mice and humans. Endogenous retroviruses (ERVs) are retrotransposons containing long terminal repeats (LTR) that are formed by integration of ancient and modern exogenous retroviruses into the germline of the host [159]. They are mostly replication defective due to deleterious mutations or transcriptional silencing through the action of diverse mechanisms in healthy individuals [155,160]. However, under pathological conditions such as immunodeficiency, cancer, infection and autoimmunity, the expression levels of ERVs are significantly upregulated [155,160]. It was also recently shown that recombination of defective ERVs can restore infectivity and lead to spontaneous development of leukaemias and lymphoma in antibody-deficient mice [155]. We therefore investigated the expression levels of replication-defective native ERVs and recombined ERVs that could become replication-competent virus in B lymphomas obtained from three individual aging M-TRAF3-/- mice. Interestingly, we found that replication-defective ecotropic murine leukemia virus (eMLV) *env* mRNA was significantly upregulated compared to LMC in two of the three mice examined (291-6 and 291-7; Figure 21). In wild type C57BL6 mice, endogenous eMLV is

transcribed from a single copy of replication-defective *Emv2* locus [155]. Expression of the replication-defective mouse mammary tumor virus (MMTV) *env* mRNA was also significantly upregulated in B lymphomas developed in the third examined mouse (274-11; Figure 21). Most importantly, expression of the reactivated eMLV (RARV; formed by correction of inactivating mutation G-to-C at position 3576 of the *pol* region of *Emv2* locus [155]) was strikingly higher in B lymphomas of mice 291-6 and 291-7 compared to LMC (Figure 21). Interestingly, B lymphomas of mice 291-6 and 291-7 also showed significant upregulation of the ecotropic gp70 envelope glycoprotein, suggesting that the reactivated RARV may be packaged into infectious retroviruses in these B lymphomas. Overall, these results demonstrate the reactivation of ERVs in B lymphomas spontaneously developed in aging M-TRAF3-/- mice, suggesting a potential role of ERV reactivation in B lymphomagenesis observed in M-TRAF3-/- mice.

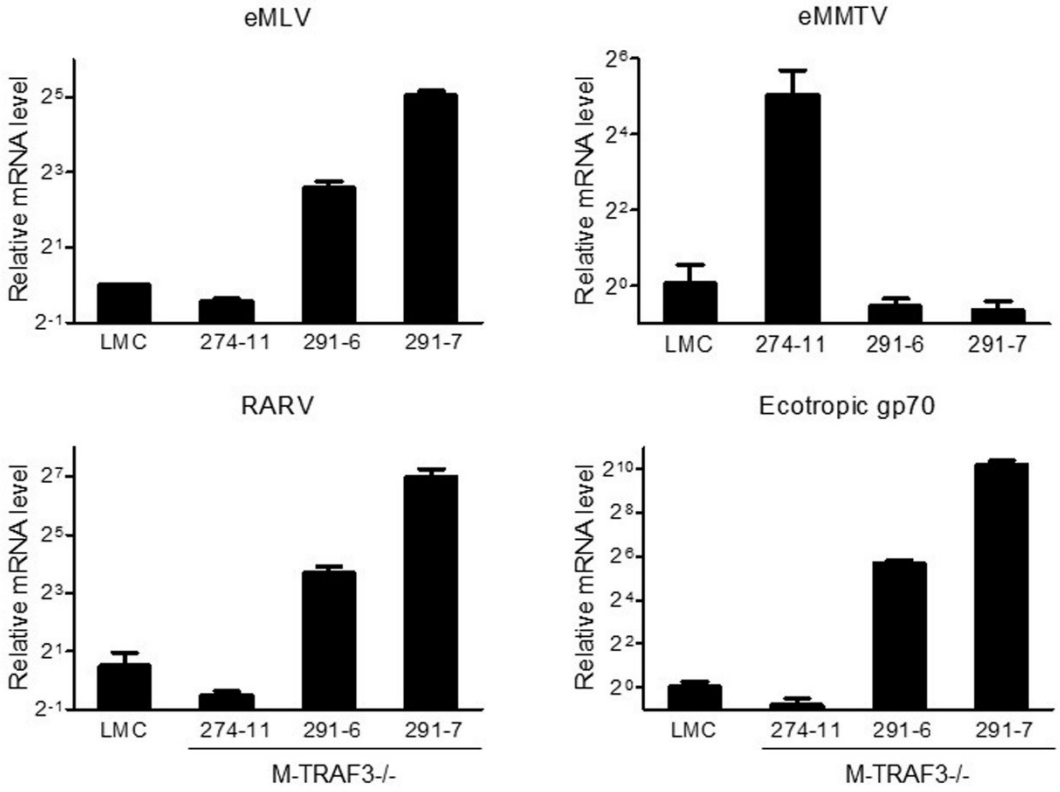

Figure 21: Endogenous retrovirus (ERV) transcripts are upregulated in B lymphoma samples.
Total cellular RNA was extracted from splenocytes of LMC mice and B lymphoma-bearing M-TRAF3-/- mice (274-11, 291-6 and 291-7), and reverse transcribed into cDNA. Quantitative real-time PCR of cDNA was performed using SYBR reagents and primers specific for the transcripts of eMLV, eMMTV, RARV, ecotropic gp70, or hprt. Relative mRNA expression levels of endogenous retroviruses represented as fold-change compared to the LMC sample. The data of ERVs of each sample were first normalized to endogenous control *hprt* mRNA expression, and then fold of change was calculated using ΔΔCt method as described in Methods section. Graphs represent three individual experiments with duplicate reactions in each experiment. eMLV and MMTV represent mRNAs of replication-defective ERVs, whereas RARV and gp70 represent mRNAs of reactivated ERVs that are likely replication-competent.

3.3.5 DEPLETION OF COMMENSAL BACTERIA PREVENTED THE DEVELOPMENT OF B LYMPHOMA IN AGING M-TRAF3-/- MICE

Bacterial products such as lipopolysaccharides (LPS) have been shown to induce the expression of endogenous MLV in mouse cells [161]. Intestinal commensal microbiota have also been implicated in successful transmission of MMTV through mucosal surfaces [162] as well as in inflammation and carcinogenesis via their direct interaction with immune cells following epithelial barrier damage [163-166]. Therefore, we were interested to test the hypothesis that commensal bacteria may induce chronic inflammation and tumor development in M-TRAF3-/- mice, either directly via activation of pro-inflammatory cytokine signaling through TLRs and NLRs or indirectly via reactivation of ERVs or other mechanisms. To address this, we treated M-TRAF3-/- mice with a cocktail of broad spectrum antibiotics to deplete commensal bacteria for four months, and monitored them for development of any abnormalities for up to 22 months of age or until moribund. We first noticed that antibiotic treatment significantly improved the life span of the M-TRAF3-/- mice as compared to the untreated mice (Figure 22). Moreover, out of the 9 antibiotics-treated M-TRAF3$^{-/-}$ mice examined, none had any incidence of B lymphoma, hepatocellular carcinoma, inflammation or infection (Table IV). Interestingly however, we

detected an increase in the incidence of histiocytic sarcomas (Table IV), which is a tumor of interstitial connective tissue resident macrophages called histiocytes [167]. Spontaneous development of these tumors were observed in 9.1% aging M-TRAF3$^{-/-}$ mice as reported in chapter I, and the incidence was increased to 33.3% in aging M-TRAF3$^{-/-}$ mice after treatment with antibiotics for 4 months. This increase is likely due to the prolonged life-span of M-TRAF3-/- mice after treatment with antibiotics, allowing histiocytes to accumulate more oncogenic mutations for malignant transformation. Taken together, these results suggest that commensal bacteria are required for chronic inflammation and B lymphoma development but are not required for histiocytic sarcoma development observed in aging M-TRAF3$^{-/-}$ mice, indicating that TRAF3 is an intrinsic tumor suppressor in histiocytes.

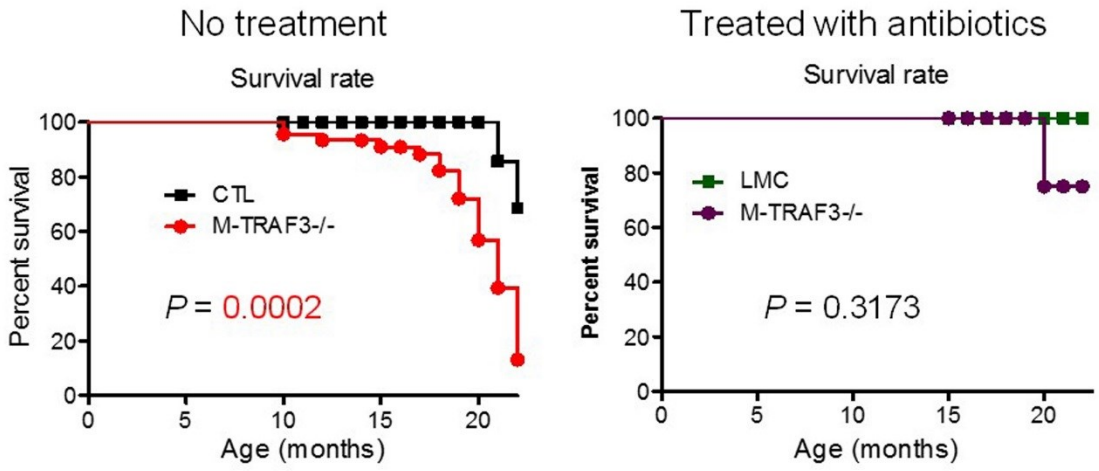

Figure 22: Antibiotic treatment inhibited disease pathogenesis and increased the survival rate in aging M-TRAF3-/- mice.
Mice were treated with a cocktail of broad spectrum antibiotics (Amp + SMZ-TMP) in drinking water for 4 months and their health was monitored for up to 22 months of age. Survival curves of LMC and M-TRAF3$^{-/-}$ mice were generated using the Kaplan–Meier method. P values were determined by the Mantel–Cox log-rank test. n=8-13 for LMC and 8-11 for M-TRAF3-/-.

Table IV: Summary of abnormalities seen in M-TRAF3-/- mice treated with or without antibiotics

Mice examined (15-22 months)	No treatment	Treated with antibiotics
Tumor		
Histiocytosis	**9.1% (2/22)**	**33.3% (3/9)**
Hepatocellular carcinoma	4.5% (1/22)	0 (0/9)
B cell lymphoma (DLBCL or FL)	40.9% (9/22)	0 (0/9)
Inflammation	27.3% (6/22)	0 (0/9)
Bacterial or entamoeba infection	13.6% (3/22)	0 (0/9)
Unknown		
hemorrhage	31.8% (7/22)	0 (0/9)
blister	9.1% (2/22)	0 (0/9)
Normal	31.2% (7/22)	66.7% (6/9)

Mice with or without antibiotic treatment were diagnosed as described in chapter I (Table II).

3.3.6 CHARACTERIZATION OF HISTIOCYTIC SARCOMAS (HS) OBSERVED IN ANTIBIOTICS-TREATED M-TRAF3$^{-/-}$ MICE

Upon treatment with a cocktail of broad spectrum antibiotics, we found that 3 out of the 9 M-TRAF3$^{-/-}$ examined developed HS. Our initial analysis showed that antibiotics-treated M-TRAF3$^{-/-}$ mice with HS display near complete loss of B and T lymphocytes as compared to antibiotics-treated LMC and M-TRAF3-/- mice that did not exhibit pathologies (Figure 23A). M-TRAF3-/- mice with HS contained a significant increase in the percentage of cells expressing low levels of CD14, Gr1, F4/80 and CD11b markers (Figure 23A). Similar expression pattern of Gr1 and CD11b markers were reported in the histiocytic sarcoma cells derived from aging M-TRAF3-/- mice in the absence of antibiotic treatment (Figure 10). Two out of the three M-TRAF3-/- mice with HS (369-2 and 369-4) also displayed significant expansion of myeloid derived suppressor cells (MDSC) (data not shown). Further immunophenotypic analyses revealed that all the three cases of histiocytic sarcoma cells were positive for intracellular markers CD68 and Mac2, which are commonly used for tissue resident macrophages and histiocytes [167,168] (Figure 23B).

Although CD11b expression level on histiocytic sarcoma cells was low in two HS cases (370-8 and 369-2), the majority of the histiocytic cells in the third case (369-4) showed high expression level of CD11b (Figure 23B). Morphological examination of TRAF3-/- HS cells by Wright-Giemsa staining of cytospin slides revealed that these malignant cells displayed the typical morphology of HS cells with abundant eosinophilic cytoplasm, and accompanied by frequent mitotic figures and occasional multinucleated giant cells (Figure 23C).

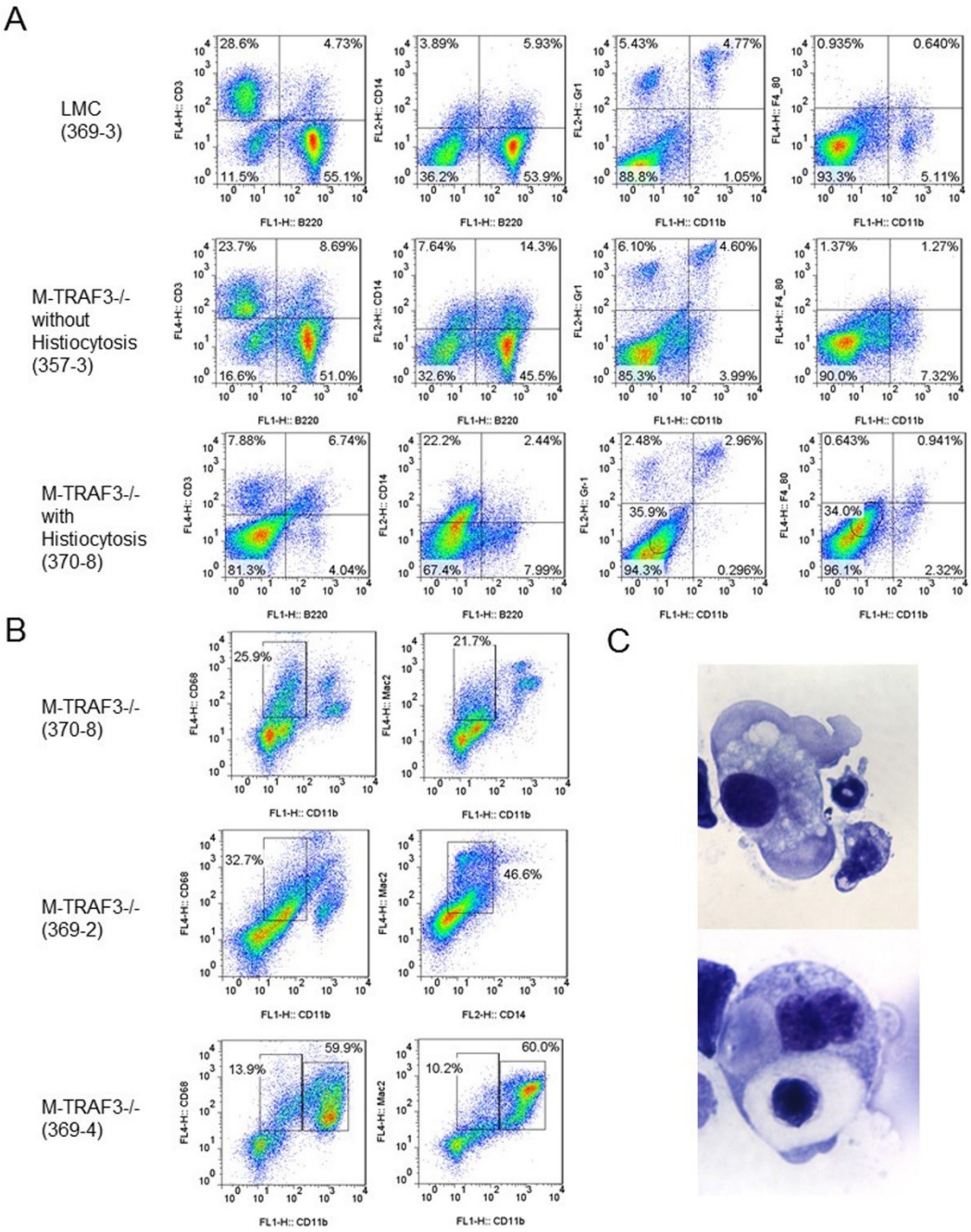

Figure 23: Characterization of histiocytic sarcomas from antibiotics-treated M-TRAF3-/- mice.

(A) Representative FACS profile of splenocytes from antibiotics-treated LMC and M-TRAF3-/- mice using surface markers. **(B)** Representative FACS profile of splenocytes from antibiotics-treated M-TRAF3$^{-/-}$ mice with histiocytic sarcomas using intracellular markers. **(C)** Representative micrographs of splenocytes harvested from an antibiotics-treated M-TRAF3$^{-/-}$ mouse (369-4). A large histiocytic sarcoma cell with abundant eosinophilic cytoplasm accompanied by 2 MDSC are shown in the top panel, and another giant histiocytic sarcoma cell with clearly visible multinucleated morphology is shown in the bottom panel.

3.3.7 HISTIOCYTIC SARCOMAS SPONTANEOUSLY DEVELOPED IN M-TRAF3$^{-/-}$ MICE ARE TRANSPLANTABLE IN NOD SCID MICE

To determine the malignant nature of histiocytic sarcomas spontaneously developed in antibiotics-treated M-TRAF3-/- mice, we transplanted HS-containing splenocytes of M-TRAF3-/- mice intraperitoneally into immunodeficient NOD SCID recipient mice. At 3-4 months after transplantation, tumor growth was observed in multiple systems including intestine, spleen and liver in NOD SCID recipient mice. Immunophenotypic analysis revealed that the histiocytic sarcoma cells grown in transplanted NOD SCID mice exhibited similar expression profiles of markers to those observed in the primary HS population of M-TRAF3-/- mice (Figure 23B and 24A). HS cells grown in the intestine and liver of transplanted NOD SCID mice exhibited high expression levels of CD68, Mac2, CD11b and CD14 markers, whereas the spleen contained heterogeneous HS populations with varying expression levels of these 4 examined markers (Figure 24A). Thus, our results of transplantation experiments demonstrate that the histiocytic sarcoma cells spontaneously developed in antibiotics-treated M-TRAF3$^{-/-}$ mice are malignant and transplantable in immunodeficient recipient mice.

3.3.8 GENERATION OF CELL LINES FROM TRANSPLANTED TRAF3-/- HISTIOCYTIC SARCOMAS

Molecular mechanisms underlying the tumorigenesis of histiocytes are poorly understood. To generate new model systems that allow us to gain insights into this area, we sought to generate HS cell lines from transplanted histiocytic sarcoma cells using a similar approach as described under section 3.2.2 for the generation of B lymphoma cell

lines. Briefly, after one or two passages through NOD SCID mice, tumor cells were harvested from the spleen or liver, and cultured *in vitro* continuously. Malignant clones were selected and further propagated *in vitro* via successive passages. Interestingly, immunophenotypic characterization of two HS cell lines generated revealed that there two distinct populations of histiocytic sarcoma cells in each cell line, which differ in terms of their expression levels of markers CD11b, CD68, F4/80 and CD14 (Figure 24B). Specifically, one HS cell population in the cell lines is $CD11b^{hi}$ $Mac2^{hi}$ CD68+ F4/80+ CD14+ Gr1-, and the other HS cell population is characterized as $CD11b^{low}$ $Mac2^{hi}$ CD68- F4/80- CD14- Gr1-. Nevertheless, the positive expression of CD11b and Mac2 on both populations confirms their HS origin. These HS cell lines will serve as important model systems in future studies to better understand the intrinsic role of TRAF3 in suppressing the tumorigenesis of histiocytes as well as the underlying mechanisms.

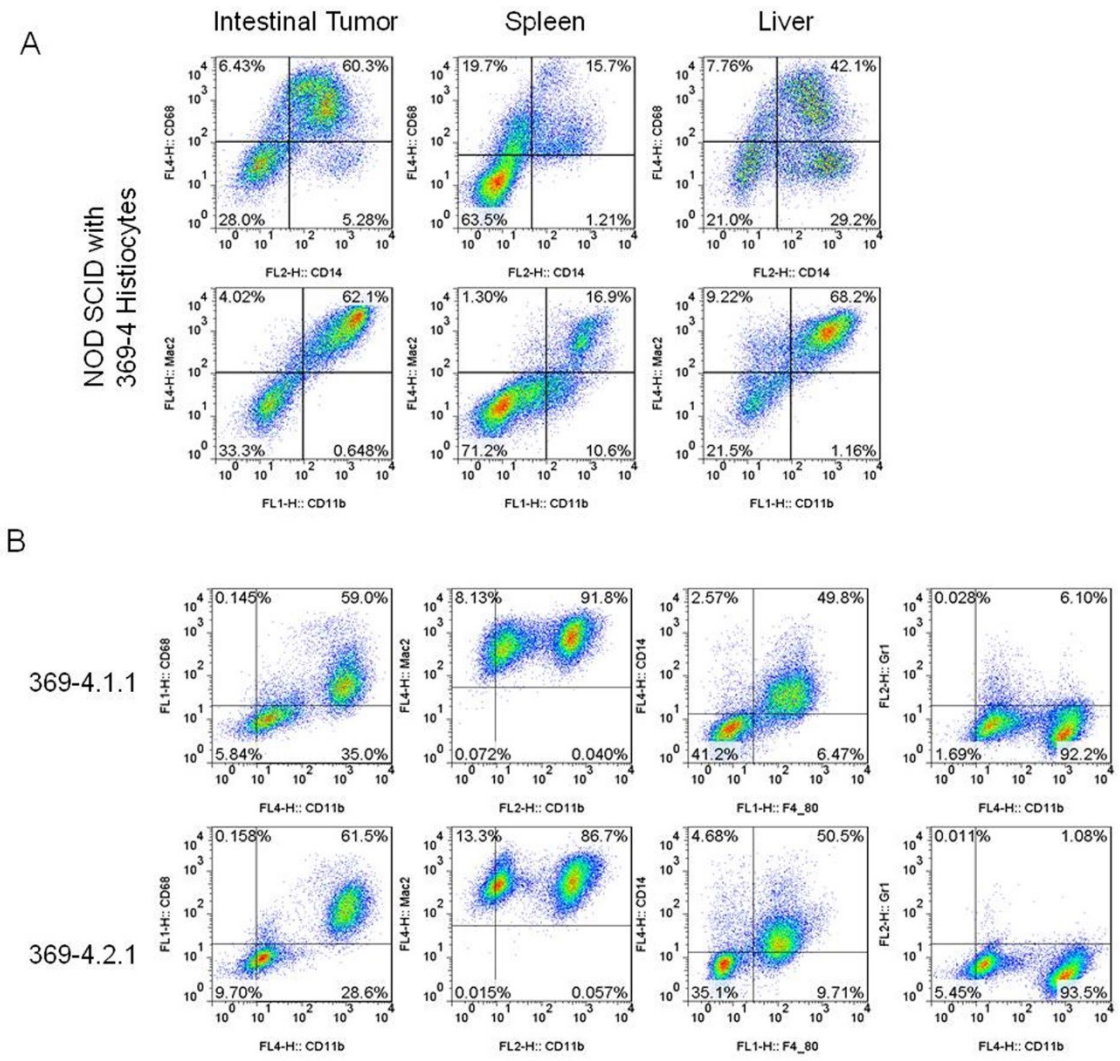

Figure 24: Immunophenotypic characterization of transplanted TRAF3-/- histiocytic sarcomas and HS cell lines generated in this study.
(A) Representative FACS profiles of cells harvested from the spleen, liver, and peritoneal tumors associated with intestines of NOD SCID mice transplanted with primary HS cells of an antibiotics-treated M-TRAF3-/- mouse (369-4). **(B)** Representative FACS profiles of histiocytic sarcoma cell lines derived from transplanted HS tumor cells of mouse 369-4. Two distinct populations of histiocytic sarcoma cells are identified in each HS cell line: one is CD11b^{hi} Mac2^{hi} CD68+ F4/80+ CD14+ Gr1-, and the other is CD11b^{low} Mac2^{hi} CD68- F4/80- CD14- Gr1-.

3.4 DISCUSSION AND CONCLUSIONS

In this chapter, we demonstrated that the B lymphoma cells observed in M-TRAF3$^{-/-}$ mice were originated from GC or post- GC B cells since they have undergone SHM and class switch recombination. Moreover, these cells are monoclonal or oligoclonal. Interestingly, the heavy chain genes of these B lymphomas show strong preference for IGHV5-9-3*01 and IGHV5-17*02 clones and are often switched to IgG isotypes, including IgG1, IgG2b and IgG3. Notably, the B lymphomas show significant upregulation of native and reactivated ERVs. Furthermore, we found that B lymphoma development along with other abnormalities observed in aging M-TRAF3-/- mice can be prevented by depletion of commensal bacteria, with the exception of HS. In contrast, the occurrence of HS was more frequent in antibiotics-treated aging M-TRAF3-/- mice and the TRAF3-/- HS cells were characterized as CD68^{+} Mac2^{+} cells with abundant eosinophilic cytoplasm or multinucleated giant cell morphology. Taken together, our results indicate that commensal bacteria are required for chronic inflammation and B lymphoma development but are not required for histiocytic sarcoma development observed in aging M-TRAF3$^{-/-}$ mice. These data provide conclusive evidence demonstrating that TRAF3 is an intrinsic tumor suppressor in tissue-resident macrophages - histiocytes.

Endogenous retroviruses are germline encoded and constitute approximately 10% of the mouse genome and 8% of the human genome[159]. The expression of ERVs is tightly controlled in C57BL/6 mice via epigenetic silencing mechanisms such as DNA[169] and histone methylation[170] and via cell-intrinsic mechanisms that prevent successful viral replication through functions of Apobec3, TRIM5-α, tetherin and SAMHD1[171,172]. However, in pathological conditions including cancer and infection, the expression of

ERVs is significantly upregulated[155,160]. In support of this, we found significantly upregulated ERV transcripts in B lymphomas harvested from aging M-TRAF3-/- mice (Figure 21). B lymphoma is the most frequent type of tumor observed in these mice and this could be explained by several mechanisms linking to findings obtained in this chapter [124]. One possible mechanism could be induction of tumor by recombined ERVs observed in B cells either via insertional mutagenesis involving activation of oncogenes or disruption of tumor suppressor genes or via other mechanisms [173]. In support of this, Johnson et al., demonstrated that aggressive B-cell leukemia can be developed by participation of repetitive MuLV-related ERV sequences in aberrant end-joining events [174]. They identified a novel class of activating mutations in *Fms-like tyrosine kinase 3 (Flt3)*, a receptor tyrosine kinase important for normal hematopoiesis, which was created by complex genomic rearrangements with Moloney leukemia virus (MuLV)-related endogenous retroviral (ERV) elements in Rag-2$^{-/-}$p53$^{-/-}$Prkdc$^{scid/scid}$ triple-mutant (TM) mice [174]. Moreover, Young et al., reported development of B and T cell lymphomas in thymus, spleen and liver of aging *Rag1*$^{-/-}$ mice which showed significant upregulation of recombined and fully infectious MLV [155]. Furthermore, they observed that the infectious ERVs in *Rag1*$^{-/-}$ mice exhibited B cell-tropism [155]. Since, such a mechanism is highly likely, it would be interesting to check the DNA integration sites of activated ERVs against commonly associated oncogenes and tumor suppressors in B lymphoma from M-TRAF3-/- mice [157,175].

In addition to ERVs, a second possible mechanism of high incidence of B lymphoma development observed in aging M-TRAF3$^{-/-}$ mice could be activation of B cells by opportunistic strains of commensal bacteria known as Pathobionts. This may drive

specific clones of B cells to undergo massive proliferation, affinity maturation and Ig isotype switching processes in germinal centers (GC), leading to a precise humoral adaptive immune response against the pathobionts [52-54]. In this regard, B cells are especially susceptible to genetic alterations due to the unique features of GC reactions, which include somatic hypermutation (SHM) and class switch recombination (CSR) of Ig genes. All of these processes produce double strand DNA breaks (DSBs), which increase the risk of genomic instability in B cells [92-94]. Moreover, proliferating cells like B and T cells are targets of spontaneous mutations and retroviral transformation, and therefore more susceptible to leukemia or lymphoma development [176,177]. Zeng et. al. recently reported that activation of mouse B cells *in vivo* by immunization with T-cell independent type 2 antigen leads to upregulation of ERV RNAs in antigen-specific B cells, which is required for specific IgM production [178]. In support of this, we found bacteria and Entamoeba infections in aging M-TRAF3-/- mice (chapter I), and confirmed the origin of B lymphoma cells as GC or post-GC and having undergone SHM (Table III). Most notably, our initial investigation showed that depletion of commensal bacteria by antibiotic treatment prevented the development of B lymphoma, chronic inflammation and infection in aging M-TRAF3$^{-/-}$ mice. Overall, these results point towards a role of commensal bacteria in B lymphomagenesis in the context of TRAF3 deficiency in myeloid cells. However, further investigation is warranted to better understand the underlying complex molecular mechanisms.

Surprisingly, antibiotic treatment of M-TRAF3-/- mice leads to greater incidence of HS. HS in humans is a rare malignancy with a dismal prognosis, and its pathologic and cytogenetic data are sparse [179-181]. Because the genetic etiology of HS is largely unknown

and patients with HS respond poorly to conventional chemotherapy, there is no standard therapy for human HS [179-181]. In M-TRAF3$^{-/-}$ mice with histiocytic sarcomas, whitish nodules of tumors are observed in the liver, and tumor cells are also identified as the major cell type in the spleen that disrupt the splenic architecture [124]. TRAF3$^{-/-}$ histiocytic sarcomas have the typical morphology of HS cells with abundant eosinophilic cytoplasm, and accompanied by frequent mitotic figures and occasional multinucleated giant cells and erythrophagocytosis [124] (Figure 23). Immunophenotypically, TRAF3$^{-/-}$ HS cells were identified as CD68^{+}Mac2^{+}CD11b^{+}, and are negative for markers of the B and T lymphoid lineages, including B220, CD19, IgM, CD3, CD4, and CD8 and granulocytic lineage marker Gr1 [124] (Figure 23 and data not shown). The predominance of HS in antibiotics-treated aging M-TRAF3-/- mice led us to hypothesize that HS is a late-onset tumor and its lower frequency in aging M-TRAF3-/- mice could be due to relatively early onset of B lymphoma and chronic inflammation proceeding to death of the affected animal and denying a chance for HS to take its root. The results of antibiotics treatment experiments also showed that commensal bacteria do not play a critical role in the development of HS, indicating that a cell intrinsic mechanism is at play as a consequence of TRAF3 deficiency in this cell type. We speculate that TRAF3 deficiency may gradually cause prolonged survival or increased proliferation of histiocytes, and eventually result in the development of HS in M-TRAF3$^{-/-}$ mice. Detailed tumorigenesis mechanisms of TRAF3-/- histiocytes remain to be investigated in future studies.

Similar to M-TRAF3$^{-/-}$ mice, several other mouse models were previously reported to spontaneously develop histiocytic sarcomas, including p21$^{-/-}$ [182], Cyp1b1$^{-/-}$ [183], p19ARF$^{-/-}$Bax$^{-/-}$ [184], PTEN$^{-/-}$INK4a/ARF$^{-/-}$ [179], Dok1$^{-/-}$Dok2$^{-/-}$Dok3$^{-/-}$ [185], and humanized TLR7/TLR8

transgenic [186] mice, implicating these genes in the pathogenesis of HS. Among these, TRAF3 is functionally linked to TLR7, TLR8, and DOK3 [10,187]. TRAF3 is recruited to the TLR7 and TLR8 signaling complex through direct interaction with MyD88 [10] (Figure 2). Snyder et al. found that transgenic expression of human TLR7/TLR8 in mice deficient for endogenous TLR7/TLR8 drives proliferative histiocytosis with multisystem infiltration of histiocytes that efface normal tissue architecture [186]. Compound deletion of MyD88 in humanized TLR7/TLR8 transgenic mice prevents the inflammatory phenotype and the development of HS, suggesting that the illness is caused by constitutive activation of humanized TLR7/TLR8 and exuberant MyD88-mediated signaling [186]. Interestingly, a recent study by Kim et al. identified TRAF3 as a new interacting protein for DOK3, a negative regulator of protein tyrosine kinase-mediated signaling [187]. As observed in $TRAF3^{-/-}$ macrophages, $DOK3^{-/-}$ macrophages are also impaired in IRF3 phosphorylation and IFNβ production upon influenza virus infection or polyI:C stimulation [187]. Some $DOK3^{-/-}$ mice exhibit abnormal accumulation of macrophages in the lung, and $Dok1^{-/-}$ $Dok2^{-/-}Dok3^{-/-}$ mice succumb to spontaneous HS at a high incidence [185]. Taken together, the above findings reinforce the notion that dysregulation of TRAF3-dependent signaling pathways in macrophages contributes to the pathogenesis of histiocytic sarcoma.

Overall, the results presented here provide significant evidence for the involvement of commensal bacteria and ERVs in the pathogenesis of B lymphoma and chronic inflammation observed in $M\text{-}TRAF3^{-/-}$ mice and also for the unique cell intrinsic mechanism of TRAF3 in suppressing the malignant transformation of histiocytes. It would therefore be interesting to further dissect the underlying molecular mechanisms to gain a better understanding of these two types of cancer in the context of TRAF3 loss in myeloid

cells. The B lymphoma and HS cell lines developed in this study will be instrumental in achieving these goals in future studies.

SIGNIFICANCE

Studying the roles of TRAF3 has clinical relevance since alteration in its function is associated with several human diseases. Given its significant role in the homeostasis of B cells, deletions, inactivating mutations and single nucleotide polymorphisms (SNPs) of TRAF3 are frequently detected in primary human samples of various B cell malignancies including multiple myeloma, splenic marginal zone lymphoma, Hodgkin lymphoma, B cell chronic lymphocytic leukemia, mantle cell lymphoma, Waldenström's macroglobulinemia and diffuse large B-cell lymphoma [4]. Recently, a heterozygous germline mutation of TRAF3 (R118W) was found in a young patient with a history of herpes simplex encephalitis[115]. The mutation is a loss-of-function, loss-of-expression and dominant negative one which leads to defective type I IFNs and enhanced pro-inflammatory cytokine expression in myeloid cells. Such a role of TRAF3 in myeloid cells was corroborated by our *in vivo* mouse model – M-TRAF3$^{-/-}$ mice, suggesting conservation of TRAF3 functions between mice and humans. The results from the study of M-TRAF3$^{-/-}$ mice by our lab and other groups have linked TRAF3 deficiency in myeloid cells to the pathogenesis of tumors, inflammatory diseases, metabolic diseases, and infectious diseases [124,151,188] . Therefore, these findings suggest that disruption of TRAF3-dependent signaling pathways might be one of the leading causes of the above mentioned diseases and that restoration of TRAF3 signaling pathways could be a potential therapeutic strategy for their successful treatment.

Restoration of TRAF3 signaling could also lead to suppression of MDSC population in the context of cancer and chronic inflammation as supported by our results presented in the present study. MDSC, a heterogeneous group of immature myeloid cells, are recognized as primary drivers of immune suppression and chronic inflammation in

tumor microenvironment [76,118]. MDSC potently suppress both tumor-specific CD8 cytotoxic T cell responses and anti-tumor innate immune responses, and promote angiogenesis, invasion and metastasis of solid tumors [74,118,119]. Therefore, intensive efforts are currently directed at developing therapeutic agents and strategies to target MDSC for the prevention and treatment of cancers [74,118]. Our results demonstrated that TRAF3 is a critical regulator of MDSC expansion in chronic inflammation. Further research in this line will lead to a better understanding of the role of TRAF3 signaling in regulating MDSC physiology and will provide a novel approach for targeting this highly immune-suppressive and tumor promoting cell type in disease settings.

Finally, we obtained interesting findings that endogenous retroviruses (ERVs) are reactivated in B lymphomas spontaneously developed in aging M-TRAF3$^{-/-}$ mice and that commensal bacteria are required for chronic inflammation and B lymphoma development in these mice. Further research efforts in the study of reactivated ERVs identified in B lymphomas derived from M-TRAF3$^{-/-}$ mice could lead to identification of new tumor-specific antigens, elucidation of novel mechanisms of B lymphomagenesis, and development of novel tumor-specific immunotherapy. Such a possibility is supported by reports from the study of human endogenous retroviruses (HERV) in at least three different types of human cancers - gastrointestinal cancer, clear cell kidney cancer and breast cancer [189-191]. All of these cancers showed tumor-specific expression of unique HERV proteins, which were highly immunogenic and were the target of humoral and cell-mediated immune responses launched by antigen-specific B cells and T cells, respectively [189-191]. In summary, my dissertation research has led to a better understanding of the *in vivo* functions of TRAF3 in myeloid cells and has provided new avenues for therapeutic intervention of

inflammatory diseases, infectious diseases and cancers in the context of TRAF3 deficiency in myeloid cells.

SUMMARY AND DISCUSSION

TRAF3 is a cytoplasmic adaptor protein that is involved in signaling downstream of a variety of adaptive and innate immune receptors as well as cytokine receptors [10,24]. TRAF3 is a highly versatile regulator of different lymphocyte subpopulations, including B and T cells, in the adaptive immune system and serves as a tumor suppressor in B lymphocytes [192]. Previous *in vitro* evidence indicates that TRAF3 regulates pro-inflammatory cytokine and type I IFN production in myeloid cells including macrophages and DCs [26,27]. However, the *in vivo* functions of TRAF3 in myeloid cells had remained unexplored. My dissertation research presented here has addressed this significant gap in knowledge by using a newly created mouse model, where TRAF3 is specifically deleted from myeloid cells (M-TRAF3-/-). We found that deletion of TRAF3 from myeloid cells does not affect the development and homeostasis of myeloid cells, but leads to interesting changes in young adult M-TRAF3-/- mice in response to different stimuli. These include enhanced pro-inflammatory cytokine production upon stimulation of TLR3 and TLR4 receptors and also enhanced antibody production of selected isotypes in response to T-cell independent and dependent antigens. As M-TRAF3-/- mice age (15-22 months old) they develop abnormalities ranging from chronic inflammation and infection to development of tumors including TRAF3-sufficient B lymphomas and hepatocellular adenoma and TRAF3-deficient histiocytic sarcomas (HS), resulting in decreased lifespan compared to littermate control mice. Moreover, these mice showed substantial expansion of immature and immunosuppressive myeloid cells called myeloid derived suppressor cells (MDSC) and upregulation of several cytokines and chemokines that are implicated in chronic inflammation and tumor development. Our results thus provide conclusive *in vivo* evidence

that TRAF3 is a critical regulator of chronic inflammation and a new tumor suppressor in myeloid cells.

Our new model of chronic inflammation in young adult M-TRAF3-/- mice by repeated BCG injections reasserted the inhibitory role of myeloid cell TRAF3 in chronic inflammation and as a suppressor of MDSC expansion. In addition, further analysis of B lymphomas developed in aging M-TRAF3-/- mice showed that they are either monoclonal or oligoclonal and display significantly high expression of native and reactivated endogenous retroviruses (ERVs). The development of chronic inflammation and B lymphomas is prevented by treatment with broad spectrum antibiotics, indicating the requirement of commensal microbiota for the development of chronic inflammation and B lymphomas observed in aging M-TRAF3-/- mice. However, antibiotic treatment does not affect HS development pointing towards a cell intrinsic role of TRAF3 in suppressing the oncogenesis of this tumor type. Taken together, the results from my dissertation research establish myeloid cell TRAF3 as a critical regulator of innate and adaptive immune responses that is required to maintain tissue homeostasis, host-commensal mutualism and successful suppression of endogenous retroviruses to prevent development of cancer and chronic inflammation.

The anti-inflammatory role of myeloid cell TRAF3 is further supported by two other groups from the study of similar M-TRAF3$^{-/-}$ mouse model. Jin J. et. al., showed that in a dextran sulfate sodium (DSS)-induced colitis model, M-TRAF3$^{-/-}$ mice exhibit exacerbated colon inflammation, as demonstrated by reduced survival rate, worsened bodyweight loss, as well as more severe mucosal damage and colon shortening [151]. Moreover, colonic macrophages purified from the DSS-treated M-TRAF3$^{-/-}$ mice express

significantly higher levels of proinflammatory cytokines, including IL-6, IL-12 and IL-23 [151]. Chen et al. also found a similar anti-inflammatory role of myeloid cell TRAF3 in lean mice. Interestingly however, they observed that the anti-inflammatory function of TRAF3 in macrophages is not static, but is dynamically modulated according to the metabolic states [188]. Macrophages in adipose tissue and the liver are the major mediators of metabolic inflammation, promoting insulin resistance and metabolic disease progression in obesity [193]. Obesity is associated with chronic, low-grade inflammation, which contributes to insulin resistance and metabolic disease [193]. Chen et al. found that myeloid cell-specific deletion of TRAF3 has opposite effects on inflammation between lean and obese mice [188]. In lean mice, myeloid cell-specific deletion of TRAF3 increases the expression of proinflammatory cytokines in the liver and adipose tissue [188]. In contrast, TRAF3 deficiency in myeloid cells decreases the expression of proinflammatory cytokines in the liver and adipose tissue of obese mice, and largely prevents high-fat diet (HFD)-induced inflammation in these metabolic tissues [188]. Consequently, M-TRAF3$^{-/-}$ mice exhibit significantly attenuated insulin resistance and hepatic steatosis in models of either genetic (ob/ob) or HFD-induced obesity [188]. Chen et al. also showed evidence to suggest that in obese state, TRAF3 may promote metabolic inflammation by increasing the expression of proinflammatory cytokines in myeloid cells and by facilitating macrophage infiltration into metabolic tissues [188]. Thus, during metabolic inflammation and obesity progression, TRAF3 functionally switches its activity from anti-inflammatory to pro-inflammatory modes in macrophages, but in normal physiological conditions it plays an anti-inflammatory role[188].

To understand the mechanisms underlying TRAF3-mediated inhibition of proinflammatory cytokine production, several groups have carefully compared the early signaling events of TLR4 engagement in macrophages in the presence or absence of TRAF3. The findings from these investigations indicate that elevated production of proinflammatory cytokines IL-6, IL-12 and IL-23 in response to TLR4 stimulation observed in TRAF3-deficient macrophages could not be attributed to the hyperactivation of MAPKs and constitutive activation of the NIK-NF-κB2 pathway only plays a minor role in mediating the hyper-induction of the proinflammatory cytokine IL-23 [26,124,151]. Rather, recent findings point towards a major role of c-Rel and IRF5 in the hyper-induction of above mentioned proinflammatory cytokines. As revealed by Jin et al., TRAF3 constitutively binds to c-Rel and IRF5, and therefore is responsible for recruiting c-Rel and IRF5 to the TRAF3-TRAF2-cIAP1/2 complexes [151]. In these complexes, the E3 ligases cIAP1/2 catalyze the K48-linked ubiquitination on c-Rel and IRF5, thereby targeting them for proteasome-mediated degradation in resting macrophages [151]. Indeed, elevated protein levels of c-Rel and IRF5 are observed in both TRAF3- and TRAF2-deficient macrophages in the absence of stimulation [151]. TRAF2$^{-/-}$ macrophages also exhibit hyper-induction of proinflammatory cytokines in response to TLR4 stimulation and M-TRAF2$^{-/-}$ mice are also more susceptible to DSS-induced colon inflammation [151]. It is known that c-Rel is specifically required for TLR-stimulated expression of IL-12 and IL-23 [151,194,195]. Similarly, IRF5 mediates the expression of multiple proinflammatory cytokines, including IL-6, IL-12, and IL-23, and inhibits the expression of the anti-inflammatory cytokine IL-10 [151,196]. Taken together, the above findings support the model that stabilized c-Rel and IRF5 are the major transcription factors that drive the hyper-induction of the

proinflammatory cytokines IL-6, IL-12, and IL-23 in TRAF3- or TRAF2-deficient macrophages in response to TLR agonists (Figure 25A).

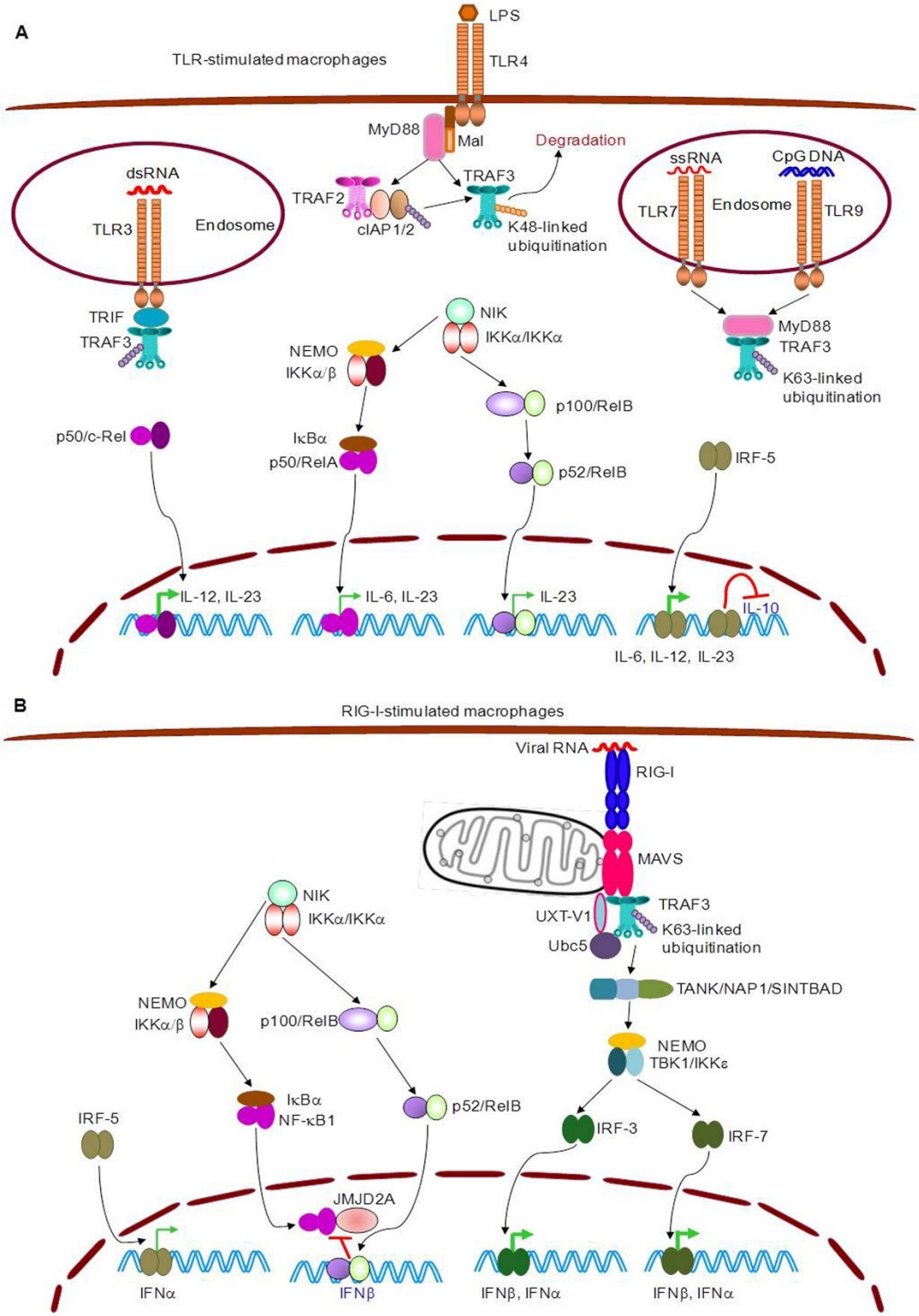

Figure 25: TRAF3 in pro-inflammatory cytokine and type I interferon signaling.
(A) TRAF3 inhibits TLR-induced proinflammatory cytokine production in macrophages. In response to LPS stimulation, dimerized or oligomerized TLR4 recruits Mal and MyD88, which in turn recruits TRAF3 and the associated TRAF2-cIAP1/2 complex to the receptor signaling complex at the plasma membrane. This allows the activation of cIAP1/2 to target TRAF3 for K48-linked ubiquitination and degradation. Similarly, stimulation of TLR7 by ssRNA or stimulation of TLR9 by CpG DNA also recruits TRAF3 via MyD88, while engagement of TLR3 by dsRNA recruits TRAF3 via TRIF to the receptor signaling complexes at the endosome membrane. Recruitment of TRAF3 by dimerized or oligomerized TLRs via MyD88 or TRIF disrupts the interaction between TRAF3 and NIK, c-Rel, or IRF5. This results in the accumulation of NIK, c-Rel and IRF5, and subsequent activation of NF-κB2 (p52/RelB), p50/c-Rel, and IRF5, which promote the expression of the proinflammatory cytokines IL-6, IL-12, and IL-23 in stimulated macrophages. In addition, nuclear IRF5 also inhibits the expression of the anti-inflammatory cytokine IL-10. Ablation of TRAF3 from macrophages mimics TLR engagement and also releases NIK, c-Rel and IRF5 from the TRAF2-cIAP1/2 complexes, allowing the accumulation of NIK, c-Rel and IRF5. Therefore, TLR agonists induce enhanced production of the proinflammatory cytokines IL-6, IL-12 and IL-23 but decreased production of the anti-inflammatory cytokine IL-10 in TRAF3-/- macrophages. Transcription factors (p50/c-Rel and IRF5) that play major roles in driving the production of IL-6, IL-12 and IL-23 are shown in bold green arrows. TRAF3-independent TLR signaling pathways, including TRAF6- or TRAF2-induced activation of ERK1/2, p38, JNK1/2 and NF-κB1 (p50/RelA), are not depicted in the figures. **(B)** Roles of TRAF3 in type I IFN production induced by RIG-I signaling. Upon viral RNA binding, RIG-I recruits TRAF3 via MAVS to the receptor signaling complex at the mitochondrial membrane. This induces the self-ubiquitination of TRAF3 and subsequent activation of TBK1/IKKε, leading to the activation and nuclear translocation of IRF3 and IRF7 to promote the expression of IFNβ and IFNα in infected macrophages. Similar to TLR signaling, recruitment of TRAF3 by engaged RIG-I via MAVS also allows the accumulation of IRF5 and NIK, which promotes the expression of IFNα and inhibits the expression of IFNβ, respectively. Therefore, TRAF3-/- macrophages are defective in producing type I IFN in response to TLR agonists or viral infections, due to both impaired activation of stimulatory IRFs (IRF3 and IRF7) and constitutive activation of repressive NIK-NF-κB2. TRAF3-independent TLR or RIG-I signaling pathways, including TRAF6- or TRAF2-induced activation of MAPKs and NF-κB1, are not depicted in the figures.

Previous *in vitro* evidence indicates that TRAF3 is required for the innate anti-viral responses and type I IFN production triggered by TLRs or RLRs in macrophages and DCs [26,27,77]. Consistent with this, TLR4-induced expression of *Ifnb* and *Ifna4* is almost abolished and phosphorylation of IRF3 is markedly reduced in BMDMs and PEMs derived from M-TRAF3$^{-/-}$ mice [124,151]. Moreover, Jin et al. obtained an interesting finding that another signaling pathway affected by TRAF3 deletion, constitutive activation of NIK-IKKα-NF-

κB2, also contributes to the defective type I IFN production observed in TRAF3$^{-/-}$ macrophages [25]. Macrophages derived from NIKΔT3-transgenic mice overexpressing a stable form of NIK, which lacks its TRAF3-binding motif and thus results in constitutive activation of IKKα-NF-κB2, show remarkably impaired production of type I IFN in response to TLR agonists [25]. Jin et al. further revealed that NF-κB2suppresses TLR or RLR-induced histone modifications at the *Ifnb* promoter, an action that involves attenuated recruitment of the transactivator RelA and the histone demethylase JMJD2A[25]. It is known that JMJD2A, recruited to the *Ifnb* promoter by RelA, induces activating modifications of histone H3 such as trimethylation of H3K4 (H3K4me3) and H3 acetylation (H3Ac), and also decreases the repressive histone modifications such as H3K9me2 and H3K9me3 [25,197]. Elevated nuclear levels of NF-κB2 (p52-RelB) lead to inhibition of RelA-JMJD2A recruitment to the *Ifnb* promoter, as p52-RelB bind to the *Ifnb* promoter more strongly than RelA [25]. Consequently, RelA-JMJD2A-mediated activation of chromatin structures at the *Ifnb* promoter is suppressed by constitutive NF-κB2 activation, which is present in TRAF3$^{-/-}$ macrophages [124,151]. Taken together, TRAF3 promotes TLR- or RLR-induced type I IFN production by facilitating the phosphorylation of IRF3 and IRF7 via its adaptor function and E3 ligase activity, and also by suppressing the inhibitory roles of the NIK-IKKα-NF-κB2 pathway via targeting NIK for degradation (Figure 25B).

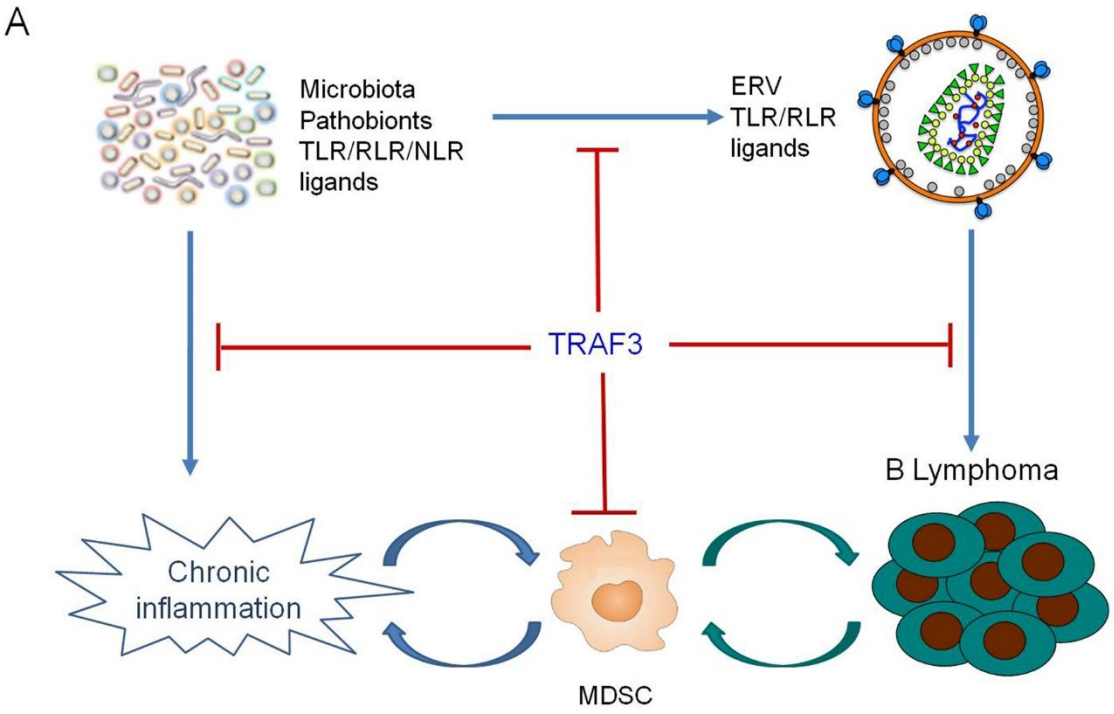
A
Microbiota
Pathobionts
TLR/RLR/NLR
ligands
ERV
TLR/RLR
ligands
TRAF3
B Lymphoma
Chronic
inflammation
MDSC

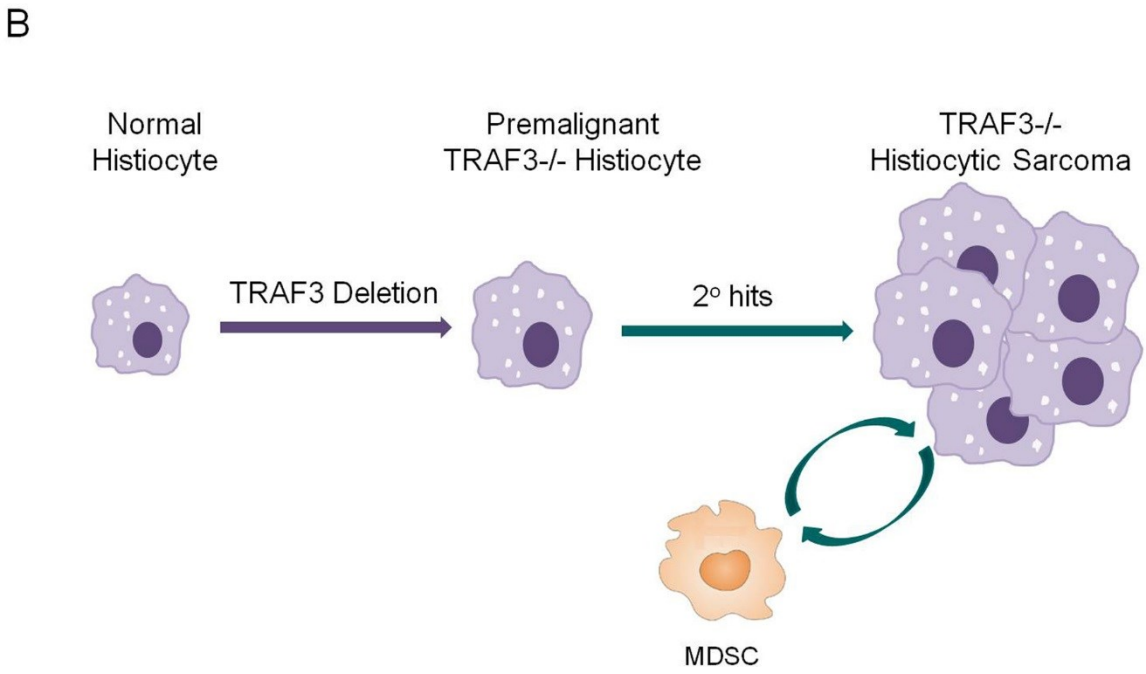
B
Normal
Histiocyte
Premalignant
TRAF3-/- Histiocyte
TRAF3-/-
Histiocytic Sarcoma
TRAF3 Deletion
2° hits
MDSC

Figure 26: Model for the *in vivo* functions of myeloid cell TRAF3 discovered in this study. **(A)** Myeloid cell TRAF3 prevents B lymphoma development by inhibiting several different pathways. It inhibits chronic inflammation mediated by commensal microbiota. It also potentially inhibits reactivation of ERVs induced by commensal bacteria. Pathobionts of commensal bacteria and reactivated ERVs may engage specific clones of B cells to undergo GC reactions, which introduce double-stranded DNA breaks and increase the risk of genetic alterations. Reactivated ERVs further increase genomic instability in such B cell clones. Moreover, TRAF3 is required for suppression of MDSC expansion, which is regulated by and also a potent driver of chronic inflammation and may contribute to the progression of B lymphomas. Therefore, aging M-TRAF3-/- mice exhibit spontaneous development of chronic inflammation and B lymphoma development in the absence of antibiotic treatment. **(B)** TRAF3 acts as a tumor suppressor in histiocytes. Its deletion predisposes histiocytes to malignant transformation possibly via dysregulation of the survival and proliferation responses of histiocytes to different innate immune recepotrs and cytokine receptors. However, the development of histiocytic sarcoma in M-TRAF3-/- displays a long latency, suggesting that accumulation of secondary genetic and epigenetic alterations are required for histiocytic malignant transformation. Additionally, hyperexpansion of TRAF3-/- MDSC in the tumor microenvironment may suppress tumor immunity and accelerate the progression and metastasis of histiocytic sarcomas. Because of the loss of such cell intrinsic tumor suppressive function of TRAF3, aging M-TRAF3-/- mice spontaneously develop histiocytic sarcomas regardless of the absence or presence of antibiotic treatment.

In conclusion, evidence obtained by my dissertation research demonstrates that specific ablation of TRAF3 in myeloid cells leads to chronic inflammation, significant expansion of MDSC, spontaneous development of different types of tumors, reactivation of endogenous retroviruses in B lymphoma and infections by commensal microbiota in mice. These results were corroborated by two other laboratories which showed that deletion of myeloid cell TRAF3 leads to inflammatory diseases and altered progression of diabetes. These new findings indicate that myeloid cell TRAF3 acts as an anti-inflammatory factor, and is required to resist infections and reactivation of endogenous retroviruses and control development of hematopoietic and solid tumors. Our evidence thus identifies TRAF3 as a novel tumor suppressor in macrophages (Figure 26). Although information about TRAF3 mutations or malfunctions in human macrophages is limited, available evidence indicates that TRAF3 mutation and aberrant expression exist in myeloid cells of human patients with viral infectious diseases and inflammatory bowel diseases. Therefore, the functions of

TRAF3 in myeloid cells appear to be conserved between mice and humans, suggesting that findings obtained from M-TRAF3$^{-/-}$ mice may be extrapolated to human diseases and merit further systematic investigations of TRAF3 in human patients. Furthermore, TRAF3 is now recognized as a converging point of numerous signaling pathways, including the TNF-R superfamily, TLRs, RLRs, and cytokine receptors. It would thus be especially interesting to further decipher how TRAF3 integrates or modulates different signals in situations that involve simultaneous or sequential engagement of multiple receptors present on macrophages and DCs, such as chronic inflammation, co-infections, or tumorigenesis. Deeper mechanistic insights into TRAF3 signaling pathways will be valuable for understanding the molecular pathogenesis of TRAF3 inactivation-associated diseases, and will provide new opportunities for developing effective therapeutic modalities for chronic inflammation, infection, and cancer.

APPENDIX 1: LIST OF ABBREVIATIONS USED

M-TRAF3-/-: Myeloid cell-specific TRAF3 deficient

LMC: Littermate control

BMDM: Bone-marrow derived macrophages

PEM: Peritoneal exudate macrophages

TLR: Toll-like receptor

RLR: RIG-I like receptor

NLR: NOD-like receptor

LPS: lipopolysaccharide

Poly I:C: polyinosinic:polycytidylic acid

TI: T-cell independent

TD: T-cell dependent

SHM: Somatic hypermutation

CSR: Class switch recombination

GC: Germinal center

V(D)J: Variable, Diversity and Joining domains

MDSC: Myeloid derived suppressor cell/s

BCG: Bacillus Calmette-Guérin

CSF: Colony stimulating factor

ERV: Endogenous retroviruses

HS: Histiocytic sarcoma

eMLV: ecotropic murine leukemia virus

MMTV: mouse mammary tumor virus

PUBLISHED PAPERS REPORTING FINDINGS OF THIS DISSERTATION RESEARCH

Lalani, A. I. *et al.* Myeloid Cell TRAF3 Regulates Immune Responses and Inhibits Inflammation and Tumor Development in Mice. *Journal of immunology* **194**, 334-348, doi:10.4049/jimmunol.1401548 (2015).

Lalani, A. I., Luo, C., Han, Y. & Xie, P. TRAF3: a novel tumor suppressor gene in macrophages. *Macrophage (Houst)* **2**, e1009, doi:10.14800/macrophage.1009 (2015).

REFERENCES CITED

1 Akira, S., Uematsu, S. & Takeuchi, O. Pathogen recognition and innate immunity. *Cell* **124**, 783, doi:10.1016/j.cell.2006.02.015 (2006).

2 Murphy, K. Janeway's Immunobiology. **8th Edition**, 1 (2012).

3 Aderem, A. & Underhill, D. M. Mechanisms of phagocytosis in macrophages. *Annu.Rev.Immunol.* **17**, 593, doi:10.1146/annurev.immunol.17.1.593 (1999).

4 Xie, P. TRAF molecules in cell signaling and in human diseases. *J.Mol.Signal.* **8**, 7, doi:10.1186/1750-2187-8-7; 10.1186/1750-2187-8-7 (2013).

5 Hacker, H., Tseng, P. H. & Karin, M. Expanding TRAF function: TRAF3 as a tri-faced immune regulator. *Nat.Rev.Immunol.* **11**, 457, doi:10.1038/nri2998; 10.1038/nri2998 (2011).

6 Kawai, T. & Akira, S. The role of pattern-recognition receptors in innate immunity: update on Toll-like receptors. *Nat.Immunol.* **11**, 373, doi:10.1038/ni.1863; 10.1038/ni.1863 (2010).

7 Inoue, J. *et al.* Tumor necrosis factor receptor-associated factor (TRAF) family: adapter proteins that mediate cytokine signaling. *Exp.Cell Res.* **254**, 14, doi:10.1006/excr.1999.4733 (2000).

8 Wajant, H., Henkler, F. & Scheurich, P. The TNF-receptor-associated factor family: scaffold molecules for cytokine receptors, kinases and their regulators. *Cell.Signal.* **13**, 389 (2001).

9 Ha, H., Han, D. & Choi, Y. TRAF-mediated TNFR-family signaling. *Curr.Protoc.Immunol.* **Chapter 11**, Unit11.19D, doi:10.1002/0471142735.im1109ds87; 10.1002/0471142735.im1109ds87 (2009).

10 Xie, P. TRAF molecules in cell signaling and in human diseases. *J Mol Signal* **8**, 7, doi:10.1186/1750-2187-8-7 (2013).

11 Ostuni, R., Zanoni, I. & Granucci, F. Deciphering the complexity of Toll-like receptor signaling. *Cell Mol.Life Sci.* **67**, 4109, doi:10.1007/s00018-010-0464-x; 10.1007/s00018-010-0464-x (2010).

12 Xie, P., Stunz, L. L., Larison, K. D., Yang, B. & Bishop, G. A. Tumor necrosis factor receptor-associated factor 3 is a critical regulator of B cell homeostasis in secondary lymphoid organs. *Immunity* **27**, 253-267 (2007).

13 Gardam, S., Sierro, F., Basten, A., Mackay, F. & Brink, R. TRAF2 and TRAF3 signal adapters act cooperatively to control the maturation and survival signals delivered to B cells by the BAFF receptor. *Immunity* **28**, 391-401 (2008).

14 Moore, C. R. *et al.* Specific deletion of TRAF3 in B lymphocytes leads to B lymphoma development in mice. *Leukemia* **26**, 1122-1127 (2012).

15 Xie, P. *et al.* Enhanced Toll-like receptor (TLR) responses of TNFR-associated factor 3 (TRAF3)-deficient B lymphocytes. *Journal of leukocyte biology* **90**, 1149-1157 (2011).

16 Xie, P., Kraus, Z. J., Stunz, L. L., Liu, Y. & Bishop, G. A. TNF Receptor-Associated Factor 3 Is Required for T Cell-Mediated Immunity and TCR/CD28 Signaling. *Journal of immunology* **186**, 143-155 (2011).

17 Yi, Z., Stunz, L. L., Lin, W. W. & Bishop, G. A. TRAF3 regulates homeostasis of CD8+ central memory T cells. *PloS one* **9**, e102120, doi:10.1371/journal.pone.0102120 (2014).

18 Yi, Z., Stunz, L. L. & Bishop, G. A. TNF receptor associated factor 3 plays a key role in development and function of invariant natural killer T cells. *The Journal of experimental medicine* **210**, 1079-1086, doi:10.1084/jem.20122135 (2013).

19 Yi, Z., Lin, W. W., Stunz, L. L. & Bishop, G. A. The adaptor TRAF3 restrains the lineage determination of thymic regulatory T cells by modulating signaling via the receptor for IL-2. *Nature immunology* **15**, 866-874, doi:10.1038/ni.2944 (2014).

20 Chang, J. H. *et al.* TRAF3 regulates the effector function of regulatory T cells and humoral immune responses. *The Journal of experimental medicine* **211**, 137-151, doi:10.1084/jem.20131019 (2014).

21 Yi, Z., Wallis, A. M. & Bishop, G. A. Roles of TRAF3 in T cells: many surprises. *Cell Cycle* **14**, 1156-1163, doi:10.1080/15384101.2015.1021524 (2015).

22 Kawamoto, H. & Minato, N. Myeloid cells. *The international journal of biochemistry & cell biology* **36**, 1374-1379, doi:10.1016/j.biocel.2004.01.020 (2004).

23 Galli, S. J., Borregaard, N. & Wynn, T. A. Phenotypic and functional plasticity of cells of innate immunity: macrophages, mast cells and neutrophils. *Nature immunology* **12**, 1035-1044, doi:10.1038/ni.2109 (2011).

24 Hacker, H., Tseng, P. H. & Karin, M. Expanding TRAF function: TRAF3 as a tri-faced immune regulator. *Nature reviews. Immunology* **11**, 457-468 (2011).

25 Jin, J. *et al.* Noncanonical NF-kappaB pathway controls the production of type I interferons in antiviral innate immunity. *Immunity* **40**, 342-354, doi:10.1016/j.immuni.2014.02.006 (2014).

26 Hacker, H. *et al.* Specificity in Toll-like receptor signalling through distinct effector functions of TRAF3 and TRAF6. *Nature* **439**, 204-207 (2006).

27 Oganesyan, G. *et al.* Critical role of TRAF3 in the Toll-like receptor-dependent and -independent antiviral response. *Nature* **439**, 208-211 (2006).

28 Chuang, T. & Ulevitch, R. J. Identification of hTLR10: a novel human Toll-like receptor preferentially expressed in immune cells. *Biochim.Biophys.Acta* **1518**, 157 (2001).

29 Hochrein, H. & Kirschning, C. J. Bacteria evade immune recognition via TLR13 and binding of their 23S rRNA by MLS antibiotics by the same mechanisms. *Oncoimmunology* **2**, e23141, doi:10.4161/onci.23141 (2013).

30 Shi, Z. *et al.* A novel Toll-like receptor that recognizes vesicular stomatitis virus. *J.Biol.Chem.* **286**, 4517, doi:10.1074/jbc.M110.159590; 10.1074/jbc.M110.159590 (2011).

31 Yarovinsky, F. *et al.* TLR11 activation of dendritic cells by a protozoan profilin-like protein. *Science* **308**, 1626, doi:10.1126/science.1109893 (2005).

32 Bishop, G. A. & Xie, P. Multiple roles of TRAF3 signaling in lymphocyte function. *Immunologic research* **39**, 22-32 (2007).

33 Rickert, R. C., Jellusova, J. & Miletic, A. V. Signaling by the tumor necrosis factor receptor superfamily in B-cell biology and disease. *Immunological reviews* **244**, 115-133, doi:10.1111/j.1600-065X.2011.01067.x (2011).

34 Lundberg, A. M. *et al.* Toll-like receptor 3 and 4 signalling through the TRIF and TRAM adaptors in haematopoietic cells promotes atherosclerosis. *Cardiovasc.Res.* **99**, 364, doi:10.1093/cvr/cvt033; 10.1093/cvr/cvt033 (2013).

35 Paz, S. *et al.* A functional C-terminal TRAF3-binding site in MAVS participates in positive and negative regulation of the IFN antiviral response. *Cell Res.* **21**, 895, doi:10.1038/cr.2011.2; 10.1038/cr.2011.2 (2011).

36 Zhang, P. *et al.* Single amino acid substitutions confer the antiviral activity of the TRAF3 adaptor protein onto TRAF5. *Sci.Signal.* **5**, ra81, doi:10.1126/scisignal.2003152; 10.1126/scisignal.2003152 (2012).

37 Watanabe, T. *et al.* NOD1 contributes to mouse host defense against Helicobacter pylori via induction of type I IFN and activation of the ISGF3 signaling pathway. *The Journal of clinical investigation* **120**, 1645-1662 (2010).

38 Sabbah, A. *et al.* Activation of innate immune antiviral responses by Nod2. *Nat Immunol* **10**, 1073-1080, doi:10.1038/ni.1782 (2009).

39 Tattoli, I., Travassos, L. H., Carneiro, L. A., Magalhaes, J. G. & Girardin, S. E. The Nodosome: Nod1 and Nod2 control bacterial infections and inflammation. *Seminars in immunopathology* **29**, 289-301, doi:10.1007/s00281-007-0083-2 (2007).

40 Kawai, T. & Akira, S. The role of pattern-recognition receptors in innate immunity: update on Toll-like receptors. *Nat Immunol* **11**, 373-384, doi:10.1038/ni.1863 (2010).

41 Saleh, M. The machinery of Nod-like receptors: refining the paths to immunity and cell death. *Immunological reviews* **243**, 235-246, doi:10.1111/j.1600-065X.2011.01045.x (2011).

42 Yu, M. & Levine, S. J. Toll-like receptor, RIG-I-like receptors and the NLRP3 inflammasome: key modulators of innate immune responses to double-stranded RNA viruses. *Cytokine & growth factor reviews* **22**, 63-72, doi:10.1016/j.cytogfr.2011.02.001 (2011).

43 Xu, Y., Cheng, G. & Baltimore, D. Targeted disruption of TRAF3 leads to postnatal lethality and defective T-dependent immune responses. *Immunity* **5**, 407-415. (1996).

44 Rub, A. *et al.* Cholesterol depletion associated with Leishmania major infection alters macrophage CD40 signalosome composition and effector function. *Nat Immunol* **10**, 273-280, doi:10.1038/ni.1705 (2009).

45 Clausen, B. E., Burkhardt, C., Reith, W., Renkawitz, R. & Forster, I. Conditional gene targeting in macrophages and granulocytes using LysMcre mice. *Transgenic Res* **8**, 265-277 (1999).

46 Clemens, R. A. *et al.* Loss of SLP-76 expression within myeloid cells confers resistance to neutrophil-mediated tissue damage while maintaining effective bacterial killing. *Journal of immunology* **178**, 4606-4614 (2007).

47 Zhang, X., Goncalves, R. & Mosser, D. M. The isolation and characterization of murine macrophages. *Current protocols in immunology / edited by John E. Coligan ... [et al.]* **Chapter 14**, Unit 14 11, doi:10.1002/0471142735.im1401s83 (2008).

48 Weischenfeldt, J. & Porse, B. Bone Marrow-Derived Macrophages (BMM): Isolation and Applications. *CSH protocols* **2008**, pdb prot5080, doi:10.1101/pdb.prot5080 (2008).

49 Manzanero, S. Generation of mouse bone marrow-derived macrophages. *Methods in molecular biology* **844**, 177-181, doi:10.1007/978-1-61779-527-5_12 (2012).

50 Edwards, S. K. *et al.* N-benzyladriamycin-14-valerate (AD 198) exhibits potent anti-tumor activity on TRAF3-deficient mouse B lymphoma and human multiple myeloma. *BMC cancer* **13**, 481, doi:10.1186/1471-2407-13-481 (2013).

51 Morse, H. C., 3rd *et al.* Bethesda proposals for classification of lymphoid neoplasms in mice. *Blood* **100**, 246-258 (2002).

52 Hao, X. *et al.* The histopathologic and molecular basis for the diagnosis of histiocytic sarcoma and histiocyte-associated lymphoma of mice. *Veterinary pathology* **47**, 434-445, doi:10.1177/0300985810363705 (2010).

53 King, C. G. *et al.* TRAF6 is a T cell-intrinsic negative regulator required for the maintenance of immune homeostasis. *Nature medicine* **12**, 1088-1092 (2006).

54 Fredrickson, T. N., Hartley, J. W. & Morse, H. C., 3rd. Citrobacter-induced colitis in mice with murine acquired immunodeficiency syndrome. *Veterinary pathology* **47**, 312-317, doi:10.1177/0300985809358605 (2010).

55 Lin, T. M. Colonization and encystation of Entamoeba muris in the rat and the mouse. *The Journal of parasitology* **57**, 375-382 (1971).

56 Cobo, E. R. *et al.* Entamoeba histolytica induces intestinal cathelicidins but is resistant to cathelicidin-mediated killing. *Infection and immunity* **80**, 143-149, doi:10.1128/IAI.05029-11 (2012).

57 Dzhagalov, I., St John, A. & He, Y. W. The antiapoptotic protein Mcl-1 is essential for the survival of neutrophils but not macrophages. *Blood* **109**, 1620-1626 (2007).

58 Yang, Y. *et al.* Heat shock protein gp96 is a master chaperone for toll-like receptors and is important in the innate function of macrophages. *Immunity* **26**, 215-226 (2007).

59 Beekman, R. & Touw, I. P. G-CSF and its receptor in myeloid malignancy. *Blood* **115**, 5131-5136, doi:10.1182/blood-2010-01-234120 (2010).

60 Greenbaum, A. M. & Link, D. C. Mechanisms of G-CSF-mediated hematopoietic stem and progenitor mobilization. *Leukemia* **25**, 211-217, doi:10.1038/leu.2010.248 (2011).

61 Gaffen, S. L. Recent advances in the IL-17 cytokine family. *Curr Opin Immunol* **23**, 613-619, doi:10.1016/j.coi.2011.07.006 (2011).

62 Das, S. *et al.* Tumor cell entry into the lymph node is controlled by CCL1 chemokine expressed by lymph node lymphatic sinuses. *The Journal of experimental medicine* **210**, 1509-1528, doi:10.1084/jem.20111627 (2013).

63 Kyriakides, T. R. *et al.* The CC chemokine ligand, CCL2/MCP1, participates in macrophage fusion and foreign body giant cell formation. *The American journal of pathology* **165**, 2157-2166, doi:10.1016/S0002-9440(10)63265-8 (2004).

64 Conti, I. & Rollins, B. J. CCL2 (monocyte chemoattractant protein-1) and cancer. *Seminars in cancer biology* **14**, 149-154, doi:10.1016/j.semcancer.2003.10.009 (2004).

65 Sarafi, M. N., Garcia-Zepeda, E. A., MacLean, J. A., Charo, I. F. & Luster, A. D. Murine monocyte chemoattractant protein (MCP)-5: a novel CC chemokine that is a structural and functional homologue of human MCP-1. *The Journal of experimental medicine* **185**, 99-109 (1997).

66 Charo, I. F. & Peters, W. Chemokine receptor 2 (CCR2) in atherosclerosis, infectious diseases, and regulation of T-cell polarization. *Microcirculation* **10**, 259-264, doi:10.1038/sj.mn.7800191 (2003).

67 Liu, M. *et al.* CXCL10/IP-10 in infectious diseases pathogenesis and potential therapeutic implications. *Cytokine & growth factor reviews* **22**, 121-130, doi:10.1016/j.cytogfr.2011.06.001 (2011).

68 Liu, M., Guo, S. & Stiles, J. K. The emerging role of CXCL10 in cancer (Review). *Oncology letters* **2**, 583-589, doi:10.3892/ol.2011.300 (2011).

69 Sharif, O. & Knapp, S. From expression to signaling: roles of TREM-1 and TREM-2 in innate immunity and bacterial infection. *Immunobiology* **213**, 701-713, doi:10.1016/j.imbio.2008.07.008 (2008).

70 Arts, R. J., Joosten, L. A., van der Meer, J. W. & Netea, M. G. TREM-1: intracellular signaling pathways and interaction with pattern recognition receptors. *Journal of leukocyte biology* **93**, 209-215, doi:10.1189/jlb.0312145 (2013).

71 Jenkinson, S. R. *et al.* TRAF3 enforces the requirement for T cell cross-talk in thymic medullary epithelial development. *Proceedings of the National Academy of Sciences of the United States of America* **110**, 21107-21112, doi:10.1073/pnas.1314859111 (2013).

72 Xiu, Y. *et al.* Chloroquine reduces osteoclastogenesis in murine osteoporosis by preventing TRAF3 degradation. *The Journal of clinical investigation* **124**, 297-310, doi:10.1172/JCI66947 (2014).

73 Baniyash, M., Sade-Feldman, M. & Kanterman, J. Chronic inflammation and cancer: suppressing the suppressors. *Cancer immunology, immunotherapy : CII* **63**, 11-20, doi:10.1007/s00262-013-1468-9 (2014).

74 Wesolowski, R., Markowitz, J. & Carson, W. E., 3rd. Myeloid derived suppressor cells - a new therapeutic target in the treatment of cancer. *Journal for immunotherapy of cancer* **1**, 10, doi:10.1186/2051-1426-1-10 (2013).

75 Brandau, S., Moses, K. & Lang, S. The kinship of neutrophils and granulocytic myeloid-derived suppressor cells in cancer: cousins, siblings or twins? *Seminars in cancer biology* **23**, 171-182, doi:10.1016/j.semcancer.2013.02.007 (2013).

76 Ostrand-Rosenberg, S. & Sinha, P. Myeloid-derived suppressor cells: linking inflammation and cancer. *Journal of immunology* **182**, 4499-4506, doi:10.4049/jimmunol.0802740 (2009).

77 Saha, S. K. *et al.* Regulation of antiviral responses by a direct and specific interaction between TRAF3 and Cardif. *Embo J* **25**, 3257-3263 (2006).

78 Perkins, D. J. *et al.* Reprogramming of Murine Macrophages through TLR2 Confers Viral Resistance via TRAF3-Mediated, Enhanced Interferon Production. *PLoS pathogens* **9**, e1003479, doi:10.1371/journal.ppat.1003479 (2013).

79 Izcue, A., Coombes, J. L. & Powrie, F. Regulatory lymphocytes and intestinal inflammation. *Annu Rev Immunol* **27**, 313-338, doi:10.1146/annurev.immunol.021908.132657 (2009).

80 Chow, J., Tang, H. & Mazmanian, S. K. Pathobionts of the gastrointestinal microbiota and inflammatory disease. *Curr Opin Immunol* **23**, 473-480, doi:10.1016/j.coi.2011.07.010 (2011).

81 Kamada, N., Chen, G. Y., Inohara, N. & Nunez, G. Control of pathogens and pathobionts by the gut microbiota. *Nat Immunol* **14**, 685-690, doi:10.1038/ni.2608 (2013).

82 Ivory, C. P., Prystajecky, M., Jobin, C. & Chadee, K. Toll-like receptor 9-dependent macrophage activation by Entamoeba histolytica DNA. *Infection and immunity* **76**, 289-297, doi:10.1128/IAI.01217-07 (2008).

83 Philpott, D. J., Sorbara, M. T., Robertson, S. J., Croitoru, K. & Girardin, S. E. NOD proteins: regulators of inflammation in health and disease. *Nature reviews. Immunology* **14**, 9-23, doi:10.1038/nri3565 (2014).

84 Biswas, A. & Kobayashi, K. S. Regulation of intestinal microbiota by the NLR protein family. *International immunology* **25**, 207-214, doi:10.1093/intimm/dxs116 (2013).

85 Buchanan, R. M., Arulanandam, B. P. & Metzger, D. W. IL-12 enhances antibody responses to T-independent polysaccharide vaccines in the absence of T and NK cells. *Journal of immunology* **161**, 5525-5533 (1998).

86 Kopf, M., Herren, S., Wiles, M. V., Pepys, M. B. & Kosco-Vilbois, M. H. Interleukin 6 influences germinal center development and antibody production via a contribution of C3 complement component. *The Journal of experimental medicine* **188**, 1895-1906 (1998).

87 Poudrier, J. *et al.* A soluble form of IL-13 receptor alpha 1 promotes IgG2a and IgG2b production by murine germinal center B cells. *Journal of immunology* **163**, 1153-1161 (1999).

88 Choi, Y. S., Eto, D., Yang, J. A., Lao, C. & Crotty, S. Cutting edge: STAT1 is required for IL-6-mediated Bcl6 induction for early follicular helper cell differentiation. *Journal of immunology* **190**, 3049-3053, doi:10.4049/jimmunol.1203032 (2013).

89 Sweet, R. A., Lee, S. K. & Vinuesa, C. G. Developing connections amongst key cytokines and dysregulated germinal centers in autoimmunity. *Curr Opin Immunol* **24**, 658-664, doi:10.1016/j.coi.2012.10.003 (2012).

90 Chakarov, S. & Fazilleau, N. Monocyte-derived dendritic cells promote T follicular helper cell differentiation. *EMBO molecular medicine* **6**, 590-603, doi:10.1002/emmm.201403841 (2014).

91 Pratama, A. & Vinuesa, C. G. Control of TFH cell numbers: why and how? *Immunology and cell biology* **92**, 40-48, doi:10.1038/icb.2013.69 (2014).

92 Shaffer, A. L., Rosenwald, A. & Staudt, L. M. Lymphoid malignancies: the dark side of B-cell differentiation. *Nature reviews. Immunology* **2**, 920-932 (2002).

93 Kuppers, R. & Dalla-Favera, R. Mechanisms of chromosomal translocations in B cell lymphomas. *Oncogene* **20**, 5580-5594 (2001).

94 Peled, J. U. *et al.* The biochemistry of somatic hypermutation. *Annu Rev Immunol* **26**, 481-511 (2008).

95 Karin, M., Lawrence, T. & Nizet, V. Innate immunity gone awry: linking microbial infections to chronic inflammation and cancer. *Cell* **124**, 823-835 (2006).

96 Mechtcheriakova, D., Svoboda, M., Meshcheryakova, A. & Jensen-Jarolim, E. Activation-induced cytidine deaminase (AID) linking immunity, chronic inflammation, and cancer. *Cancer immunology, immunotherapy : CII* **61**, 1591-1598, doi:10.1007/s00262-012-1255-z (2012).

97 Hasselbalch, H. C. Chronic inflammation as a promotor of mutagenesis in essential thrombocythemia, polycythemia vera and myelofibrosis. A human inflammation model for cancer development? *Leukemia research* **37**, 214-220, doi:10.1016/j.leukres.2012.10.020 (2013).

98 Kamp, D. W., Shacter, E. & Weitzman, S. A. Chronic inflammation and cancer: the role of the mitochondria. *Oncology (Williston Park)* **25**, 400-410, 413 (2011).

99 Rakoff-Nahoum, S., Paglino, J., Eslami-Varzaneh, F., Edberg, S. & Medzhitov, R. Recognition of commensal microflora by toll-like receptors is required for intestinal homeostasis. *Cell* **118**, 229-241, doi:10.1016/j.cell.2004.07.002 (2004).

100 Pradere, J. P., Dapito, D. H. & Schwabe, R. F. The Yin and Yang of Toll-like receptors in cancer. *Oncogene* **33**, 3485-3495, doi:10.1038/onc.2013.302 (2014).

101 Sato, Y., Goto, Y., Narita, N. & Hoon, D. S. Cancer Cells Expressing Toll-like Receptors and the Tumor Microenvironment. *Cancer microenvironment : official journal of the International Cancer Microenvironment Society* **2 Suppl 1**, 205-214, doi:10.1007/s12307-009-0022-y (2009).

102 Saxena, M. & Yeretssian, G. NOD-Like Receptors: Master Regulators of Inflammation and Cancer. *Frontiers in immunology* **5**, 327, doi:10.3389/fimmu.2014.00327 (2014).

103 Wang, J. Q., Jeelall, Y. S., Ferguson, L. L. & Horikawa, K. Toll-Like Receptors and Cancer: MYD88 Mutation and Inflammation. *Frontiers in immunology* **5**, 367, doi:10.3389/fimmu.2014.00367 (2014).

104 Allen, I. C. *et al.* NLRP12 suppresses colon inflammation and tumorigenesis through the negative regulation of noncanonical NF-kappaB signaling. *Immunity* **36**, 742-754 (2012).

105 Wimmer, N. *et al.* Lymphotoxin beta receptor activation on macrophages induces cross-tolerance to TLR4 and TLR9 ligands. *Journal of immunology* **188**, 3426-3433, doi:10.4049/jimmunol.1103324 (2012).

106 Hoshi, N. *et al.* MyD88 signalling in colonic mononuclear phagocytes drives colitis in IL-10-deficient mice. *Nature communications* **3**, 1120, doi:10.1038/ncomms2113 (2012).

107 Fukata, M. *et al.* Toll-like receptor-4 promotes the development of colitis-associated colorectal tumors. *Gastroenterology* **133**, 1869-1881, doi:10.1053/j.gastro.2007.09.008 (2007).

108 Keats, J. J. *et al.* Promiscuous mutations activate the noncanonical NF-kappaB pathway in multiple myeloma. *Cancer cell* **12**, 131-144 (2007).

109 Annunziata, C. M. *et al.* Frequent engagement of the classical and alternative NF-kappaB pathways by diverse genetic abnormalities in multiple myeloma. *Cancer cell* **12**, 115-130 (2007).

110 Demchenko, Y. N. *et al.* Classical and/or alternative NF-kappaB pathway activation in multiple myeloma. *Blood* **115**, 3541-3552 (2010).

111 Nagel, I. *et al.* Biallelic inactivation of TRAF3 in a subset of B-cell lymphomas with interstitial del(14)(q24.1q32.33). *Leukemia* **23**, 2153-2155 (2009).

112 Rossi, D. *et al.* Alteration of BIRC3 and multiple other NF-{kappa}B pathway genes in splenic marginal zone lymphoma. *Blood* **118**, 4930-4934 (2011).

113 Braggio, E. *et al.* Identification of copy number abnormalities and inactivating mutations in two negative regulators of nuclear factor-kappaB signaling pathways in Waldenstrom's macroglobulinemia. *Cancer research* **69**, 3579-3588 (2009).

114 Otto, C. *et al.* Genetic lesions of the TRAF3 and MAP3K14 genes in classical Hodgkin lymphoma. *British journal of haematology* **157**, 702-708 (2012).

115 Perez de Diego, R. *et al.* Human TRAF3 adaptor molecule deficiency leads to impaired Toll-like receptor 3 response and susceptibility to herpes simplex encephalitis. *Immunity* **33**, 400-411, doi:10.1016/j.immuni.2010.08.014 (2010).

116 Momeni, M. *et al.* Decreased expression of toll like receptor signaling molecules in chronic HBV infected patients. *Human immunology* **75**, 15-19, doi:10.1016/j.humimm.2013.09.015 (2014).

117 Gabrilovich, D. I. & Nagaraj, S. Myeloid-derived suppressor cells as regulators of the immune system. *Nature reviews. Immunology* **9**, 162-174, doi:10.1038/nri2506 (2009).

118 Khaled, Y. S., Ammori, B. J. & Elkord, E. Myeloid-derived suppressor cells in cancer: recent progress and prospects. *Immunology and cell biology* **91**, 493-502, doi:10.1038/icb.2013.29 (2013).

119 Gabrilovich, D. I., Ostrand-Rosenberg, S. & Bronte, V. Coordinated regulation of myeloid cells by tumours. *Nature reviews. Immunology* **12**, 253-268, doi:10.1038/nri3175 (2012).

120 Marvel, D. & Gabrilovich, D. I. Myeloid-derived suppressor cells in the tumor microenvironment: expect the unexpected. *The Journal of clinical investigation* **125**, 3356-3364, doi:10.1172/JCI80005 (2015).

121 Kumar, V., Patel, S., Tcyganov, E. & Gabrilovich, D. I. The Nature of Myeloid-Derived Suppressor Cells in the Tumor Microenvironment. *Trends in immunology* **37**, 208-220, doi:10.1016/j.it.2016.01.004 (2016).

122 Messmer, M. N., Netherby, C. S., Banik, D. & Abrams, S. I. Tumor-induced myeloid dysfunction and its implications for cancer immunotherapy. *Cancer immunology, immunotherapy : CII* **64**, 1-13, doi:10.1007/s00262-014-1639-3 (2015).

123 Solito, S. *et al.* Myeloid-derived suppressor cell heterogeneity in human cancers. *Annals of the New York Academy of Sciences* **1319**, 47-65, doi:10.1111/nyas.12469 (2014).

124 Lalani, A. I. *et al.* Myeloid Cell TRAF3 Regulates Immune Responses and Inhibits Inflammation and Tumor Development in Mice. *J Immunol* **194**, 334-348, doi:10.4049/jimmunol.1401548 (2015).

125 Sade-Feldman, M. *et al.* Tumor necrosis factor-alpha blocks differentiation and enhances suppressive activity of immature myeloid cells during chronic inflammation. *Immunity* **38**, 541-554, doi:10.1016/j.immuni.2013.02.007 (2013).

126 Youn, J. I., Collazo, M., Shalova, I. N., Biswas, S. K. & Gabrilovich, D. I. Characterization of the nature of granulocytic myeloid-derived suppressor cells in tumor-bearing mice. *Journal of leukocyte biology* **91**, 167-181, doi:10.1189/jlb.0311177 (2012).

127 Youn, J. I. *et al.* Epigenetic silencing of retinoblastoma gene regulates pathologic differentiation of myeloid cells in cancer. *Nat Immunol* **14**, 211-220, doi:10.1038/ni.2526 (2013).

128 Ezernitchi, A. V. *et al.* TCR zeta down-regulation under chronic inflammation is mediated by myeloid suppressor cells differentially distributed between various lymphatic organs. *Journal of immunology* **177**, 4763-4772 (2006).

129 Vaknin, I. *et al.* A common pathway mediated through Toll-like receptors leads to T- and natural killer-cell immunosuppression. *Blood* **111**, 1437-1447, doi:10.1182/blood-2007-07-100404 (2008).

130 Younos, I. H., Dafferner, A. J., Gulen, D., Britton, H. C. & Talmadge, J. E. Tumor regulation of myeloid-derived suppressor cell proliferation and trafficking. *International immunopharmacology* **13**, 245-256, doi:10.1016/j.intimp.2012.05.002 (2012).

131 Connolly, M. K. *et al.* Distinct populations of metastases-enabling myeloid cells expand in the liver of mice harboring invasive and preinvasive intra-abdominal tumor. *Journal of leukocyte biology* **87**, 713-725, doi:10.1189/jlb.0909607 (2010).

132 Swirski, F. K. *et al.* Identification of splenic reservoir monocytes and their deployment to inflammatory sites. *Science* **325**, 612-616, doi:10.1126/science.1175202 (2009).

133 Zhu, B. *et al.* CD11b+Ly-6C(hi) suppressive monocytes in experimental autoimmune encephalomyelitis. *Journal of immunology* **179**, 5228-5237 (2007).

134 Gomez-Garcia, L. *et al.* Intact glycans from cestode antigens are involved in innate activation of myeloid suppressor cells. *Parasite Immunol* **27**, 395-405, doi:10.1111/j.1365-3024.2005.00790.x (2005).

135 Sunderkotter, C. *et al.* Subpopulations of mouse blood monocytes differ in maturation stage and inflammatory response. *Journal of immunology* **172**, 4410-4417 (2004).

136 Mencacci, A. *et al.* CD80+Gr-1+ myeloid cells inhibit development of antifungal Th1 immunity in mice with candidiasis. *Journal of immunology* **169**, 3180-3190 (2002).

137 Van Ginderachter, J. A., Beschin, A., De Baetselier, P. & Raes, G. Myeloid-derived suppressor cells in parasitic infections. *European journal of immunology* **40**, 2976-2985, doi:10.1002/eji.201040911 (2010).

138 Solito, S., Pinton, L., Damuzzo, V. & Mandruzzato, S. Highlights on molecular mechanisms of MDSC-mediated immune suppression: paving the way for new working hypotheses. *Immunol Invest* **41**, 722-737, doi:10.3109/08820139.2012.678023 (2012).

139 Bunt, S. K. *et al.* Reduced inflammation in the tumor microenvironment delays the accumulation of myeloid-derived suppressor cells and limits tumor progression. *Cancer research* **67**, 10019-10026, doi:10.1158/0008-5472.CAN-07-2354 (2007).

140 Beury, D. W. *et al.* Cross-talk among myeloid-derived suppressor cells, macrophages, and tumor cells impacts the inflammatory milieu of solid tumors. *Journal of leukocyte biology* **96**, 1109-1118, doi:10.1189/jlb.3A0414-210R (2014).

141 Condamine, T., Mastio, J. & Gabrilovich, D. I. Transcriptional regulation of myeloid-derived suppressor cells. *Journal of leukocyte biology* **98**, 913-922, doi:10.1189/jlb.4RI0515-204R (2015).

142 Parker, K. H., Beury, D. W. & Ostrand-Rosenberg, S. Myeloid-Derived Suppressor Cells: Critical Cells Driving Immune Suppression in the Tumor Microenvironment. *Advances in cancer research* **128**, 95-139, doi:10.1016/bs.acr.2015.04.002 (2015).

143 Xin, H. *et al.* Sunitinib inhibition of Stat3 induces renal cell carcinoma tumor cell apoptosis and reduces immunosuppressive cells. *Cancer research* **69**, 2506-2513, doi:10.1158/0008-5472.CAN-08-4323 (2009).

144 Nefedova, Y. *et al.* Activation of dendritic cells via inhibition of Jak2/STAT3 signaling. *Journal of immunology* **175**, 4338-4346 (2005).

145 Cheng, P. *et al.* Inhibition of dendritic cell differentiation and accumulation of myeloid-derived suppressor cells in cancer is regulated by S100A9 protein. *The Journal of experimental medicine* **205**, 2235-2249, doi:10.1084/jem.20080132 (2008).

146 Marigo, I. *et al.* Tumor-induced tolerance and immune suppression depend on the C/EBPbeta transcription factor. *Immunity* **32**, 790-802, doi:10.1016/j.immuni.2010.05.010 (2010).

147 Corzo, C. A. *et al.* Mechanism regulating reactive oxygen species in tumor-induced myeloid-derived suppressor cells. *Journal of immunology* **182**, 5693-5701, doi:10.4049/jimmunol.0900092 (2009).

148 Parker, K. H. *et al.* HMGB1 enhances immune suppression by facilitating the differentiation and suppressive activity of myeloid-derived suppressor cells. *Cancer research* **74**, 5723-5733, doi:10.1158/0008-5472.CAN-13-2347 (2014).

149 Maenhout, S. K., Thielemans, K. & Aerts, J. L. Location, location, location: functional and phenotypic heterogeneity between tumor-infiltrating and non-infiltrating myeloid-derived suppressor cells. *Oncoimmunology* **3**, e956579, doi:10.4161/21624011.2014.956579 (2014).

150 Lechner, M. G., Liebertz, D. J. & Epstein, A. L. Characterization of cytokine-induced myeloid-derived suppressor cells from normal human peripheral blood mononuclear cells. *Journal of immunology* **185**, 2273-2284, doi:10.4049/jimmunol.1000901 (2010).

151 Jin, J. *et al.* Proinflammatory TLR signalling is regulated by a TRAF2-dependent proteolysis mechanism in macrophages. *Nature communications* **6**, 5930, doi:10.1038/ncomms6930 (2015).

152 Yu, J. *et al.* T cell-intrinsic function of the noncanonical NF-kappaB pathway in the regulation of GM-CSF expression and experimental autoimmune encephalomyelitis pathogenesis. *J Immunol* **193**, 422-430, doi:10.4049/jimmunol.1303237 (2014).

153 Paschall, A. V. *et al.* IFN regulatory factor 8 represses GM-CSF expression in T cells to affect myeloid cell lineage differentiation. *Journal of immunology* **194**, 2369-2379, doi:10.4049/jimmunol.1402412 (2015).

154 Yu, J. *et al.* Noncanonical NF-kappaB activation mediates STAT3-stimulated IDO upregulation in myeloid-derived suppressor cells in breast cancer. *J Immunol* **193**, 2574-2586, doi:10.4049/jimmunol.1400833 (2014).

155 Young, G. R. *et al.* Resurrection of endogenous retroviruses in antibody-deficient mice. *Nature* **491**, 774-778, doi:10.1038/nature11599 (2012).

156 Jolly, C. J., Klix, N. & Neuberger, M. S. Rapid methods for the analysis of immunoglobulin gene hypermutation: application to transgenic and gene targeted mice. *Nucleic Acids Res* **25**, 1913-1919 (1997).

157 Moore, C. R. *et al.* Specific deletion of TRAF3 in B lymphocytes leads to B-lymphoma development in mice. *Leukemia* **26**, 1122-1127, doi:10.1038/leu.2011.309 (2012).

158 Yu, W. J., Yang, W. H., Shi, Z. X., Yang, X. D. & Wang, H. J. [Application of NOD/SCID mice in research of experimental hematology - review]. *Zhongguo shi yan xue ye xue za zhi / Zhongguo bing li sheng li xue hui = Journal of experimental hematology / Chinese Association of Pathophysiology* **16**, 964-968 (2008).

159 Stocking, C. & Kozak, C. A. Murine endogenous retroviruses. *Cell Mol Life Sci* **65**, 3383-3398, doi:10.1007/s00018-008-8497-0 (2008).

160 Stoye, J. P. Studies of endogenous retroviruses reveal a continuing evolutionary saga. *Nat Rev Microbiol* **10**, 395-406, doi:10.1038/nrmicro2783 (2012).

161 McCubrey, J. & Risser, R. Genetic interactions in induction of endogenous murine leukemia virus from low leukemic mice. *Cell* **28**, 881-888 (1982).

162 Kane, M. *et al.* Successful transmission of a retrovirus depends on the commensal microbiota. *Science* **334**, 245-249, doi:10.1126/science.1210718 (2011).

163 Peek, R. M., Jr. & Blaser, M. J. Helicobacter pylori and gastrointestinal tract adenocarcinomas. *Nature reviews. Cancer* **2**, 28-37, doi:10.1038/nrc703 (2002).

164 Dzutsev, A., Goldszmid, R. S., Viaud, S., Zitvogel, L. & Trinchieri, G. The role of the microbiota in inflammation, carcinogenesis, and cancer therapy. *European journal of immunology* **45**, 17-31, doi:10.1002/eji.201444972 (2015).

165 Jobin, C. Colorectal cancer: CRC--all about microbial products and barrier function? *Nat Rev Gastroenterol Hepatol* **9**, 694-696, doi:10.1038/nrgastro.2012.220 (2012).

166 Rao, V. P. *et al.* Innate immune inflammatory response against enteric bacteria Helicobacter hepaticus induces mammary adenocarcinoma in mice. *Cancer research* **66**, 7395-7400, doi:10.1158/0008-5472.CAN-06-0558 (2006).

167 Murray, P. J. & Wynn, T. A. Protective and pathogenic functions of macrophage subsets. *Nature reviews. Immunology* **11**, 723-737, doi:10.1038/nri3073 (2011).

168 Vos, J. A. *et al.* Histiocytic sarcoma: a study of five cases including the histiocyte marker CD163. *Mod Pathol* **18**, 693-704, doi:10.1038/modpathol.3800346 (2005).

169 Chiappinelli, K. B. *et al.* Inhibiting DNA Methylation Causes an Interferon Response in Cancer via dsRNA Including Endogenous Retroviruses. *Cell* **164**, 1073, doi:10.1016/j.cell.2015.10.020 (2016).

170 Collins, P. L., Kyle, K. E., Egawa, T., Shinkai, Y. & Oltz, E. M. The histone methyltransferase SETDB1 represses endogenous and exogenous retroviruses in B lymphocytes. *Proceedings of the National Academy of Sciences of the United States of America* **112**, 8367-8372, doi:10.1073/pnas.1422187112 (2015).

171 Wolf, D. & Goff, S. P. Host restriction factors blocking retroviral replication. *Annu Rev Genet* **42**, 143-163, doi:10.1146/annurev.genet.42.110807.091704 (2008).

172 Yan, N. & Chen, Z. J. Intrinsic antiviral immunity. *Nat Immunol* **13**, 214-222, doi:10.1038/ni.2229 (2012).

173 Kassiotis, G. Endogenous retroviruses and the development of cancer. *Journal of immunology* **192**, 1343-1349, doi:10.4049/jimmunol.1302972 (2014).

174 Johnson, R. M. *et al.* MuLV-related endogenous retroviral elements and Flt3 participate in aberrant end-joining events that promote B-cell leukemogenesis. *Genes Dev* **28**, 1179-1190, doi:10.1101/gad.240820.114 (2014).

175 Hachem, A. & Gartenhaus, R. B. Oncogenes as molecular targets in lymphoma. *Blood* **106**, 1911-1923, doi:10.1182/blood-2004-12-4621 (2005).

176 Triviai, I. *et al.* Endogenous retrovirus induces leukemia in a xenograft mouse model for primary myelofibrosis. *Proceedings of the National Academy of Sciences of the United States of America* **111**, 8595-8600, doi:10.1073/pnas.1401215111 (2014).

177 Yu, P. *et al.* Nucleic acid-sensing Toll-like receptors are essential for the control of endogenous retrovirus viremia and ERV-induced tumors. *Immunity* **37**, 867-879, doi:10.1016/j.immuni.2012.07.018 (2012).

178 Zeng, M. *et al.* MAVS, cGAS, and endogenous retroviruses in T-independent B cell responses. *Science* **346**, 1486-1492, doi:10.1126/science.346.6216.1486 (2014).

179 Carrasco, D. R. *et al.* The PTEN and INK4A/ARF tumor suppressors maintain myelolymphoid homeostasis and cooperate to constrain histiocytic sarcoma development in humans. *Cancer cell* **9**, 379-390, doi:10.1016/j.ccr.2006.03.028 (2006).

180 Been, R. A. *et al.* Genetic signature of histiocytic sarcoma revealed by a sleeping beauty transposon genetic screen in mice. *PloS one* **9**, e97280, doi:10.1371/journal.pone.0097280 (2014).

181 Hedan, B. *et al.* Molecular cytogenetic characterization of canine histiocytic sarcoma: A spontaneous model for human histiocytic cancer identifies deletion of tumor suppressor genes and highlights influence of genetic background on tumor behavior. *BMC cancer* **11**, 201, doi:10.1186/1471-2407-11-201 (2011).

182 Martin-Caballero, J., Flores, J. M., Garcia-Palencia, P. & Serrano, M. Tumor susceptibility of p21(Waf1/Cip1)-deficient mice. *Cancer research* **61**, 6234-6238 (2001).

183 Ward, J. M. *et al.* Progressive glomerulonephritis and histiocytic sarcoma associated with macrophage functional defects in CYP1B1-deficient mice. *Toxicologic pathology* **32**, 710-718 (2004).

184 Eischen, C. M., Rehg, J. E., Korsmeyer, S. J. & Cleveland, J. L. Loss of Bax alters tumor spectrum and tumor numbers in ARF-deficient mice. *Cancer research* **62**, 2184-2191 (2002).

185 Mashima, R. *et al.* Mice lacking Dok-1, Dok-2, and Dok-3 succumb to aggressive histiocytic sarcoma. *Laboratory investigation; a journal of technical methods and pathology* **90**, 1357-1364, doi:10.1038/labinvest.2010.121 (2010).

186 Snyder, J. M. *et al.* Humanized TLR7/8 expression drives proliferative multisystemic histiocytosis in C57BL/6 mice. *PloS one* **9**, e107257, doi:10.1371/journal.pone.0107257 (2014).

187 Kim, S. S. *et al.* DOK3 is required for IFN-beta production by enabling TRAF3/TBK1 complex formation and IRF3 activation. *J Immunol* **193**, 840-848, doi:10.4049/jimmunol.1301601 (2014).

188 Chen, Z. *et al.* Myeloid cell TRAF3 promotes metabolic inflammation, insulin resistance, and hepatic steatosis in obesity. *American journal of physiology. Endocrinology and metabolism* **308**, E460-469, doi:10.1152/ajpendo.00470.2014 (2015).

189 Mullins, C. S. & Linnebacher, M. Endogenous retrovirus sequences as a novel class of tumor-specific antigens: an example of HERV-H env encoding strong CTL epitopes. *Cancer immunology, immunotherapy : CII* **61**, 1093-1100, doi:10.1007/s00262-011-1183-3 (2012).

190 Cherkasova, E. *et al.* Detection of an Immunogenic HERV-E Envelope with Selective Expression in Clear Cell Kidney Cancer. *Cancer research* **76**, 2177-2185, doi:10.1158/0008-5472.CAN-15-3139 (2016).

191 Wang-Johanning, F. *et al.* Human endogenous retrovirus K triggers an antigen-specific immune response in breast cancer patients. *Cancer research* **68**, 5869-5877, doi:10.1158/0008-5472.CAN-07-6838 (2008).

192 Lalani, A. I., Luo, C., Han, Y. & Xie, P. TRAF3: a novel tumor suppressor gene in macrophages. *Macrophage (Houst)* **2**, e1009, doi:10.14800/macrophage.1009 (2015).

193 Chawla, A., Nguyen, K. D. & Goh, Y. P. Macrophage-mediated inflammation in metabolic disease. *Nature reviews. Immunology* **11**, 738-749, doi:10.1038/nri3071 (2011).

194 Goriely, S., Neurath, M. F. & Goldman, M. How microorganisms tip the balance between interleukin-12 family members. *Nature reviews. Immunology* **8**, 81-86, doi:10.1038/nri2225 (2008).

195 Lu, Y. C. *et al.* Differential role for c-Rel and C/EBPbeta/delta in TLR-mediated induction of proinflammatory cytokines. *J Immunol* **182**, 7212-7221, doi:10.4049/jimmunol.0802971 (2009).

196 Gunthner, R. & Anders, H. J. Interferon-regulatory factors determine macrophage phenotype polarization. *Mediators of inflammation* **2013**, 731023, doi:10.1155/2013/731023 (2013).

197 Whetstine, J. R. *et al.* Reversal of histone lysine trimethylation by the JMJD2 family of histone demethylases. *Cell* **125**, 467-481, doi:10.1016/j.cell.2006.03.028 (2006).